A PID FEEDBACK CONTROL SYSTEM FOR UTILIZING A RF EMISSION TUBE AT THE MAXIMUM EFFICIENCY

Senaka Bandara Wijayakoon

(148470N)

Degree of Master of Science

Department of Electronic and Telecommunication Engineering

University of Moratuwa

Sri Lanka

January 2019

A PID FEEDBACK CONTROL SYSTEM FOR UTILIZING A RF EMISSION TUBE AT THE MAXIMUM EFFICIENCY

Senaka Bandara Wijayakoon

(148470N)

Thesis submitted in partial fulfillment of the requirements for the degree Master of Science in Electronics and Automation

Department of Electronic and Telecommunication Engineering

University of Moratuwa

Sri Lanka

January 2019

DECLARATION, COPYRIGHT STATEMENT AND THE STATEMENT OF THE SUPERVISOR

"I declare that this is my own work and this thesis does not incorporate without acknowledgement any material previously submitted for a Degree or Diploma in any other University or institute of higher learning and to the best of my knowledge and belief it does not contain any material previously published or written by another person except where the acknowledgement is made in the text".

"Also, I hereby grant to University of Moratuwa the non-exclusive right to reproduce and distribute my thesis, in whole or in part in print, electronic or other medium. I retain the right to use this content in whole or part in future works (such as articles or books)".

Signature: Date:

The above candidate has carried out research for the Master's Thesis under my supervision.

Name of the supervisor: **Dr. Jayathu Samarawickrama**

Signature of the supervisor: Date:

ABSTRACT

Thermal emission tubes are expensive electron devices regularly used in numerous applications such as Radio Frequency (RF) amplifiers, medical instruments, etc. Such a thermal tube designated as TH558E is used as a RF amplifier within a 250kW Short Wave transmitter in the Sri Lanka Broadcasting Corporation in Trincomalee. In this RF amplifier circuit, a control scheme is integrated with the fine tuning of RF amplifier's final stage to maintain the desired power efficiency and the output power. The present control system configured by the transmitter manufacturer shows poor control capabilities for some broadcasting frequencies and, as a consequence power efficiency and life time of the thermal emission tube is significantly reduced. In this work, we propose a control scheme which is based on multiple Proportional Integration Derivation (PID) controllers and H-infinity optimality criterion to overcome the deficiencies of the original control scheme. Here, a new controller is embedded with an optimal automated tuning method. It is tested for fine-tuning of the RF amplifier's final stage. The PID control gains are found using an algorithm based on Linear Matrix Inequality [LMI] ensuring the stability. The simulation and test results prove that the proposed control architecture is capable of providing the desired performance.

ACKNOWLEDGEMENT

This master thesis project was initiated and funded by Engineering section of Sri Lanka Broadcasting Corporation (SLBC). I would like to express my sincere gratitude to Eng. H.V.K. Zoysa; Engineer in Charge of International High power Radio Station, Kuburupiddi, Trincomalee, Eng. H.M. Jackson; Former Deputy Director General in Engineering, Sri Lanka Broadcasting Corporation and fellow staff members of Engineering section for consulting engineering crew in International High power Radio Station as the technology provider of this project. I heartily appreciate all the supports and encouragements given by Eng. B.B. Basnayake; Information and Networks, Eng. T.D. Somarathna; power and high voltage, Eng. M.S.K. Rakeeb; antenna system and Eng. B. Shankaran; Generator system, who are working with me at the International High Power Radio Station.

I would like to express my special gratitude and thanks to project supervisor, Dr. Jayathu Samarawickrama for giving me such attention, time and extending relentless guidance in a successful completion of this thesis. I am also heartily thankful to course coordinators of the MSc program in Electronics and Automation; Prof. Rohan Munasinghe and Dr. Chamira Edussooriya who always spent their valuable time for keeping the progress of this project at scheduled time line. Additionally, I would like to thank course assistant; Mr. Damith Kandage for arranging everything in the infrastructure level throughout MSc program. Finally, I am also thankful to all academic and non-academic staff members; Department of Electronic and Telecommunication Engineering of University of Moratuwa, for giving their supports to complete this master thesis.

Senaka Bandara Wijayakoon,
BSc Eng(SL), MIEEE, AMIE(SL)
International High Power Radio Station of Sri Lanka Broadcasting Corporation,
Trincomalee, Sri Lanka,
January 2019.

TABLE OF CONTENTS

LIST OF FIGURES

LIST OF TABLES

CHAPTER 1
INTRODUCTION

Chapter 1 discusses the inducement and background behind the research. It explains why this project was selected as a master thesis. The major goal of this project is to design a control scheme and synthesize a controller which ensures expected performances from the plant. Performances are directly related to the power efficiency and life time of electron emission tube, TH558E [17]. Proposed controller is engaged with the fine tuning of final RF amplifier stage in which TH558E is employed as active amplifying module. Section 1.1 is devoted to reveal the motivation of research. Section 1.2 clearly discusses problem definition of research work. Section 1.3 focusses on assumptions and limitations of the project. Section 1.4 discusses the contribution of project to the organization, and Lastly, Section 1.5 outlines the rest of the chapters of the report.

1.1.Motivation

Sri Lanka Broadcasting Corporation (SLBC) [18] is a government radio service which owns eight island wide Frequency Modulation (FM) services and two international high power Medium Wave/Short Wave (MW/SW) radio stations. This research has focused on a matter which exists in one of high power radio station located in Trincomalee, Sri Lanka. This radio station was previously run and maintained by German government's radio service named Voice of German (DW). They handed over the project to SLBC after expiring the agreement between DW and SLBC, in year of 2012. This radio station has four SW transmitters and one MW transmitter. Programs are broadcasted to Asia, Middle East, Australia, Europe and Africa. Each SW transmitter is capable to deliver 250kW maximum carrier RF power within the frequency range of 6MHz – 26MHz. Target area of MW transmitter of which RF power limits to 400kW is south Asian region.

Programs which should be broadcasted to target locations are given by several international radio services like AWR (Adventist World Radio), GFA (Gospel for Asia), PCJ (Phillips Radio), BBC (British Broadcasting Corporation) and NHK (Japan's National Public Broadcasting Service). The main income way of the firm is the air time which is based on transmitter's output RF power. SW transmitters can be powered in two levels named full power (250kW) and half power (125kW). Output RF power level is mainly decided based on distance of target area to which program needs to be broadcasted. Power efficiencies of high power transmitters vary with respect to their modulation techniques. The maximum power efficiency of the oldest SW transmitter which has a linear modulation technique, limits only to 25%. Therefore this one is mainly used in a case of one SW transmitter gets out of order. There are other two SW transmitters from same model which has an efficiency about 70%. Contemporary SW transmitter which has the matter this thesis discusses, has an efficiency around 85%. MW transmitter made of class F solid state amplifier modules has an efficiency more than 90%. The net profit of the station mainly depends on the overall power efficiency contributed by each transmitter. The modulation methods of all SW transmitters, except oldest one are based on switching amplifier technique.

The final modulation device of SW transmitter we discuss, is high power electron emission tube, TH558E. It works as a class C amplifier. The power efficiency of transmitter mainly depends on the efficiency of this device. In other words, device must be capable to convert input electrical power to RF power as much as possible. Because the device operates as a class C amplifier, the phase difference between input and output RF of emission tube must be 180 degrees at its highest efficiency. The phase of the output RF depends on the load or antenna connected to the output terminal (anode) of the emission tube. The anode impedance of the emission tube, TH558E is 290Ω. Then, final tuning stage which is employed between load and anode must be capable to transform the impedance of load (or antenna) to 290Ω at the anode terminal of emission tube. There are two tuning criteria named coarse and fine tuning for pre and final RF amplifier stages. In coarse tuning, variable elements like capacitors and inductors coupled to permanent magnet DC motors [19] are positioned to their pre-defined values.

Fine tuning control scheme of final RF stage which is considered in this thesis should vary two fine tuning elements, a capacitor and an inductor until phase difference designated as PHI2, between input and output RF of the emission tube becomes close to 180 degrees, and RF power designated as PWR to the antenna or load reaches expected value set by operator. Then it is obvious to see that control scheme is inherently bonded to optimize two output variables, phase difference and output RF power. This nature leads to identify the plant as a Multi Input Multi Output (MIMO) system which has a loop interaction between two controlled variables. In other words, when controller tries to optimize one controlled variable, then other controlled variable also gets affected. Two manipulated or so called input variables are the position of two fine tuning elements. The reactance of capacitor and inductor appear in final stage RF circuit depends on their tuning positions. Positions are set by two permanent magnet DC motors [19] coupled to fine tuning elements through gear wheels and transmission belts. Supply voltages for motors are given by two servo amplifiers. The magnitude and polarity of motor's supply voltages are governed by a control voltage. This control voltage is the input of the servo amplifier and it lies within the range of -10V ... +10V. In the existing system, this control voltage is generated by a digital motor control board coming under transmitter's control system. According to the literatures of transmitter, it emphasizes that the existing controller has been designed as an ON/OFF (Bang-Bang) controller. With respect to controller, Output variables (controlled variables) are same as the measured variables. Phase difference (PHI2) and output RF power (PWR) are measured by two dedicated sensor probes. Sensed variables are then transduced to form of electrical signals and conditioned prior to send motor control board. In this research work, same conditioned electrical signals of measured controlled variables are used while only controller is replaced by the proposed one. In other words, existing control algorithm for fine tuning of final amplifier stage is bypassed through proposed controller.

Original fine tuning control scheme occasionally fails to generate RF power at an expected level of efficiency. As a result, input electrical power is wasted in the form of heat within the tube itself. This scenario is capable to deteriorate the internal structure of tube besides decreasing the overall efficiency of the transmitter.

From the view of control engineering terms, existing system always ends up with a steady state error for RF power efficiency (PHI2). Otherwise it experiences sustained oscillations by showing its instability nature. In such a case, many number of overshoots or undershoots for both controlled variables may occur. Therefore there is a considerable chance to dissipate input electrical power as heat spikes which may cause catastrophic failure of emission tube. By taking those drawbacks in to account, the main priority of proposed controller is going to maintain the stability of whole closed loop system composed by controller and transmitter (plant). Minimized settling time, overshoots and zero steady state error for both controlled variables are other supplementary design goals. The transmitter to which new control scheme is proposed is shown in Figure1. Figure 2 shows two fine tuning elements, capacitor and inductor. Sensor probes for measuring phase difference (PHI2) are shown in Figure 3 and RF directional coupler which is used to measure RF output power is shown in Figure 4. Figure 5 shows the emission tube we consider in this research.

Figure 1: Transmitter (Plant)

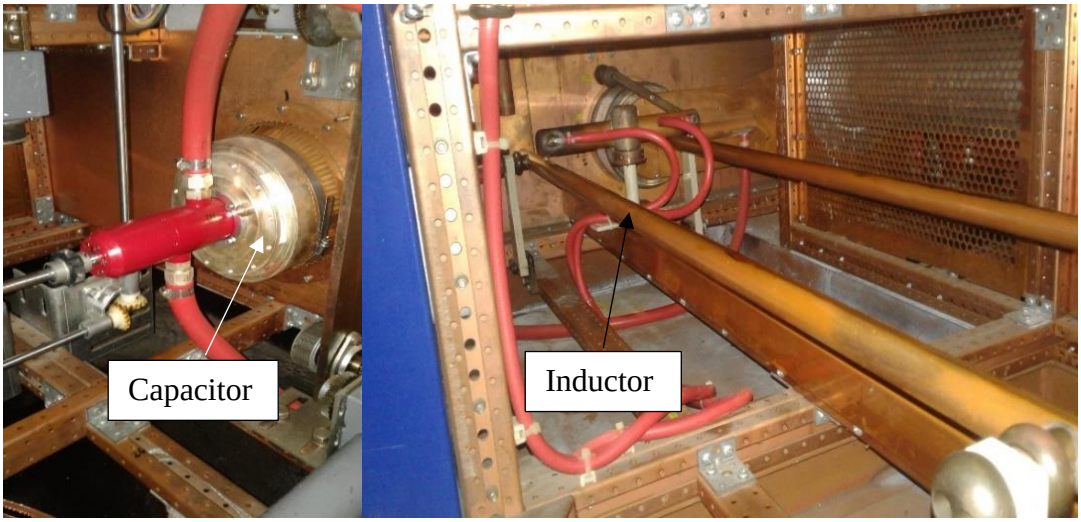

Figure 2: Two Fine Tuning Elements

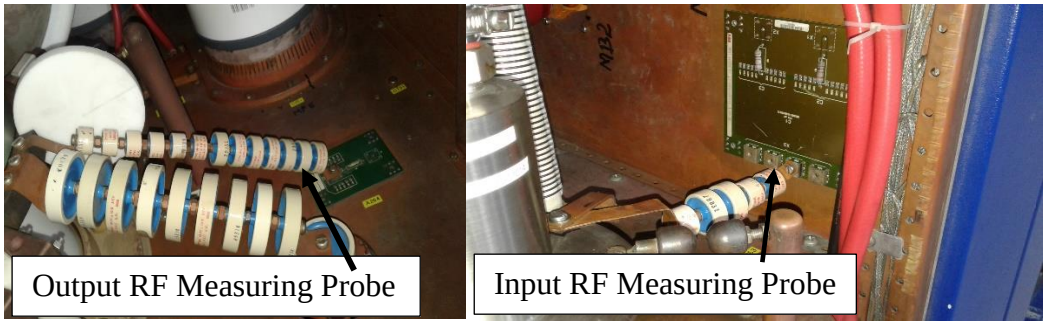

Figure 3: Sensor Probes to get RF Samples for Calculating RF Phase Difference

Figure 4: RF Directional Coupler for Measuring Output RF Power

Figure 5: TH558E Electron Emission Tube within the Transmitter

1.2. Problem Definition

Within past 6 years of operation, three emission tubes from the type of TH558E were failed prematurely. Then engineering team in the premises started to analyze the causes which can make the tube ill. Then they identified several probable causes including poor control capabilities of fine tuning of final RF stage. This mission was collaborated by the manufacturer of emission tube THALES [20] and manufacturer of transmitter, AMPEGON [21].

Eventually, AMPEGON proposed to replace some RF components like fine tuning element, inductor and components of control circuit. The total cost including their labor charges was around 10 million in LKR. Any way, they couldn't prove what the probable cause was precisely, without a site inspection. Therefore our technical crew had to find alternatives prior to welcome manufacturer for a site inspection. This research work was originated based on that decision.

The project was supervised by Dr. Jayathu Samarawickrama who is a senior lecturer in Department of Electronic and Telecommunication Engineering (ENTC), Faculty of Engineering, University of Moratuwa. Project was funded by engineering section of SLBC .The participants of this work are Mr. W.W.R.S.B.Wijayakoon; engineer who works in the radio station (author), senior technicians; Mr. E. Ockez and Mr. S. Rodrigo who also work in the radio station.

1.2.1. Thesis Definition and Objectives

The main objective of this master's thesis is to research and develop a stabilized and robust controller which is based on multiple PIDs and H-infinity optimality criterion for purpose of increasing the power efficiency and extending the life time of electron emission tube TH558E of which life time may be badly affected by poor fine tuning performance of final RF amplifier stage. Tube is employed as a class C RF amplifier within the 250kW, SW transmitter, SK 53 C3-3-P manufactured by AMPEGON [21]. In this research, input-output relationships or so called transfer functions are approximated by using best experimental data. Proposed controller can easily be validated comparing its performance with the performance of existing controller.

1.2.2. Goals

New control scheme is proposed to have following goals.

Main Goal

I. Development of an appropriate control scheme to ensure the stability of fine tuning of final RF amplifier stage which is formed by interested emission tube TH558E. Controller is robust to maintain its stability even when low frequency disturbances, high frequency noises and plant model errors are presence. As a result, power efficiency is maintained at an optimal level. Therefore dissipation of heat in long term basis or short term basis as heat spikes can be minimized as much as possible. That is directly related to the life time of tube.

Sub Goals

i. Minimizing settling time of fine tuning criteria of final RF stage.
ii. Minimizing the percentage of maximum overshoots while system is in dynamic.
iii. Ensuring a zero steady state error for both controlled variables, power efficiency (PHI2) and output RF power (PWR).

1.3. Limitations

- Proposed controller has not been tested in a situation where elements of RF circuit and/or control circuit have perturbed from their nominal values in large amount.
- System's transfer functions are approximated from experimental data which are taken while transmitter is operated under several specific frequencies. Therefore, a little chance may still exist to give unexpected results under some other frequencies
- Approximated transfer functions have an accuracy more than 90%. Therefore, a possibility to fail the controller still may be found within the range of other 10% even though controller is robust to model errors.

1.4. Contributions to the Organization

As mentioned in the problem definition, three emission tubes were failed prematurely within past 6 years. The cost of this type of an emission tube would be around 20 million in LKR. There may be several reasons for premature failures while poor fine tuning of final RF stage plays a main role. Nominal operating hours of a TH558E should be around 30,000 hours. Proposed controller certainly helps to achieve this life time because it ensures and proves a minimal heat dissipation during tube works within the RF circuit. Therefore the cost of operation of transmitter SK 53 C3-3-P [21] decreases in a considerable amount with respect to the time when transmitter's original controller was employed. Therefore this research work takes a remarkable place in the calculation of total revenue and cost of whole radio station. Since tube works with a zero steady state error of power efficiency, generation of internal heat is minimized as much as possible. This is equivalent to saving of power and hence cost for power. The cost for manufacturer of transmitter to analyse the matter and proposing a solution was approximately 10 million in LKR. It is a big amount compared with the cost of this proposal. Hence, it is obvious to conclude that this research work grants several benefits in many aspects to the SLBC

1.5. Report Outline

The rest of this thesis is outlined as follows. Chapter 2 is devoted to review some of previous works on existing control mechanisms developed for MIMO systems which usually experience loop interactions. Chapter 3 discusses how experimental data were taken and how they were processed to identify transfer functions between inputs and outputs. Chapter 4 focuses on theoretical terms which can be gathered to design a control scheme for ensuring main goal, stabilized closed loop system. The implementation of hardware and software of the proposed control scheme is discussed in Chapter 5.

Chapter 6 describes the results of the research. Furthermore, it proves the validity of developed control scheme by comparing the proposed controller's response with existing controller's response. Finally, overall success of thesis is discussed. MATLAB programing code written in language C for Linear Matrix Inequality [LMI], the convex optimization algorithm, is given in Appendix 'B'. The developed test controller is based on high speed microcontroller ATMEL MEGA- 328P [25]. The relevant programing code written in language C is given in Appendix 'C'.

CHAPTER 2
LITERATURE REVIEW

Lot of researchers and industrial people are talking about MIMO control systems. Most of practical plants and processes are inherently MIMO systems which have individual control loops with interactions among each other. This scenario leads to a situation where control design becomes a tedious task for engineers or researchers. A major difficulty encountered in a MIMO control design is the stability issues of whole system which comprises of plant (or process) and controller. All controlled variables must be regulated at same time while considering the stability. The situation may be worse when low frequency disturbances and high frequency noises interrupt the system. Then, mitigation of those unwanted, unexpected and non-manipulated external inputs become a leading factor in stability and time domain performance of a system. Therefore, since recent years, control designs for MIMO systems are considered in conjunction with noise and disturbance filtering.

2.1. Some Previous Works

It is not possible to find previous works which specifically focus on automated RF amplifier tuning. But other analogue studies of which plant and design methodologies are closely related to our work, are discussed. Such a TITO system of a wastewater treatment plant is discussed in [13]. This paper talks about three methods to find out closed loop feedback gain matrices for decentralized two PID controllers. All those methods are based on plant's frequency response. One method called Davison can only calculate the integral feedback gain matrix. It ensures the decoupling between two control loops only for low frequency response. Therefore, considering the lack of advantages from PID controlling and poor decoupling, this method does not meet our requirements. Second method, Penttinen-Koivo, proposes a way to find integral and proportional gain matrices. But its decoupling performance is better than first one.

However, due to the fact that it neglects the derivative component, a decentralized PID controller designed based on this method may have poor time domain behaviors like excessive overshooting. Third method named Maciejowski can successfully be used to find all three closed loop gain matrices of two decentralized PID controllers. It can ensure a good decoupling for whole bandwidth of plant. But, it is necessary to have frequency bandwidth of the plant in this method. Practically, it is not an easy task to find the bandwidth of a MIMO system accurately. Therefore it is concluded that this method makes the design more complex in the phase of data collecting and analysis.

Another method to design a decentralized PID control system by introducing a static decoupler is explained in [15]. It proposes an additional decoupling system between plant and controller. But the method can only be used with stable systems. In other words, step response of the opened loop system must have a stable steady state value. If transfer function matrix of MIMO system is $G(s)$ then $G(0)$ should not be singular. In our TITO system, all four transfer functions are approximated with an integrator. Therefore it is inherently an unstable system to which proposed method from this research is not possible to be used directly without extensive modifications.

A Static Output Feedback (SOF) control strategy is discussed for a TITO system of a binary distillation column, in [16]. The system is inherently stable with a delayed response in time. Time domain performance and external disturbance rejection are achieved by combining design approaches, LMI, Genetic Algorithm (GA) and H-infinity optimality criterion together. The paper clearly reveals the capability of proposed control scheme to reject external disturbances while keeping the step tracking at expected level. LMI design approach ensures the stability of closed loop system while H-infinity optimal tuning criterion takes care of robust control performances like disturbance rejection and model errors. Original transfer function matrix of distillation column which is famous as Wood and Berry is firstly approximated to a set of transfer functions using first order pade approximation method.

This method is employed to approximate the time delays coming with all four transfer functions. Then opened loop transfer function matrix is converted to state space domain as ease of handling. It emphasizes the advantage of using H-infinity control design as the ability to withstand the system at expected level of performance even in presence of uncertainty of dynamics and external disturbances. This research has considered the set point inputs as external disturbances to the system. Disturbances of low frequencies can affect the step tracking performance when they appear with tracking error, the difference between set points and outputs. Disturbances of high frequencies can affect the performance when they are present at the place from where controlled variables are measured. Therefore, two weighting functions are placed at those two places to where disturbances are likely to be added so as overall performance may be affected. Weighting function for low frequency disturbances is modeled as a low pass filter while weighting function for high frequency disturbances is modeled as a high pass filter. The guide lines for modeling necessary weighting functions are described in [14]. Then the closed loop system with presence of weighting functions is depicted as in Figure 6.

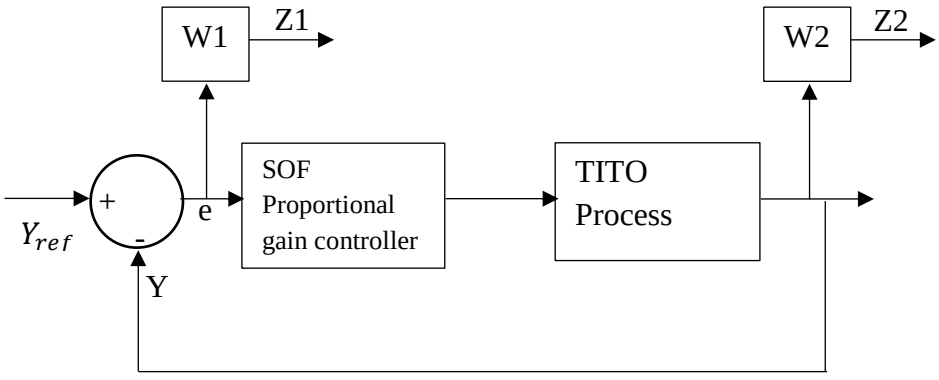

Figure 6: Closed Loop System with Controller and Weighting Functions

The generic form of weighting functions for a TITO process is defined as in equations (1) and (2).

$$w_1(s) = \begin{bmatrix} w_{e1}(s) & 0 \\ 0 & w_{e2}(s) \end{bmatrix} \qquad (1)$$

$$w_2(s) = \begin{bmatrix} w_{y1}(s) & 0 \\ 0 & w_{y2}(s) \end{bmatrix} \qquad (2)$$

Then, outputs of weighting functions, Z1 and Z2 are written in vector form as given in equations (3) and (4).

$$Z_1 = [Z_{e1}, Z_{e2}]^T \quad (3)$$

$$Z_2 = [Z_{y1}, Z_{y2}]^T \quad (4)$$

State space realization of augmented plant which comprises controller and weighting functions is given as listed by equations (5)-(8).

$$\dot{X}_{tg} = A_{tg}X_{tg} + B_{tu}U_{tc} + B_{tw}W_{td} \qquad (5)$$

$$Z_1 = C_{t1}X_{tg} + D_{t11}U_{tc} + D_{t12}W_{td} \qquad (6)$$

$$Z_2 = C_{t2}X_{tg} + D_{t21}U_{tc} + D_{t22}W_{td} \qquad (7)$$

$$Y = C_tX_{tg} \qquad (8)$$

A_{tg} is state transition matrix. X_{tg} represents the state vector which includes all the states of augmented plant. U_{tc} is the vector of manipulated control inputs. W_{td} represents the vector of tracking reference, Y_{ref} . B_{tu} , B_{tw} , D_{t11}, D_{t12}, D_{t21} and D_{t22} are control input matrices with appropriate dimensions. .Then, authors define the main control objective in H-infinity and SOF design as finding a controller K such that $U_{tc} = K * Y$ for minimizing the infinity norm of transfer function which relates the reference input W_{td} and output of weighting functions, $Z = [Z_1, Z_2]^T$. This necessity mathematically is written as given by equation (9).

$$\left\|T_{zw_{td}}\right\|_\infty = \left\| \begin{matrix} w_1(s)S(s) \\ W_2(s)T(s) \end{matrix} \right\|_\infty \qquad (9)$$

Referring to equation (9), $S(s)$ ($(I + PC)^{-1}PC$) is known as sensitivity function and $T(s)$ ($(I + PC)^{-1}$) is named as complementary sensitivity function.

P and C are opened loop transfer function matrix of plant and transfer function matrix of controller respectively. By substituting SOF control law $U_{tc} = K * Y$ in to equation (5), closed loop form of the state transition matrix is derived. Then, theoretical derivations based on Lyapunov stability condition is used to express the stability of system as a Quadratic Matrix Inequality (QMI) [3]. This inequality is given by (10).

$$\begin{bmatrix} (A_{tg} + B_{tu}KC_t)^T P + P(A_{tg} + B_{tu}KC_t) - (NB_{tu}{B_{tu}}^T P) - (NB_{tu}{B_{tu}}^T P)^T + (NB_{tu}{B_{tu}}^T N) & (B_{tu}{}^T P + KC_t)^T \\ (B_{tu}{}^T P + KC_t) & -I \end{bmatrix} < 0 \quad (10)$$

In equation (10), P $(P > 0)$ is a positive definite matrix and N is any arbitrary selected square matrix.

The authors show that QMI given in (10) can be deduced as a LMI, if one matrix variable, P or N is set as a constant. They clearly show that time domain performance mainly depends on these two matrices. Because P has a constraint, $P > 0$, matrix N is selected as decision variable of which value is found by a GA while a predefined Performance Index (PI) is being minimized. PI is defined in this paper as given by equation (11).

$$PI = q_{t1}(100) + q_{t2}\left(\left\|T_{zw_{td}}\right\|_{\infty}\right) \quad (11)$$

The values of q_{t1} and q_{t2} are selected based on stability requirements. They may have only 1 or 0. Their values depend on the eigenvalues of closed loop system matrix $A_{tg} + B_{tu}KC_t$. Therefore, PI may have 100 or a value between 0 and 1. Authors propose an iterative algorithm based on GA and LMI to achieve the stability and performance requirements. SOF gain matrix is found using proposed iterative algorithm. The successful simulation results are compared with other results taken in several other publications for same Wood and Berry distillation column. The measurement index of performance is quantified using terms, Integral Square Error (ISE) and Integral Square Value (ISV).

Not only controlled variables but also manipulated control efforts are taken in to consideration in this paper. The magnitude, polarity and rate of change of manipulated variables are important in practical control design. The capability of disturbance rejection is simulated by injecting an external step disturbance at time, 50 minutes. Results clearly show that the performance of proposed controller in view of disturbance rejection is more successful. Despite the fact that controller is proposed for a stable plant, LMI and H-infinity design approaches ensure the expected time domain performance, disturbance rejection and closed loop system stability.

A pure LMI design approach is considered in [1] for both stable and unstable processes. The main objective of the design is to stabilize the augmented plant while minimizing the infinity norm of weighted sensitivity function of the closed loop system. Control problem is mathematically formulated based on well-known Bounded Real Lemma (BRL). Nonlinear Matrix Inequalities related to BRL are decomposed in to several LMIs such that an iterative algorithm could be built for solving controller's gain matrices. The set of LMIs are solved by starting from Lyapunov stability criterion. Proposed algorithm can be used to calculate gains of a Proportional and Integration (PI) or a Proportional and Derivative (PD) controller. In a case, results don't meet required performance, then decision parameters defined in algorithm could be changed and rerun the program until we get satisfied results. According to proposed methodology, plant, controller and weighted sensitivity functions should firstly be converted in to state space domain. Controller and augmented plant in state space domain are depicted in the paper as shown by Figure 7 and Figure 8 respectively.

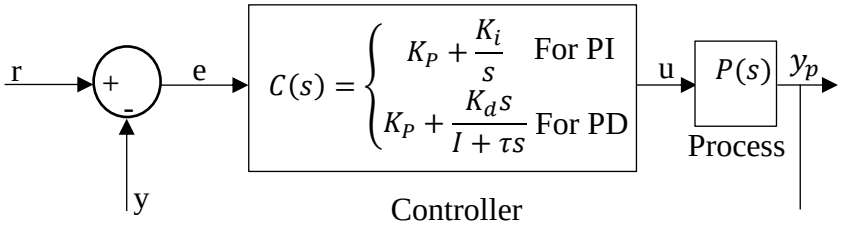

Figure 7: MIMO Feedback System with a PI/PD Controller

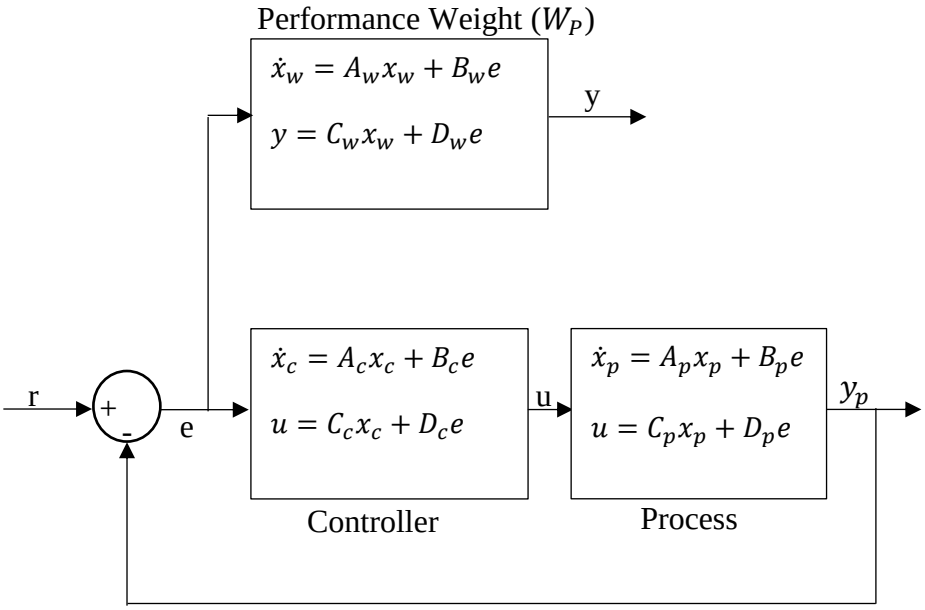

Figure 8: Augmented System with Weighted Sensitivity Function

The main design goal is to minimize $\left\|W_p(s)S(s)\right\|_\infty$ while keeping the stability of closed loop system. $W_p(s)$ is performance weight and $S(s)$ is sensitivity function as described for [16]. If a MIMO plant is with l, outputs and m, inputs then dimensions of controller's gain matrices become, K_P, K_i, $K_d \in \mathbb{R}^{m*l}$. The relationship between r and y in state space domain, is expressed as given by equation (12) and (13).

$$\dot{x}_{ws} = A_{ws}x_{ws} + B_{ws}r(t) \quad (12)$$

$$y = C_{ws}x_{ws} + D_{ws}r(t) \quad (13)$$

The parameters mentioned in equations (12) and (13) are derived from the parameters of state space equations given in Figure 8. Stability of the system given by (12) and (13) is considered based on BRL. The corresponding transfer function, $G(s)$ for the system described by (12) and (13) is given as in (14).

$$G(s) = C_{ws}(sI - A_{ws})^{-1}B_{ws} + D_{ws} \quad (14)$$

Then authors define the necessity for stability of system, by following BRL as given by (15).

$$\left\| W_p(s)S(s) \right\|_\infty < \gamma \qquad (15)$$

γ is a positive number upon which time domain performance depends and it is known as Performance Index (PI) . Moreover, inequality (15) is expressed as a Matrix Inequality (MI) as given by (16).

$$\begin{bmatrix} {A_{ws}}^T P + P A_{ws} & P B_{ws} & {C_{ws}}^T \\ {B_{ws}}^T P & -\gamma I & {D_{ws}}^T \\ C_{ws} & D_{ws} & -\gamma I \end{bmatrix} < 0 \qquad (16)$$

MI, (16) holds true and there exists a feasible solution, if and only if, there exists a symmetric matrix P such that $P = P^T > 0$. (16) is a nonlinear MI since multiplications of unknown variables appear in several places. Therefore the method followed by authors to simplify (16) as a set of LMIs, is decomposing MI in to several LMIs. Once unknown matrices A_{ws}, B_{ws}, C_{ws} and D_{ws} are found with the constraint of $P = P^T > 0$ and BRL (15), state space realization of controller (A_c, B_c, C_c, D_c) can be derived easily. Authors propose an iterative algorithm which is capable to solve all six LMIs. At the end of the algorithm, three gain matrices of PID controller are given.

Another Iterative LMI (ILMI) algorithm to find PID gain matrices of a MIMO system is proposed by [2]. This algorithm is also based on sensitivity and complementary sensitivity functions of the closed loop system. Sensitivity of plant ($S(s)$) around $s = 0$ is approximated to $(P(0) * K_I)^{-1}$. $P(0)$ is plant's transfer function at $s = 0$ and K_I is integration gain matrix. The best possible sensitivity for low frequencies is achieved by minimizing the norm $\|(P(0) * K_I)^{-1}\|$. The boundaries for two sensitivity functions and actuator's outputs are predefined to ensure the closed loop stability. Then algorithm minimizes the norm $\|(P(0) * K_I)^{-1}\|$ while considering those boundary constraints. The guide lines for selecting boundary values are given in this publication. Algorithm is proposed only for stable and strictly proper plants. But at end of the paper, the way of extending it for unstable plants like our one, are also described clearly.

2.2. Conclusion of Review

Research works [13] and [15] discusses some old methods to tune or find the gain matrices of a MIMO PID controller. The method named Maciejowski considered in [13] has remarkable advantages upon other two methods proposed in same paper. However an accurate frequency response of the plant is expected, if method, Maciejowski is used. The methods described in [13] and [15] can be used to design controllers only for stable plants. An extensive effort is needed to extend the results for unstable plants like we consider in this thesis. Since additional decouplers are proposed by [15], practical design may become somewhat complicated.

The contemporary ILMI design approaches are discussed in [16], [1] and [2]. This design method, ILMI ensures the stability of an unstable or stable closed loop system. Time domain performance depends on some decision parameters used in the algorithm. The values of decision parameters do not effect on the stability. In this research, we consider a plant which experiences instability and poor controlling behaviors for some particular operating conditions. Since ILMI approach ensures the stability for any time domain performance, it is desirable to select ILMI approach to proceed our work. Only [2] proposes an algorithm to find all three gain matrices of PID controller while [16] and [1] discuss only design of PI, PD and P controllers. Therefore the ILMI algorithm for SOF-PID controller presented in [2] is considered in this thesis while another approach to replace its weighting functions are proposed as it eases the control design [4].

CHAPTER 3
DATA ANALYSIS

This chapter explains how the process is mathematically identified using experimental data taken from transmitter (plant). It is necessary to have an overview knowledge of the plant in the process of data gathering and analysis. Therefore section 3.1 describes the overview of the plant. It includes descriptions of all functionalities related to the operation of transmitter. Section 3.2 narrates the mechanism of fine tuning criterion of final stage in RF amplifier. Section 3.3 explains how experimental data were gathered and manipulated to identify the process. It shows the path of analysis to build transfer functions which relates inputs and outputs of the process. Discussion is extended further by describing the Control Design and its theoretical background in Chapter 4.

3.1. Functional overview of plant

SK 53 C3-3-P 250kW- SW [21] transmitter is a complex composition made of many block of functionalities. Mainly, it includes RF, High Voltage (HV), Cooling and Control sections. Fine tuning criterion of final stage of RF amplifier is categorized under control section. Functional overview in block form can be shown as in Figure 9. Main supply represents the 3-phase 11KV (phase to phase voltage) high voltage input to the transmitter. It is stepped down by an auxiliary transformer for utilizing the power in Low Voltage (LV) distribution which is dedicated to supply power for other two sections, cooling and control. Pulse step modulator (PSM) is a high voltage/low current audio amplifier which is created from 40 number of individual switching amplifiers. The basic switching element in a single amplifier unit is an Insulated Gate Bipolar Transistor (IGBT). Each amplifier module is switched ON or OFF by control section of transmitter so as output of the amplifier becomes the audio to be modulated. All the amplifier modules are connected in series. RF section mainly comprises low power RF generator (synthesizer), driver amplifier stage and final amplifier stage which is connected to antenna through a RF coaxial cable. This research work focuses only on fine tuning criterion of final amplifier stage.

RF driver stage also consists a triode type thermal emission tube of which maximum RF output power is 30kW. It is working as a class A amplifier with common control grid configuration.

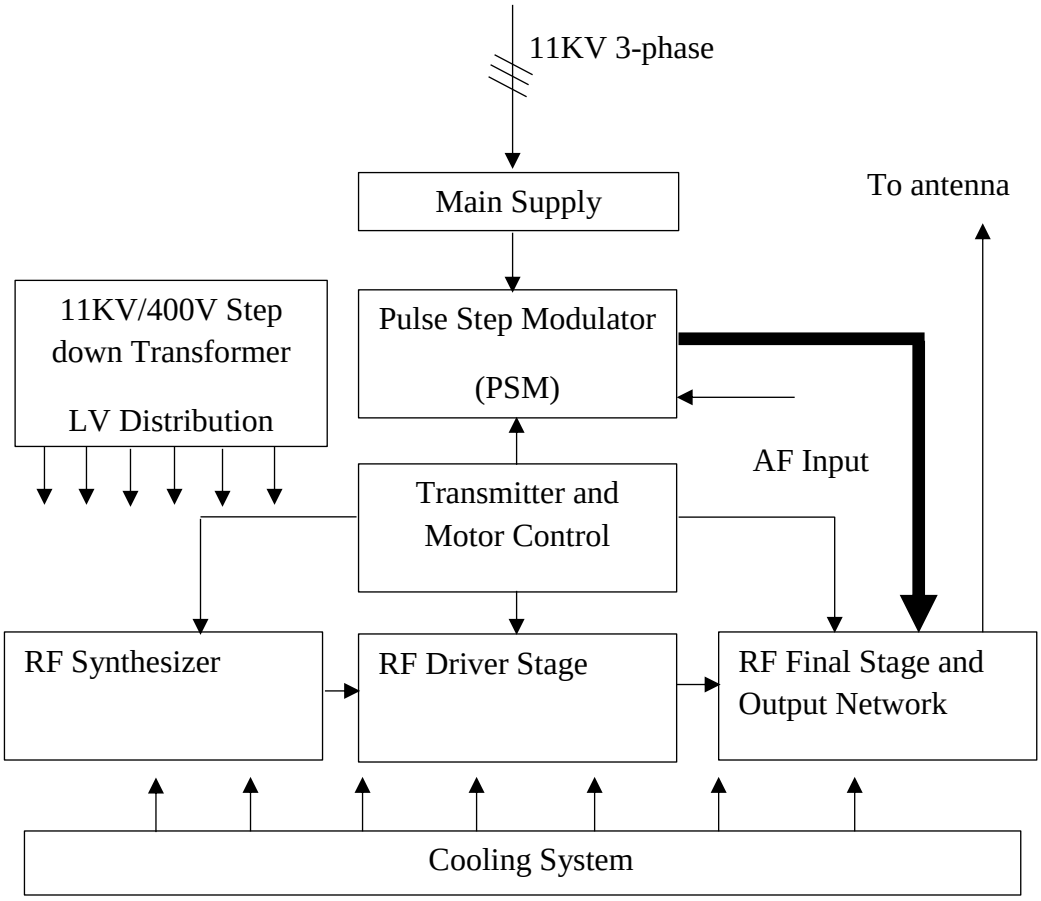

Figure 9: Functional Overview of Transmitter

Cooling system mainly contains two parts, water and air cooling. Water cooling system works as a closed circuit. The main objective of water cooling is to absorb dissipated heat from two emission tubes, high voltage capacitors and inductors. Then heated water is going through an external heat exchanger or so called a radiator. The water cooled by radiator again flows through heated elements. The purpose of low pressure air cooling circuit is to absorb surrounding air of which temperature is elevated by dissipated heat from other electronic components. Control section monitors and control each other sections to maintain expected normal operating conditions.

Control section utilizes many control methods which are attained using various hardware elements and modules like switching relays, motor actuators, servo-amplifiers, linear analog circuit devices and so on. All the monitoring parameters like measurements and feedback signals are generated by measuring probes and signal transducers. Those signals are filtered to remove induced high frequency noises before sending to processing unit. If it is necessary, measurement signals are further conditioned by dedicated analog circuit boards function between probes and processing unit. Control output signals like voltages for servo-amplifiers also go through intermediate low pass filters to remove induced high frequency noises. Control section mainly contains three sub sections named sequence, motor and PSM control. Sequence controlling ensures a proper sequence of functional states related to whole transmitter. Transmitter has five main functional states depend on the filament voltages of two emission tubes, state of the high voltage supply to PSM unit and RF output to the antenna. If filament voltages for two emission tubes are zero then cooling system is also not working. At this stage, only control electronic boards are powered. This stage is designated as OFF. Next level is auxiliary state (AUX). Filament voltages for two emission tubes are increased in a ramp manner from 0V to adequate values. Relevant filament voltages are 6V for final RF tube (TH558E) and 2.5V for driver stage RF tube, CTK-12-1 [22]. In this stage, a low pressure (0.8 bar) and slow speed water circulation (70 liters/minutes) is maintained through final RF emission tube, TH558E. Full filament designated as FIL is the next stage in which filaments of two emission tubes are increased to their nominal operating voltages. It is 20V for final RF tube and 6.3V for driver stage one. These voltages are also attained in a ramp manner. Then the strength of water circulation is elevated up to a level where flow rate is 120 liters/minutes. Low pressure air circulation is also added to the cooling system in this stage. From FIL stage onward, two emission tubes are ready to accept their other terminal voltages to operate as RF amplifiers. Other terminals of final stage emission tube, TH558E are control grid, screen grid and anode. Control grid is the terminal to which RF to be amplified should be given. Screen grid pulls the electrons from filament and pushes toward the anode. Then anode collects those electrons and makes a closed loop electric circuit with filament via the load. The working principle of an emission tube is as same as it is for a Bipolar Junction Transistor (BJT).

Next operating stage is named as standby (STBY). In this stage, PSM unit which is the high voltage anode supplier of final RF tube is prepared. After that, transmitter can be powered up by giving all terminal supplies, input RF signal and audio needed to modulate. Then, transmitter is said to be in ON stage.

3.2. Present fine tuning algorithm

The purpose of fine tuning of final RF stage is to optimize two parameters

1. Phase difference between sinusoidal input and out RF of TH558E emission tube
2. RF power on the transmitting antenna

In the view of control engineering terms, these are the controlled variables. These two variables are interacted each other. When control algorithm tries to optimize one variable, other variable may also be affected in positive or negative manner. Therefore the control strategy becomes somewhat complicated. Phase difference, PHI2 can be measured by using two RF sensing probes designated as phase probe 1 and probe 2. The places at where probes are employed are shown in Figure 10. Then sensed RF wave forms are routed via two low pass filters to a device called phase detector where phase difference is calculated. The purpose of low pass filters is to filter out harmonic components and RF interferences from other transmitters, and keep the needed RF wave as expected. The output of phase detector is a DC voltage which is linearly varying between -5V and +5V corresponds to phase difference. In other words, -5V corresponds to 0° phase difference while +5V corresponds to 360°. But, according to the design, the board designated as motor control board in which fine tuning algorithm is embedded accepts the input voltages vary within the range of 0V - +10V. Therefore this voltage level conversion is achieved within a signal conditioning circuit employed between phase detector and algorithm board, as shown in Figure 10.

The other variable, PWR, the output RF power of emission tube, TH558E is measured using a probe commonly known as RF directional coupler.

Measured RF sample is directed to a power detector where a DC voltage which is proportional to square root of RF power is generated. A constant RF attenuator is employed between detector and coupler for purpose of attenuating the power since detector accepts only up to 10 watts. Output DC voltage from power detector varies between 0V and 5V while RF power on antenna varies between 0kW and 300kW. But, that voltage range must also be converted to a range of 0V – +10V before sending to motor control board. That task is achieved in signal conditioning circuit as shown in Figure 10.

Motor control board is dedicated to control the reactance values of all coarse and fine tuning elements by varying their physical positions. Fine tuning algorithm works for both driver and final amplifier stages. In this work, only final stage is considered. According to design details of algorithm given by manufacturer, present controller is an ON/OFF or so called bang-bang controller. Control DC voltages for intermediate servo amplifiers are issued from motor control board as depicted in Figure 10. They vary between -10V and +10V. Those are amplified by servo amplifiers so as input DC voltages for DC motors which are connected with fine tuning elements, vary between -24V and +24V. Polarity governs the rotating direction of motors and hence the rotating (capacitor) or sliding (inductor) direction of moving elements attached to fine tuning capacitor and inductor. By considering two control loops which incorporate with two controlled variables, it is not difficult to identify two main transfer functions and two cross coupled transfer functions. Transfer functions can be built between inputs of the servo amplifiers (or output of motor control board) and input of the motor control board to where measured output variables are fed (Figure 10). The DC motor designated as Motor Position 10 (MP10) is connected to a sliding conducting bar moving on fine tuning inductor. That sliding bar and inductor is shown in Figure 11. The Position of sliding bar governs the value of inductance. The torque or power of DC motor is transferred to the bar via a flexible transmission belt. Motor Position 11 (MP11) is connected to fine tuning variable capacitor via coupling gears as shown in Figure 12.

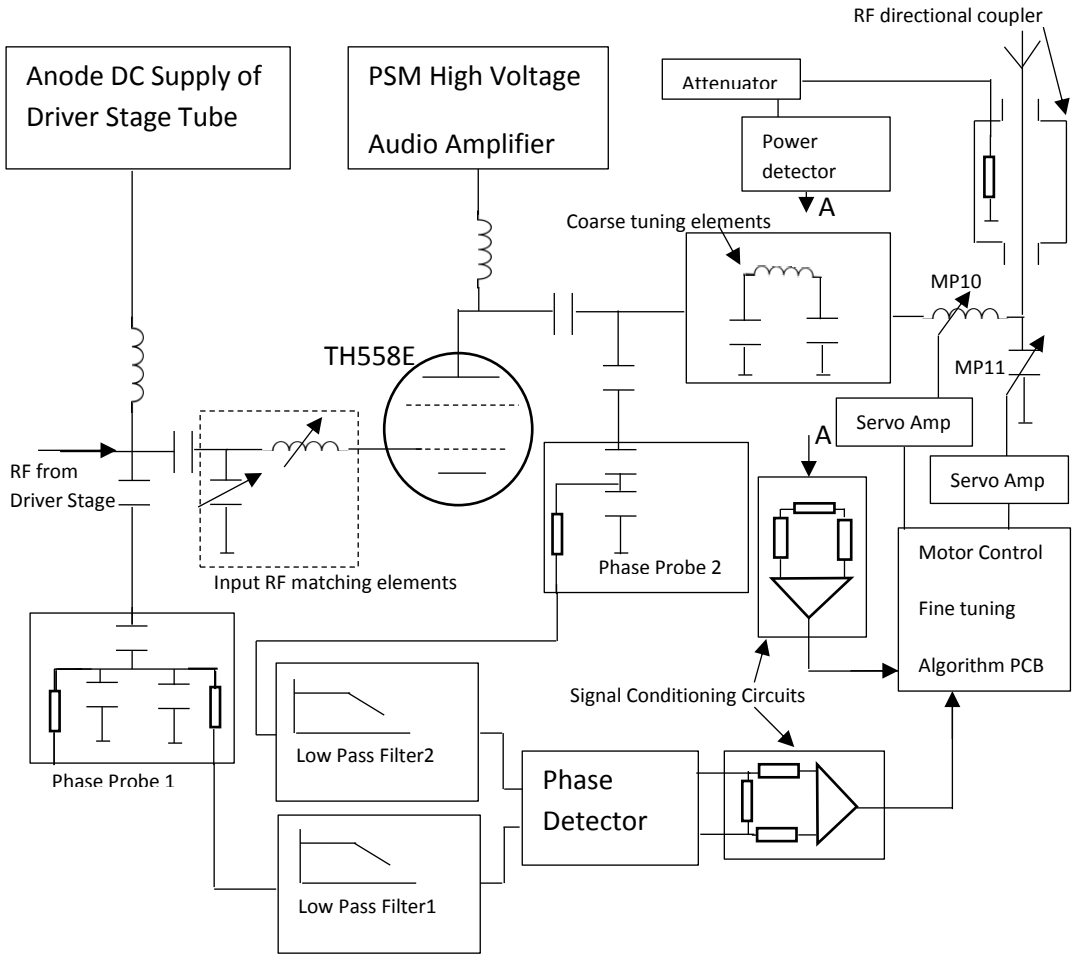

Figure 10: Overview of Final RF Stage-Fine Tuning

Figure 11: Moving Sliding Bar for Varying the Inductance

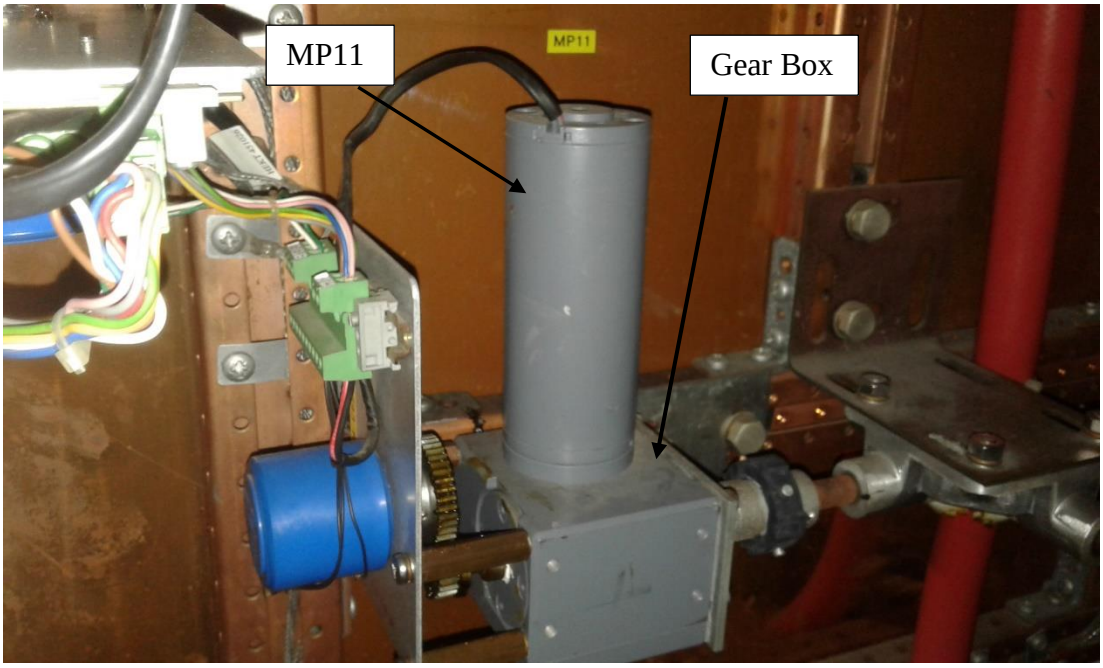

Figure 12: Coupling Gears between MP11 and Variable Capacitor

3.3. Process Identification

Identifying transfer functions between inputs and outputs is a main task in the process of control design. Inputs or manipulated variables are the control voltage signals issued by controller. There are two manipulated variables which are routed from controller to two servo amplifiers. Therefore transfer functions should be built between inputs of servo amplifiers and respective controlled variable (Figure 10). As a result of natural interactions between two main control loops, it is necessary to build four transfer functions. Therefore experimental data were taken as in Table 1. Corresponding experimental setup is shown in Figure 13 and Figure 14.

Table 01: Selected Input/output pairs for having experimental data

Manipulated Variable	Exciting Step I/P Voltage (V)	Measured O/P Variable
I/P to Servo amp of MP10	0.4V	PHI2
I/P to Servo amp of MP10	0.4V	PWR
I/P to Servo amp of MP11	1.0V	PHI2
I/P to Servo amp of MP11	1.0V	PWR

The step responses of output variables are shown in Figure 15, Figure 16, Figure 17 and Figure 18. Relevant transfer functions were identified by using nonlinear least squares error method with the help from APM regression software package [29] and MATLAB software. Each transfer function model is assumed to be second order with an integrator by considering the fact that output variables PHI2 and PWR are directly related to the position of DC motors. Therefore transfer function can be modeled as given in equation (17).

$$\frac{{\omega_n}^2}{s(s^2 + 2\zeta\omega_n s + {\omega_n}^2)} \qquad (17)$$

Time domain response can be obtained by having Inverse Laplace Transformation (ILT) of (17) for a step input. Response in Laplace domain for a step input of which amplitude is one can be expressed as given in equation (18).

$$Y(s) = \frac{{\omega_n}^2}{s^2(s^2 + 2\zeta\omega_n s + {\omega_n}^2)} \qquad (18)$$

Here, ζ is damping ratio and ω_n is natural undamped frequency.

Response in time domain can be given as in equation (19).

$$y(t) = \left(t - \frac{2\zeta}{\omega_n}\right) + \frac{2\zeta e^{-\omega_n\zeta t}}{\omega_n}\left[\cosh\left(\sqrt{\zeta^2 - 1}\omega_n t\right) - \frac{\left(\sinh\left(\sqrt{\zeta^2-1}\omega_n t\right)\right)\left(\omega_n\zeta + \left(\frac{\omega_n - 4\omega_n\zeta^2}{2\zeta}\right)\right)}{\omega_n\sqrt{\zeta^2-1}}\right] \qquad (19)$$

The unknown ζ and ω_n are easily found by minimizing the sum of squares of errors. Error is defined as the difference between measured output values (PHI2 or PWR) from the plant and the predicted output values from the model at a particular time instant. Corresponding MATLAB code and APM model are given in Appendix 'A'. Each transfer function has an accuracy of more than 95% as clearly reveal by Figures. Corresponding transfer functions which are numbered as same order as in Table 01 are given from equation 20 to 23. Two transfer functions out of four have two underdamp poles while other two have two real poles.

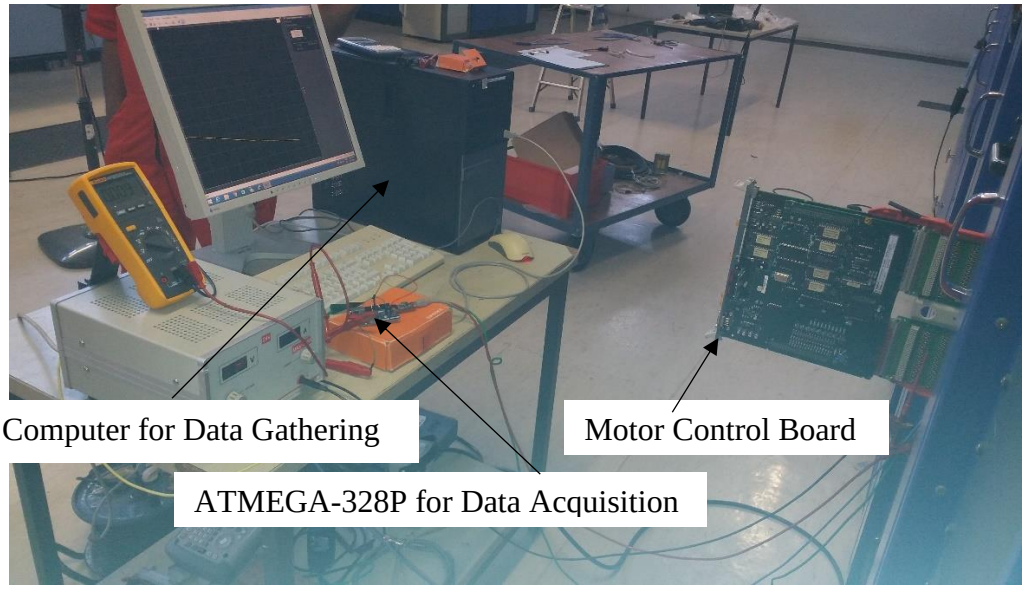

Figure 13: Complete experimental setup

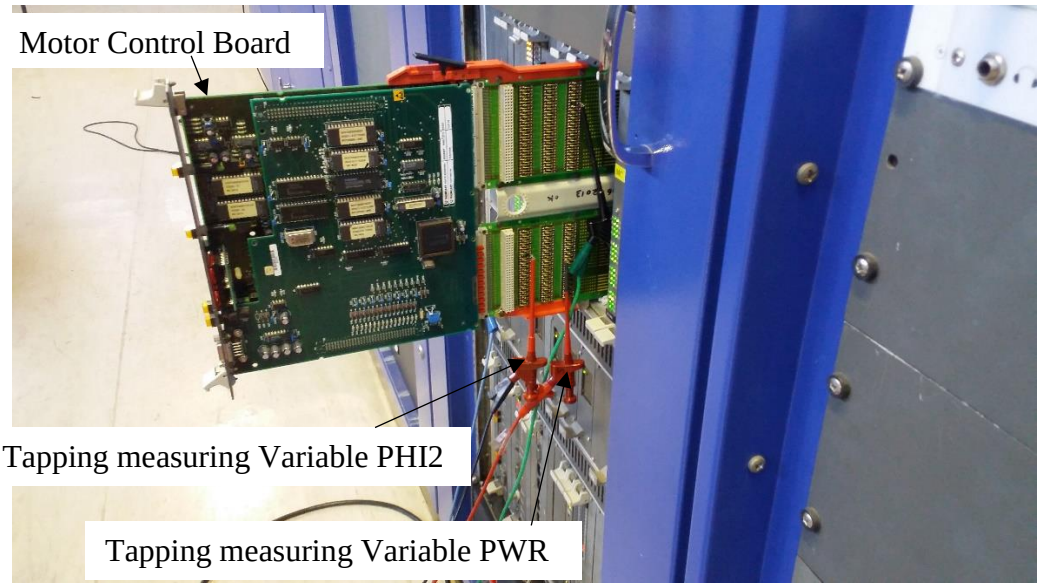

Figure 14: Tapping measuring variables (PHI2 & PWR) from motor control board

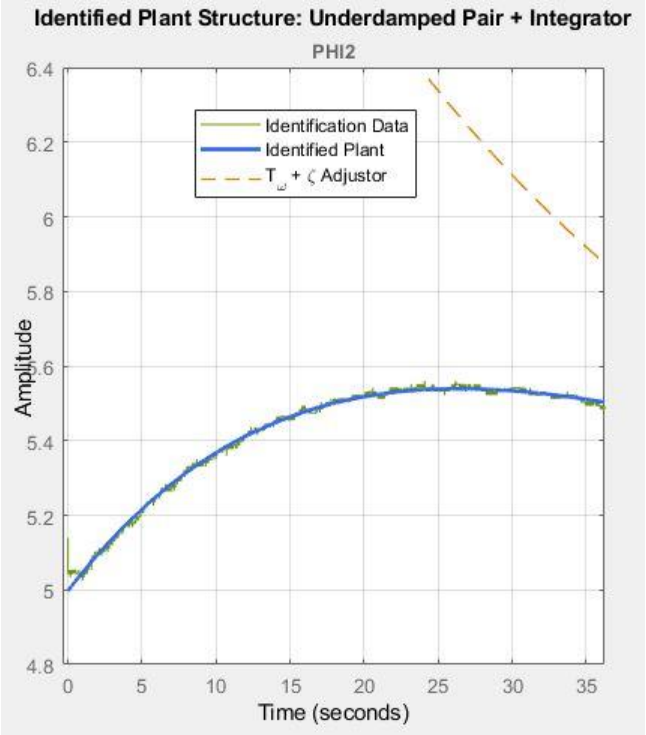

Figure 15: Step Response of PHI2 by Exciting only MP10

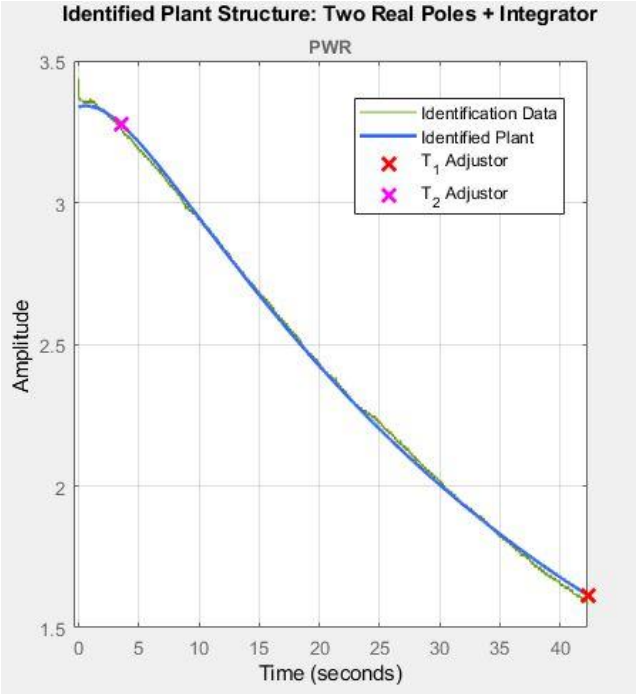

Figure 16: Step Response of PWR by Exciting only MP10

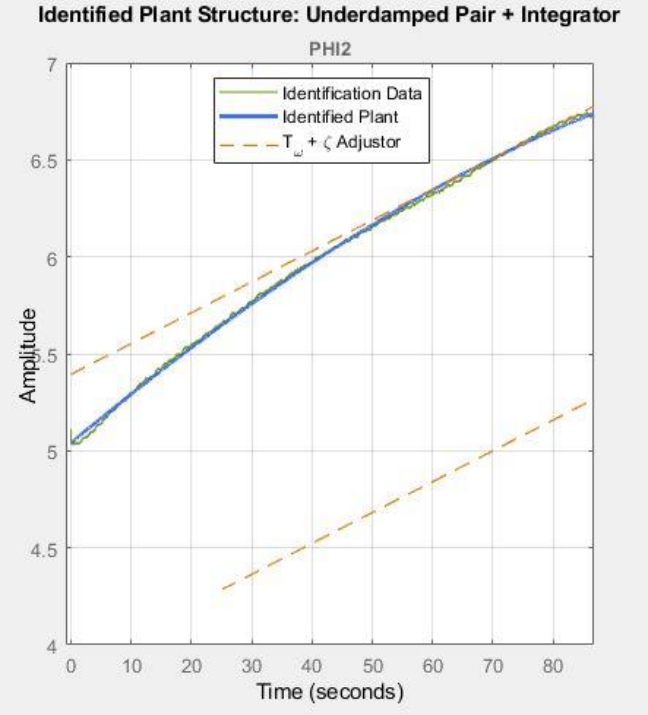

Figure 17: Step Response of PHI2 by Exciting only MP11

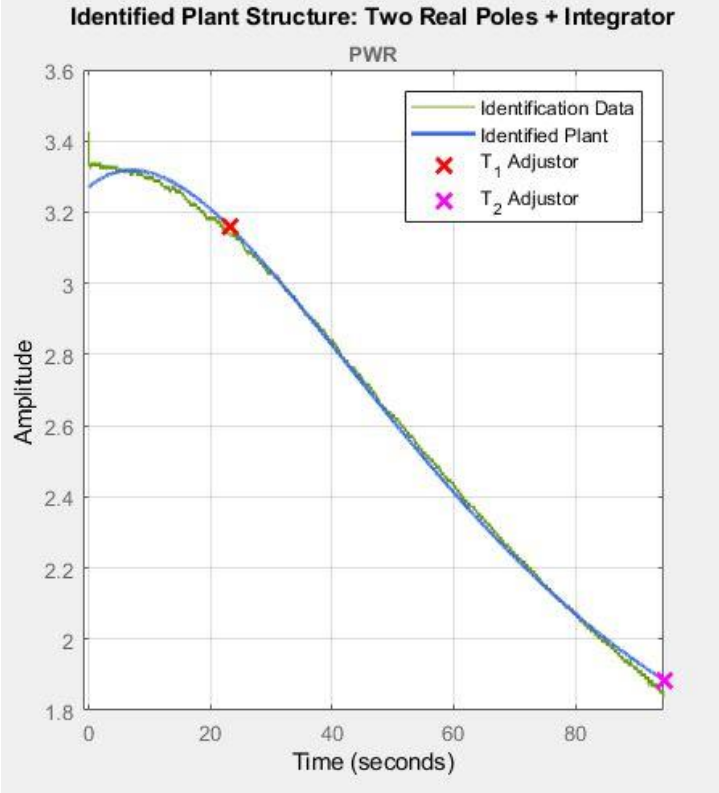

Figure 18: Step Response of PWR by Exciting only MP11

$$\frac{-0.37237}{0.0797 * S^3 + 5.689 * S^2 + S} \quad (20)$$

$$\frac{-0.2018}{6.315 * S^3 + 4.5234 * S^2 + S} \quad (21)$$

$$\frac{0.019761}{301.091 * S^3 + 27.693 * S^2 + S} \quad (22)$$

$$\frac{-0.07345}{16.112 * S^3 + 3.523 * S^2 + S} \quad (23)$$

Four transfer functions are approximated with an integrator by considering the fact that instability nature of step response of a DC motor's position which is directly related to the step response of output variables, PHI2 and PWR.

CHAPTER 4
CONTROL DESIGN

This Chapter discusses a new design approach of a control scheme for the plant mathematically identified in previous chapter. Main goal of the design is to ensure the stability of overall closed loop system which is made of transmitter (plant) and controller to be designed. Section 4.1 explains how identified transfer functions are arranged in a proper configuration to form a TITO plant. Section 4.2 briefly describes proposed control scheme. Section 4.3 illustrates a general design method which guaranties the stability of an overall closed loop system. Section 4.4 specifically focuses on a MIMO and decentralized PID control design method based on results taken in section 4.3. Section 4.5 talks about how H-infinity optimality criterion is embedded in to the results derived in section 4.4.

4.1. Identified Process

Because all identified transfer functions are approximated with an integrator, most of proposed methods and guide lines like Relative Gain Array (RGA) or Extended Relative Gain Array (ERGA) [5], [7] for coupling inputs with outputs can't be used directly and easily. Therefore a manner based on individual responsivities of controlled variables to step inputs is followed to couple inputs and outputs. Figure from 15 to 18 clearly reveal that controlled variable PHI2 has the fastest step response for MP10. Therefore it is logical to couple control input of the MP10's servo amplifier and PHI2. Because the system is TITO, control input of the MP11's servo amplifier is coupled with controlled variable PWR. This configuration is shown in Figure 19. In this selection, control voltage for servo amplifier of MP10 is considered as input variable 1 while input variable 2 becomes the control voltage for servo amplifier of MP11. Output variable 1 is the phase difference, PHI2 and output variable 2 is RF output power, PWR. Figure 19 represents as same input-output relationships as presented by equations from 17 to 20.

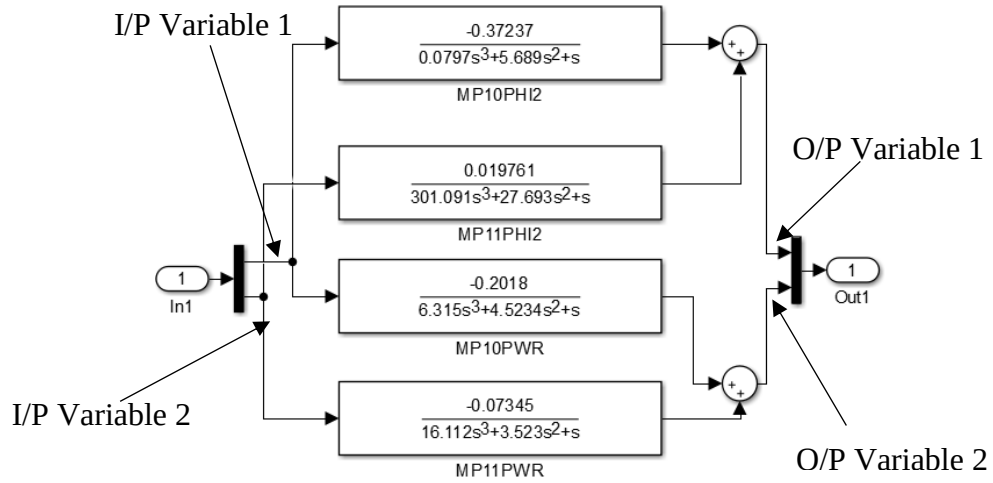

Figure 19: Input-Output coupling Configuration

4.2. Proposed Control Scheme

The proposed control system should ensure the stability time domain performances as we expect. From the point of view of control theory, closed loop poles of the system made by plant and controller must lie on the opened Left Half Plane (LHP) of the complex S- plane, if system is expected to be stabilized. Among various approaches, Static Output Feedback (SOF) method is selected to design the controller as it always ensures the stability of closed loop system. SOF technique is further extended to introduce PID controllers instead of ending the design with only a proportional controller. Finally, H-Infinity optimal control criterion is embedded in proposed controller designed based on SOF technique. Tuning or finding gains of SOF controller is achieved by a Linear Matrix Inequality (LMI) technique. In this section we talk about a generalized SOF stabilization problem and then an iterative LMI algorithm (ILMI) is developed for finding controller's gains. LMI problems can be solved practically, as an iterative algorithm using MATLAB software.

In the next section, results are further evolved to integrate PID controllers and H-Infinity criterion together.

SOF controlling is a major research topic in control engineering. Many researchers are trying to solve various kinds of problems, analytically or numerically. In SOF, control problems are solved by finding static output feedback gains so as expected stability and other performances are achieved. In our design, assumption of Linear Time Invariant (LTI) and constraint of finite dimensional system simplify the design without losing generality. The major benefit of the SOF is its ease of practical realization. Measured variables are directly tapped from the system's outputs. Therefore additional observers are not needed in the design. In this research, measured and regulated variables are same. Recently, many researchers [1], [2], [6], [8], [9], [10], [11], [16] have attempted to derive analytical and numerical solutions for SOF stabilization problems. But, it is obvious to see that most of methods are not easy to implement as numerical algorithms. Therefore, it is not possible to use them in a practical engineering design. This fact directed this research towards to LMI approach because it has many benefits in a process of developing a practical numerical algorithms.

4.3 Stabilization via SOF

Let's consider a finite dimensional and LTI system in state space

$$\dot{x} = Ax + Bu \quad (24)$$

$$y = Cx \quad (25)$$

Here, $x \epsilon R^n$ is the vector of states, $u \epsilon R^r$ is the vector of control inputs and $y \epsilon R^m$ is the vector of system outputs. A, B and C are constant matrices with appropriate dimensions. The main objective of SOF stabilization is to find a feedback constant or constant matrix (for MIMO), F such that

$$u = Fy \quad (26) \qquad \text{Here } F \epsilon R^{r \times m}$$

Then closed loop system can be written by replacing u in (24) from (26), as in (27).

$$\dot{x} = (A + BFC)x \quad (27)$$

If closed loop system is stable, poles of the system represented by (27) must be on opened LHP. We can write this requirement in matrix form by following Lyapunov's stability theorem [12], as shown by (28)

$$(A + BFC)^T P + P(A + BFC) < 0 \quad (28)$$

Here P is any positive definite matrix such that $P = P^T$.

If we define another positive definite matrix which is made of SOF matrix, F and output matrix, C as shown by (29)

$$C^T F^T FC \geq 0 \quad (29)$$

And combine with (28), a new relationship can be obtained as follows in (30)

$$(A + BFC)^T P + P(A + BFC) \leq (A + BFC)^T P + P(A + BFC) + C^T F^T FC \quad (30)$$

Equation (30) can be further rearranged as shown in equation (31)

$$A^T P + PA - PBB^T P + (B^T P + FC)^T (B^T P + FC) < 0 \quad (31)$$

This matrix inequality can be considered as a sufficient condition for the system to be stable. The necessity may be proven as follows.

Let's say system is stable for some SOF matrix F.

From Lyapunov theorem, equation (28) and equation (29) we can derive (34) as follows

$$(A + BFC)^T P + P(A + BFC) < 0 \quad (28)$$

A scalar $\delta > 0$ should exist such that

$$(A + BFC)^T P + P(A + BFC) + \frac{C^T F^T FC}{\delta^2} < 0 \quad (32)$$

$$A^T P + PA - \delta^2 PBB^T P + (\delta B^T P + \frac{FC}{\delta})^T (\delta B^T P + \frac{FC}{\delta}) < 0 \quad (33)$$

Equation (30) can be rearranged as shown in equation (31)

$$\delta^2 A^T P + \delta^2 PA - \delta^4 PBB^T P + (\delta^2 B^T P + FC)^T (\delta^2 B^T P + FC) < 0 \quad (34)$$

It is obvious to see that, $\delta^2 P$ can be replaced by P without losing inequality expressed by (34). Then equation (34) is equivalent to equation (31). Therefore there exists a $P > 0$. This is the necessity for having a stable closed loop system.

Because there are two unknown matrices in their product form, equation (31) can be identified as a Quadratic Matrix Inequality (QMI). If we try to simplify this inequality in to a Linear Matrix Inequality (LMI), minus term $-PBB^TP$ makes the work impossible. Therefore another additional variable X which has as same dimension as P is introduced to solve this matter as shown below.

For any X ,and P

$(X-P)^T BB^T (X-P) \geq 0$ (35) Holds true

By expanding (35), we can obtain (36) as follows

$X^T BB^T P + P^T BB^T X - X^T BB^T X \leq P^T BB^T P$ (36)

If we replace term PBB^TP in equation (31) by equation (36), (37) can be obtained

$A^TP + PA - XBB^TP - PBB^TX + XBB^TX + (B^TP + FC)^T(B^TP + FC) < 0$ (37)

Then another sufficiency can be expressed as, closed loop system is stabilizable via a SOF matrix, F if and only if there exists matrices $P > 0$ and $X > 0$ which satisfy inequality (37).

Inequality (37) can be rearranged as a QMI by using Schur complement as given by (38)

$$\begin{bmatrix} A^TP + PA - XBB^TP - PBB^TX + XBB^TX & (B^TP + FC)^T \\ (B^TP + FC) & -I \end{bmatrix} < 0 \quad (38)$$

It is not difficulty to see that if we set X as a fixed value matrix then inequality (38) becomes a LMI. Then only $P > 0$ and F are the unknown matrix variables to be found. In other hand, they are the solution for equation (31) too.

The necessary condition for closed loop stabilization could be derived by considering a perturbed plant as well [3]. The procedure is described as follows.

Let's perturb state matrix A by an amount of $I\mu$.

Then new state matrix becomes as $A - I\mu$. Here $\mu \geq 0$.

If there exists a feasible solution for equation (31) or (37) which represent a system of state matrix, $(A - BFC)$ the necessary inequality condition can be expressed as in (39)

$$A^T P + PA - XBB^T P - PBB^T X + XBB^T X + (B^T P + FC)^T (B^T P + FC) < \mu P \quad (39)$$

Here solution is $P > 0$ and F . When solution is feasible, matrix $X > 0$ and $\mu \geq 0$ also should exist. More specifically, inequality (39) can be rearranged as in (40).

$$A^T P + PA - \mu P - XBB^T P - PBB^T X + XBB^T X + (B^T P + FC)^T (B^T P + FC) < 0 \quad (40)$$

In a situation where inequality (40) is satisfied, real parts of all eigenvalues of the state matrix $(A - BFC)$ must lie on the left hand side of vertical line which is passing through $Re(s) = \mu$. Then it is obvious to conclude that we can have many solution matrices, F for different values of matrix $X > 0$ and constant $\mu \geq 0$, if solutions are feasible. If we need to have all eigenvalues on the left hand side of any $\mu \geq 0$, it is necessary to repeat the numerical mechanism which is used to solve the inequality, (40) until μ is converged to expected value. The same argument is applied for a system of which state matrix is $(A + BFC)$. In this case μ should be a negative value. Then we have to build a numerical algorithm so that μ is always tried to minimize in each iteration. As a result, real parts of all eigenvalues of matrix $(A + BFC)$ are shifted towards the far left side of negative half of S-plane. By considering all the derivations described so far, an iterated algorithm which can easily be implemented with a computing software like MATLAB is proposed. Algorithm is decomposed in to five steps.

1. For deriving a LMI from QMI given in (40), it is necessary to fix the matrix X with a condition that X must be capable to stabilize the closed loop system of which feedback control gain matrix is $B^T X$. Therefore X can simply be found by solving Continuous time Algebraic Riccati Equation (CARE)

   $$A^T X + XA - XBB^T X + Q = 0$$

   Where Q is any positive definite symmetric matrix ($Q > 0$)

2. The X found in step 1 can easily be used as a fixed value matrix in QMI given by (40). Here SOF matrix F and P should be found while μ is minimized as much as possible. QMI constraint given by (40) can be expressed by using Schur complement as given in (38).

$$\begin{bmatrix} A^T P + PA - XBB^T P - PBB^T X + XBB^T X - \mu P & (B^T P + FC)^T \\ (B^T P + FC) & -I \end{bmatrix} < 0 \quad (41)$$

   Same time, constraint $P = P^T > 0$ should also be considered.

   $$P = P^T > 0 \quad (42)$$

   When X in (41) is fixed, It converts to a LMI.

3. If μ is minimized such that $\mu \leq \mu_{min}$ then acquired F, SOF gain matrix is the solution. μ_{min} is the value to which variable μ is converged. Let's denote the obtained P as P_i (subscript i represents the iteration number)

4. If μ is still greater than μ_{min} , let's say its value is μ_i (subscript i denotes the iteration number), then it means that real parts of some eigenvalues are still right side to the vertical line which is passing through $Re(s) = \mu_{min}$. This situation occurs as a result of matrix P obtained in step 2.

5. The summation of eigenvalues of matrix P is larger than we expect. Therefore, prior to jump next iteration, its eigenvalues must be minimized as much as possible.

   The most convenient way of doing this is to minimize the trace of P by still maintaining the inequalities given in step 2. The value of μ used in this step for inequality (41) is the μ_i which was found in step 2. Let's designate minimized P_i as P_{i_min} .

6. In this step, obtained P_{i_min} is compared with X found in step 1 before jumping to top of the flow of algorithm (step 2). This comparison is accomplished by having 2-norm of the difference between X and P_{i_min} . if $\|X_i - P_{i\_min}\| < \Delta$ (Here Δ is a prescribed tolerance which should be defined at the start of algorithm), a solution doesn't exist in next iteration because eigenvalues of X_i are already smaller than eigenvalues of P_{i_min} for expected tolerance Δ . Otherwise algorithm is continued again from step 2 by setting $i = i + 1$ and $X_i = P_{i-1\_min}$ .Algorithm described by these five steps can be demonstrated by a flow chart as shown in Figure 20.

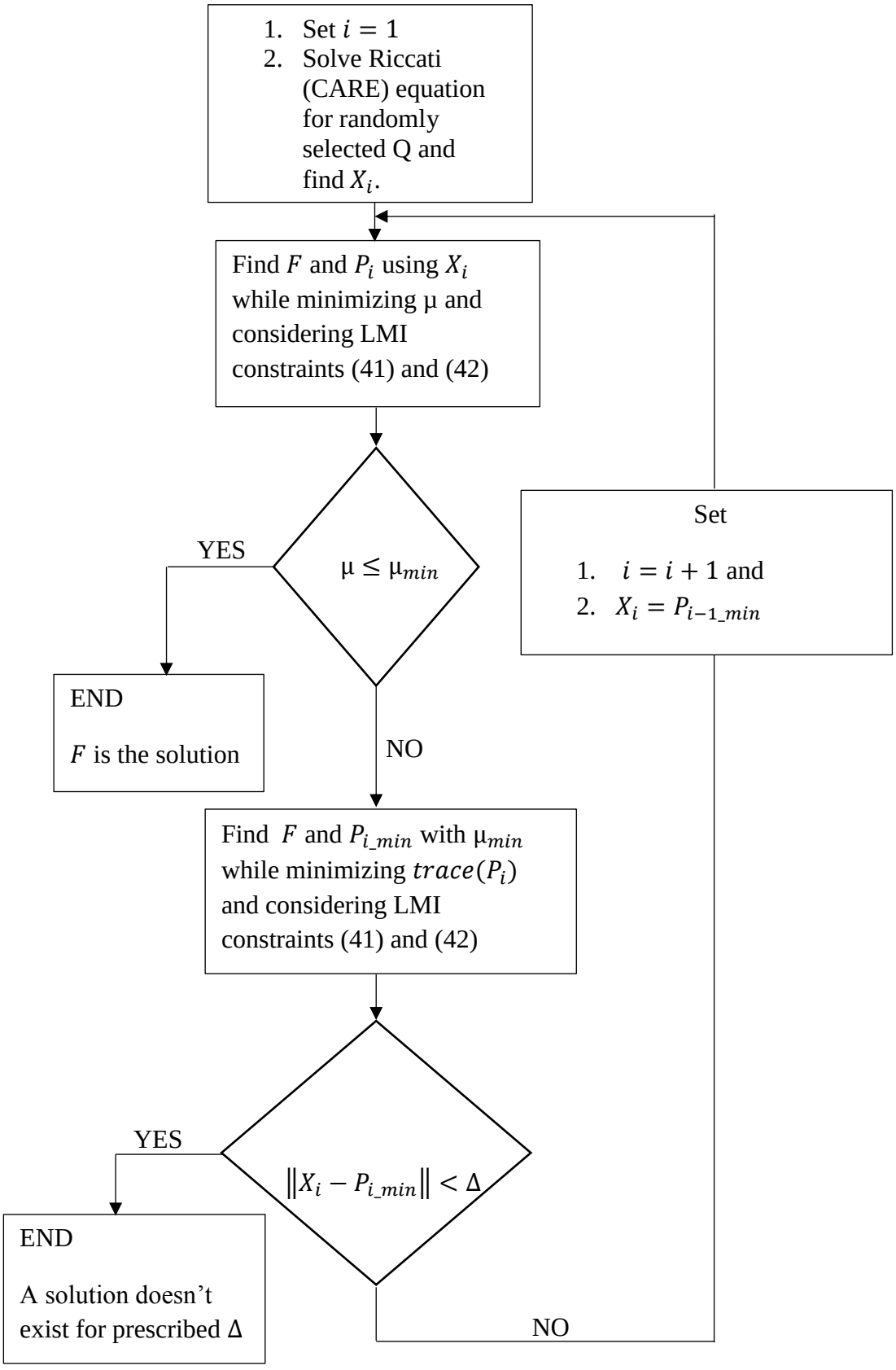

Figure 20: Flow chart of Numerical Algorithm to solve LMI

It should be noted that, time domain performances merely depend on randomly selected matrix Q in step 1. Therefore the algorithm has to be run several times until expected time domain performances are met.

4.4 Stabilization via SOF- Decentralized PID Controllers

Results obtained in previous section can be further developed to introduce decentralized PID controllers in the feedback path. Then flexibility to adjust time domain performances can further be increased. Because our system is a TITO, it is necessary to insert two PID controllers in feedback path formed by two controlled variables. Otherwise or in centralized control scheme, number of PID controllers need to be used is increased up to four. Decentralized two PID controllers must ensure closed loop stability, time domain performances and decoupling of two output variables as we expect. The scenario, decoupling means the internal interaction between two output variables while they are in control.

Let's consider our system in state space domain, represented by (24) and (25)

$$\dot{x} = Ax + Bu \qquad (24)$$

$$y = Cx \qquad (25)$$

If we introduce PID controllers in feedback path then u becomes

$$u = F1y + F2\int_0^t ydt + F3\frac{dy}{dt} \qquad (43)$$

Here, $F1$, $F2$ and $F3$ are diagonal matrices which are to be found by algorithm depicted in Figure 20.

Let's define some other variables as follows

$$z1 = x \qquad (44)$$

$$z2 = \int_0^t ydt \qquad (45)$$

$z = [z1^T, z2^T]^T$ (46)

A new system which is augmented by plant and controller is represented by state vector z in equation (46). It can further be revealed using (44) and (45) as follows

$\dot{z1} = \dot{x} = Az1 + Bu$ (47)

$\dot{z2} = y = Cz1$ (48)

By considering equations from (44) to (48), state space equation for augmented plant can be formulated in terms of original plant's parameters as given in (49).

$\dot{z} = \bar{A}z + \bar{B}u$ (49)

Here, $\bar{A} = \begin{bmatrix} A & 0 \\ C & 0 \end{bmatrix}$ and $\bar{B} = \begin{bmatrix} B \\ 0 \end{bmatrix}$

By differentiating equation (25), we have

$\dot{y} = C\dot{x}$ (50)

If we replace $\dot{x}$ in (50) by (24), we have (51) as follows

$\dot{y} = CAx + CBu$ (51)

x in (51) can be replaced by (44). Then we have (52).

$\dot{y} = CAz1 + CBu$ (52)

But, $z1 = [1\ 0]z$ (53)

If (53) is substituted in (52), we have (54) as follows.

$\dot{y} = [CA\ 0]z + CBu$ (54)

From (45), we can express $\int_0^t ydt$ in term of z as shown in (55).

$\int_0^t ydt = z2 = [0\ I]z$ (55)

From equation (48) we can derive (56) as follows.

$y = Cz1 = [C\ 0]z$ (56)

Because now we have expressions for y , $\dot{y}$ and $\int_0^t ydt$, it is possible to obtain an expression for control effort u in term of z by substituting (54), (55) and (56) in to (43) as shown by (57).

$$u = F1y + F2\int_0^t ydt + F3\frac{dy}{dt} \qquad (43)$$

$$u = F1[C\ 0]z + F2[0\ I]z + F3([CA\ 0]z + CBu)$$

$$u - F3CBu = F1[C\ 0]z + F2[0\ I]z + F3[CA\ 0]z$$

$$u = (I - F3CB)^{-1}(F1[C\ 0] + F2[0\ I] + F3[CA\ 0])z \qquad (57)$$

Here an assumption is made that $(I - F3CB)$ is invertible. Then it is obvious to see that control effort u is expressed in term of z which is the output of new augmented plant. Let's define another three new variables for augmented plant.

$$\bar{C}1 = [C\ 0] \qquad (58)$$

$$\bar{C}2 = [0\ I] \qquad (59)$$

$$\bar{C}3 = [CA\ 0] \qquad (60)$$

Then equation (57) can be expressed by using new variables defined in above three equations (58), (59) and (60) as given in (61).

$$u = F1\bar{C}1z + F2\bar{C}2z + F3\bar{C}3z + F3CBu \qquad (61)$$

If we rearrange equation (61) by introducing $\bar{y}_i$ ($i = 1,2,3$) such that

$$\bar{y}_i = \bar{C}_i z \qquad (62)$$

$$u = F1\bar{y}_1 + F2\bar{y}_2 + F3\bar{y}_3 + F3CBu \qquad (63)$$

Then composite matrices for augmented system can be defined as follows.

$$\bar{C} = [\bar{C}1^T\ \bar{C}2^T\ \bar{C}3^T]^T \qquad (64)$$

By considering (54)

$$\bar{F}1 = (I - F3CB)^{-1}F1 \qquad (65)$$

$$\bar{F}2 = (I - F3CB)^{-1}F2 \qquad (66)$$

$$\bar{F}3 = (I - F3CB)^{-1}F3 \qquad (67)$$

$$\bar{F} = [\bar{F}1 \ \bar{F}2 \ \bar{F}3] \qquad (68)$$

Then, closed loop augmented system which comprises two PID controllers and plant, can be represented in state space domain as given by equations (49) and (69). Therefore the algorithm depicted in Figure 20 can be used to find composite PID gain matrix $\bar{F}$ without any difficulty.

$$\dot{z} = \bar{A}z + \bar{B}u \quad (49)$$

$$\bar{y} = \bar{C}z \qquad (69)$$

$$u = \bar{F}\bar{y} \qquad (70)$$

It is straightforward to find original gain matrices $F1$, $F2$ and $F3$ of two PID controllers once the composite matrix $\bar{F}$ is found. Corresponding results can be obtained by solving equations (65), (66) and (67) as given in equations (71), (72) and (73).

$$F3 = \bar{F}3(I + CB\bar{F}3)^{-1} \qquad (71)$$

$$F2 = (I - F3CB)^{-1}\bar{F}2 \qquad (72)$$

$$F1 = (I - F3CB)^{-1}\bar{F}1 \qquad (73)$$

Here, both matrices $(I + CB\bar{F}3)$ and $(I - F3CB)$ should be invertible. If and only if $(I + CB\bar{F}3)$ is invertible, $(I - F3CB)$ becomes invertible. Therefore checking the invertible nature of only $(I + CB\bar{F}3)$ matrix reveals the existing of PID gain matrices as solutions. This necessity is known as well-posedness of PID feedback controllers. Meanwhile the algorithm is run, it is necessary to avoid the singularity nature of matrix $(I + CB\bar{F}3)$ for ensuring the well-posedness. Therefore inequality constraint $I + CB\bar{F}3 + (CB\bar{F}3)^T > 0$ can be added to the step 2 and 4 of the algorithm depicted in Figure 20, in addition to the constraints which are already considered in the algorithm, or the invertible nature can be checked at end of each iteration.

In algorithm that we propose in this research work, post checking approach is selected as complexity of the algorithm and hence processing power and time to have the final solution are decreased in a considerable amount. Decentralized PID controllers can be obtained by explicitly making the off diagonal elements of gain matrices to zero.

4.5 H-infinity Suboptimal Controlling via SOF- Decentralized PID Controllers

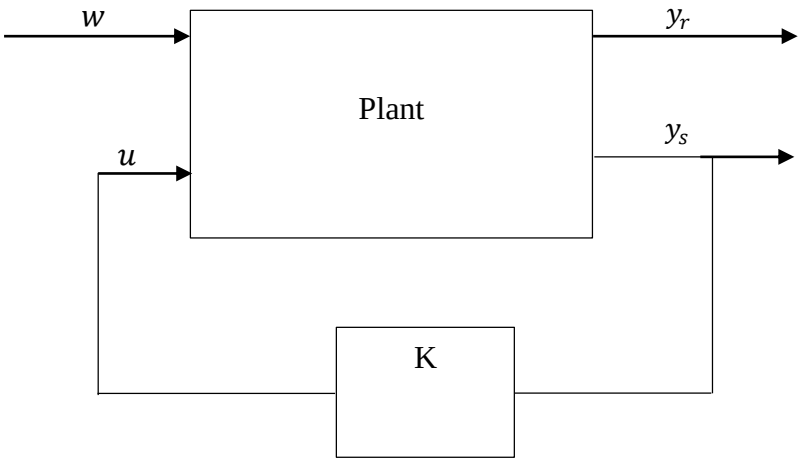

Figure 21: Closed loop, controller and plant with exogenous inputs

4.5.1 H-infinity Suboptimal Control Concept

The major expectation of embedding the H-infinity suboptimal criterion to the controller is giving the strength of robust control performances like immune to external disturbances, noises and model errors. Moreover, internal interactions between two main feedbacks loops can also be minimized as influence from other loop to a particular loop acts as a disturbance. Referring to Figure 21, w represents exogenous (external) control inputs which are not directly manipulated by controller. u is manipulated input to the plant. u is calculated by controller considering sensed or measured outputs y_s . y_r is regulated output of the plant. These outputs are considered to be controlled by controller, K. The motivation of H-infinity optimization is to reduce the energy transformation from undesired inputs to regulated outputs [4], [23].

Then the effect of exogenous input w on the regulated output y_r must be minimized as much as possible. Mathematically, this idea can be represented by H-infinity norm of the transfer function between undesired input and regulated output as follows

$$\left\|T_{wy_r}\right\|_\infty < \gamma \qquad (74)$$

Here, T_{wy_r} is the transfer function between w and y_r . $\|\,.\,\|_\infty$ represents the H-infinity operator and $\gamma > 0$ is a constant which is known as performance index. The physical meaning of H-infinity operator is to measure the power of some signal. Therefore the left side of (74) really measure the amplification or ability to represent the effect of unwanted input on regulated output. In our case, as both regulated outputs are measured for making feedback loops, regulated and measured variables are same ($y_r = y_s$). Mathematically, physical interpretation of $\|\,.\,\|_\infty$ can be expressed as a bound on the energy throughput as given by (75) [4].

$$\|y_r\|_2 \leq \left\|T_{wy_r}\right\|_\infty \|w\|_2 \quad (75)$$

Let's consider a simple plant which transfers the exogenous input $w(t)$ to an output $z(t)$

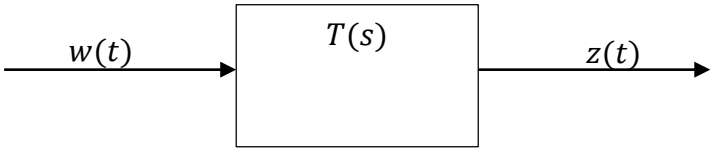

Figure 22: Relationship between only exogenous input and regulated output

If state space realization of this plant is expressed as given by (76) and (77)

$$\dot{x} = Ax + Gw \qquad (76)$$

$$z = Hx \qquad (77)$$

The bounded-real lemma can be obtained by considering (75) as shown by (78) [4]. The system is bounded real if and only if there exists a matrix $P > 0$ such that

$$\begin{bmatrix} (A^TP + PA + H^TH) & PG \\ G^TP & -I \end{bmatrix} < 0 \qquad (78)$$

In any case, if equations (75) and (74) both hold true, inequality given by (79) must also hold true.

$$\emptyset(j\omega) > 0 \qquad \forall\, \omega \in \mathbb{R} \quad (79)$$

The definition of $\emptyset(j\omega)$ is given by (77)

$$\emptyset(s = j\omega) = \gamma^2 I - T^T(-s)T(s) \qquad (80)$$

Equation (79) and (80) represent as same meaning as (74) does. $T^T(-s)T(s)$ is equivalent to the magnitude of transfer function for a particular $s = j\omega$ on the imaginary axis. Considering bounded real lemma given by (78), we can express that any matrix variable $X > 0$ should exist such that it satisfies inequality (81) [4].

$$\begin{bmatrix} (A^T X + XA + H^T H) & XG \\ G^T X & -\gamma^2 I \end{bmatrix} < 0 \quad (81)$$

When (74) and (81) hold true, Hamiltonian matrix, M_γ may have eigenvalues anywhere in complex plane except on pure imaginary axis.

$$M_\gamma = \begin{bmatrix} A & \frac{GG^T}{\gamma^2} \\ -H^T H & -A^T \end{bmatrix} \in \mathbb{R}^{2n \times 2n} \quad (82) \quad 2n \text{ is number of states of the system}$$

If $\gamma > 0$, eigenvalues of M_γ can clearly be divided into two groups. A set of eigenvalues is placed in open LHP while other set would be its mirror image on the opened Right Half Plane (RHP). If we process the M_γ using a similarity transformation method, then two sets of eigenvalues can be separated as shown below.

$$J^{-1} M_\gamma J = -J M_\gamma J = -{M_\gamma}^T \quad (83)$$

Here

$$J = \begin{bmatrix} 0 & I \\ -I & 0 \end{bmatrix} = -J^{-1} \qquad (84)$$

Then symmetric spectrum of eigenvalues can be expressed as

$$|sI - M_\gamma| = |sI + M_\gamma| \qquad (85)$$

From (85), it shows that eigenvalues are separated each other. Therefore Eigen spaces should also be separated. We can extract stable eigenvalues of M_γ by introducing basis eigenvectors V_s and V_u as follows

$$M_\gamma[V_s\ V_u] = [V_s\ V_u]\begin{bmatrix}\lambda_s & 0\\ 0 & \lambda_u\end{bmatrix} \quad (86)$$

Here, λ_s and λ_u are diagonal square matrices of which diagonal elements are the stable and unstable eigenvalues of M_γ respectively. If we further partition the eigenvector $[V_s\ V_u]$ as shown by (87). Here, we assume that $|V_{s1}| \neq 0$.

$$[V_s\ V_u] = \begin{bmatrix}V_{s1} & V_{u1}\\ V_{s2} & V_{u2}\end{bmatrix} \quad (87)$$

Let's introduce another matrix variable P such that

$$P = V_{s2}{V_{s1}}^{-1} \qquad (88)$$

From (83), we can write

$$M_\gamma V_s = V_s\lambda_s \qquad (89)$$

By substituting (87) into (89), and considering only stable space, we have

$$M_\gamma \begin{bmatrix}V_{s1}\\ V_{s2}\end{bmatrix} = \begin{bmatrix}V_{s1}\\ V_{s2}\end{bmatrix}\lambda_s \qquad (89)$$

If both side of (89) is multiplied by ${V_{s1}}^{-1}$

$$M_\gamma \begin{bmatrix}V_{s1}\\ V_{s2}\end{bmatrix}{V_{s1}}^{-1} = \begin{bmatrix}V_{s1}\\ V_{s2}\end{bmatrix}\lambda_s{V_{s1}}^{-1} \quad (90)$$

If we rearrange (90) as shown by (91)

$$M_\gamma \begin{bmatrix}V_{s1}\\ V_{s2}\end{bmatrix}{V_{s1}}^{-1} = \begin{bmatrix}V_{s1}\\ V_{s2}\end{bmatrix}{V_{s1}}^{-1}V_{s1}\lambda_s{V_{s1}}^{-1} \quad (91)$$

And defining $A_c = V_{s1}\lambda_s{V_{s1}}^{-1}$, we can write (91) by substituting (88) as given by (92)

$$M_\gamma \begin{bmatrix}I\\ P\end{bmatrix} = \begin{bmatrix}I\\ P\end{bmatrix}A_c \qquad (92)$$

Now (82) is substituted in (92) for having (93)

$$\begin{bmatrix} A & \frac{GG^T}{\gamma^2} \\ -H^TH & -A^T \end{bmatrix} \begin{bmatrix} I \\ P \end{bmatrix} = \begin{bmatrix} I \\ P \end{bmatrix} A_c \quad (93)$$

Equation (93) reveals that

$$A + \frac{GG^T}{\gamma^2} P = A_c \quad (94)$$

$$-H^TH - A^TP = PA_c \quad (95)$$

If term A_c is eliminated from (95) and (94) we have (96)

$$A^TP + PA + P\frac{GG^T}{\gamma^2}P + H^TH = 0 \quad (96)$$

This equation can be identified as Continuous time Algebraic Riccati Equation (CARE), the same one we have already considered in SOF and SOF with PID controllers. This equation has many solutions while only one can stabilize the system. Anyway, equation (96) is a quadratic one because third term has two P matrices. Related QMI can be expressed as

$$A^TP + PA + P\frac{GG^T}{\gamma^2}P + H^TH < 0 \quad (97)$$

Quadratic nature of (97) can be eliminated by having its Schur complement as follows

$$\begin{bmatrix} (A^TP + PA + H^TH) & PG \\ G^TP & -\gamma^2 I \end{bmatrix} < 0 \quad (98)$$

This is the corresponding LMI related to H-infinity suboptimal control criterion.

4.5.2 Extending the H-infinity Suboptimal Control Concept for SOF-PID

Let's consider the augmented plant as given by equation (49) and (69)

$\dot{z} = \bar{A}z + \bar{B}u$ (49)

Here, $\bar{A} = \begin{bmatrix} A & 0 \\ C & 0 \end{bmatrix}$ and $\bar{B} = \begin{bmatrix} B \\ 0 \end{bmatrix}$

$\bar{y} = \bar{C}z$ (69)

$\bar{C}$ is given by (58), (59), (60) and (64). If we write dynamics of the system by considering exogenous unwanted inputs, w

$\dot{z} = \bar{A}z + \bar{B}1w + \bar{B}2u$ (99)

$\bar{y}_s = \bar{C}_s z$ (100)

$\bar{y}_r = \bar{C}_r z + \bar{D}u$ (101)

$u = \bar{F}\bar{y}_s$ (102)

In our case, $\bar{C}_s = \bar{C}_r$ and $\bar{D} = 0$. Therefore (100) and (101) are equivalent and equal to (69). Then system dynamics can finally be represented by (69) and (99).

$\dot{z} = \bar{A}z + \bar{B}1w + \bar{B}2u$ (99)

$\bar{y} = \bar{C}z$ (69)

$\bar{B}1$ in (99) represents exogenous input matrix while $\bar{B}2$ is the manipulated input variable matrix. Exogenous inputs represent the low frequency disturbances which may appear with actuators, and high frequency noises which may mix with measured outputs, PHI2 and PWR. By considering the augmented closed loop plant which is represented by (49) and (69), QMI (97) can be written as in (103).

$$(\bar{A} + \bar{B}2\bar{F}\bar{C})^T P + P(\bar{A} + \bar{B}2\bar{F}\bar{C}) + \frac{P\bar{B}1\bar{B}1^T P}{\gamma^2} + \bar{C}^T\bar{C} < 0 \quad (103)$$

Here $(\bar{A} + \bar{B}2\bar{F}\bar{C})$ is state matrix of closed loop system. This inequality is also a QMI as it contains two P matrices in third term. Therefore (103) can easily be converted to a form of LMI by having Schur complement as shown in (104).

$$\begin{bmatrix} (\bar{A} + \bar{B}2\bar{F}\bar{C})^T P + P(\bar{A} + \bar{B}2\bar{F}\bar{C}) & P\bar{B}1 & \bar{C}^T \\ \bar{B}1^T P & -\gamma^2 I & 0 \\ \bar{C} & 0 & -I \end{bmatrix} \quad (104)$$

If we consider an augmented plant which is perturbed by μI ($\mu \geq 0$), state matrix becomes $\bar{A} - \mu I$ .Then (103) can be written by following derivation given by (39)

$$(\bar{A} + \bar{B}2\bar{F}\bar{C})^T P + P(\bar{A} + \bar{B}2\bar{F}\bar{C}) + \frac{P\bar{B}1\bar{B}1^T P}{\gamma^2} + \bar{C}^T\bar{C} < \mu P$$

$$(\bar{A} + \bar{B}2\bar{F}\bar{C})^T P + P(\bar{A} + \bar{B}2\bar{F}\bar{C}) + \frac{P\bar{B}1\bar{B}1^T P}{\gamma^2} + \bar{C}^T\bar{C} - \mu P < 0 \quad (105)$$

This QMI can be converted to a LMI by having its Schur complement as follows

$$\begin{bmatrix} \Sigma & P\bar{B}1 & \bar{C}^T & (\bar{B}2^T P + \bar{F}\bar{C})^T \\ \bar{B}1^T P & -\gamma^2 I & 0 & 0 \\ \bar{C} & 0 & -I & 0 \\ (\bar{B}2^T P + \bar{F}\bar{C}) & 0 & 0 & -I \end{bmatrix} < 0 \quad (106)$$

Here

$$\Sigma = \bar{A}^T P + P\bar{A} - X\bar{B}2\bar{B}2^T P - P\bar{B}2\bar{B}2^T X + X\bar{B}2\bar{B}2^T X - \mu P$$

The same algorithm depicted in Figure 20 can be used to find $\bar{F}$ and hence $F1$, $F2$ and $F3$, by considering LMI (106) and (42). Then modified algorithm after introducing additional LMI constraints for solving a MIMO, SOF-PID with H-infinity optimality criterion can be depicted by a flow chart as shown in Figure 23. The CARE used with this algorithm should only deal with manipulated control inputs matrix $\bar{B}2$. Therefore it should like as follows

$$\bar{A}^T X + X\bar{A} - X\bar{B}2\bar{B}2^T X + Q = 0 \quad (107)$$

As same definitions as in step 1 of the algorithm depicted by figure 20 are still valid for Q and X.

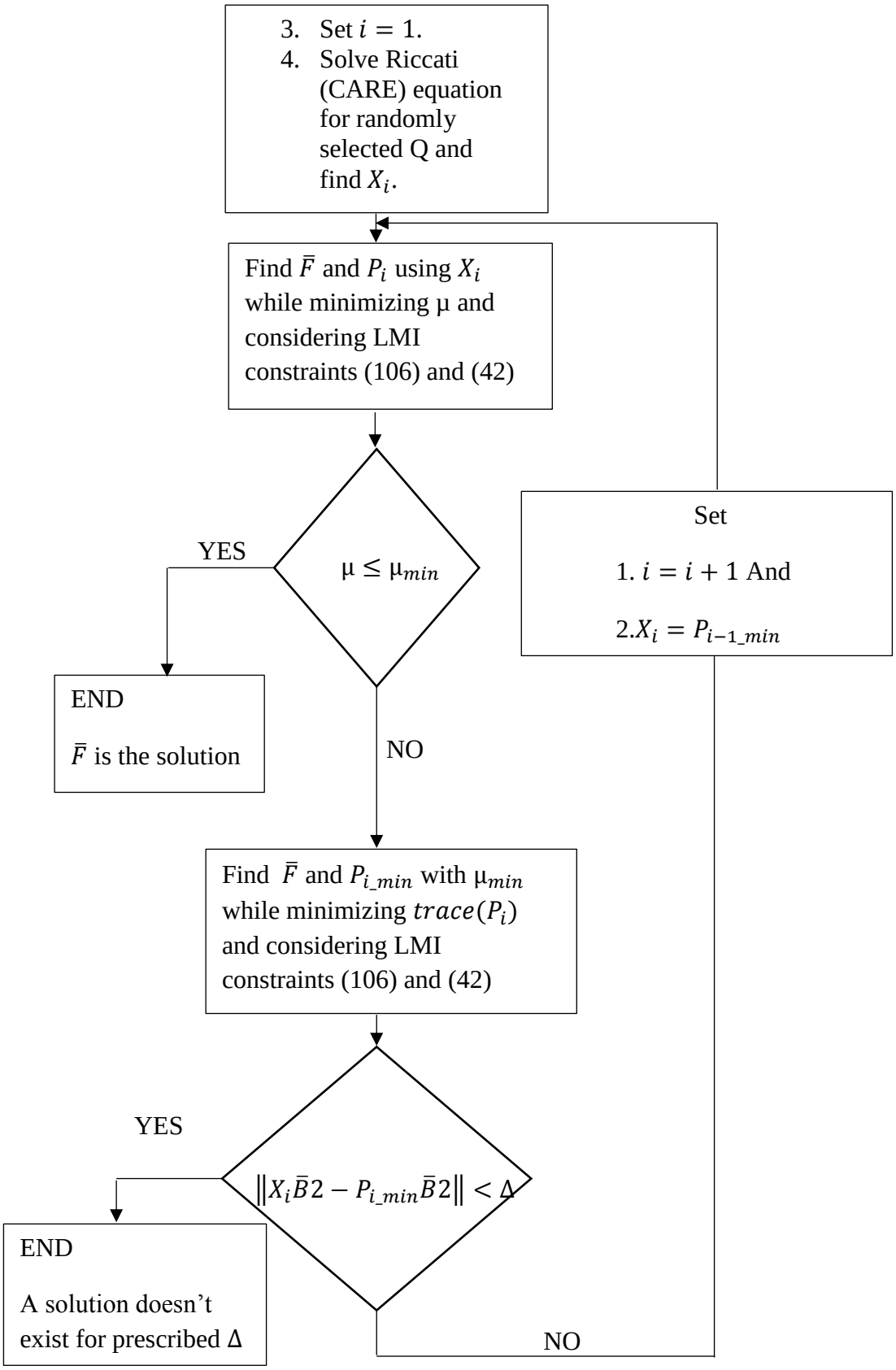

Figure 23: Flow chart of Numerical Algorithm to solve LMI for H-infinity Criterion

Algorithm given in Figure 23 is implemented in MATLAB software. A convex optimization solver called MOSEK [24] is used to solve LMIs given in (42) and (106). Algorithm is run for different values of randomly selected symmetric matrix Q. Time domain performances like percentage of overshoot/undershoot, settling time and steady state error mainly depend on this matrix. However, for any solution, $\bar{F}$ given by this algorithm is capable to stabilize the augmented plant. Therefore algorithm is run several times until time domain response reaches expected performances. Each result of $\bar{F}$ is tested in MATLB-SIMULINK prior to implement the hardware. Step response of the augmented plant is inspected to select the best collection of PID gains. But in the real plant, two controlled variables PHI2 and PWR don't follow their set points by starting from zero as in simulation. When fine tuning of final RF stage is started by the transmitter's main control system, two controlled variables are already around their nominal or set values. Therefore, settling time of actual plant is always lower than it is in simulation. MATLAB code of algorithm is given in Appendix 'B'. Simulation diagram of the closed loop system without disturbance and noise effects is depicted in Figure 24. An acceptable set of PID gain matrices which simulate expected time domain performances are listed by (108), (109) and (110). Algorithm is run for initial parameters $\Delta = 0$ and $\gamma = 10$.

$$F1 = \begin{bmatrix} 1.2491 & 0 \\ 0 & 1.5108 \end{bmatrix} \quad (108)$$

$$F2 = \begin{bmatrix} 0.0352 & 0 \\ 0 & 0.0066 \end{bmatrix} \quad (109)$$

$$F3 = \begin{bmatrix} 5.0805 & 0 \\ 0 & 6.2034 \end{bmatrix} \quad (110)$$

Here, $F1$ is proportional gain matrix, $F2$ is integral gain matrix and $F3$ is derivative gain matrix. Simulation results, step response of output and variation of control efforts will be discussed in Chapter 6, Results and Conclusion.

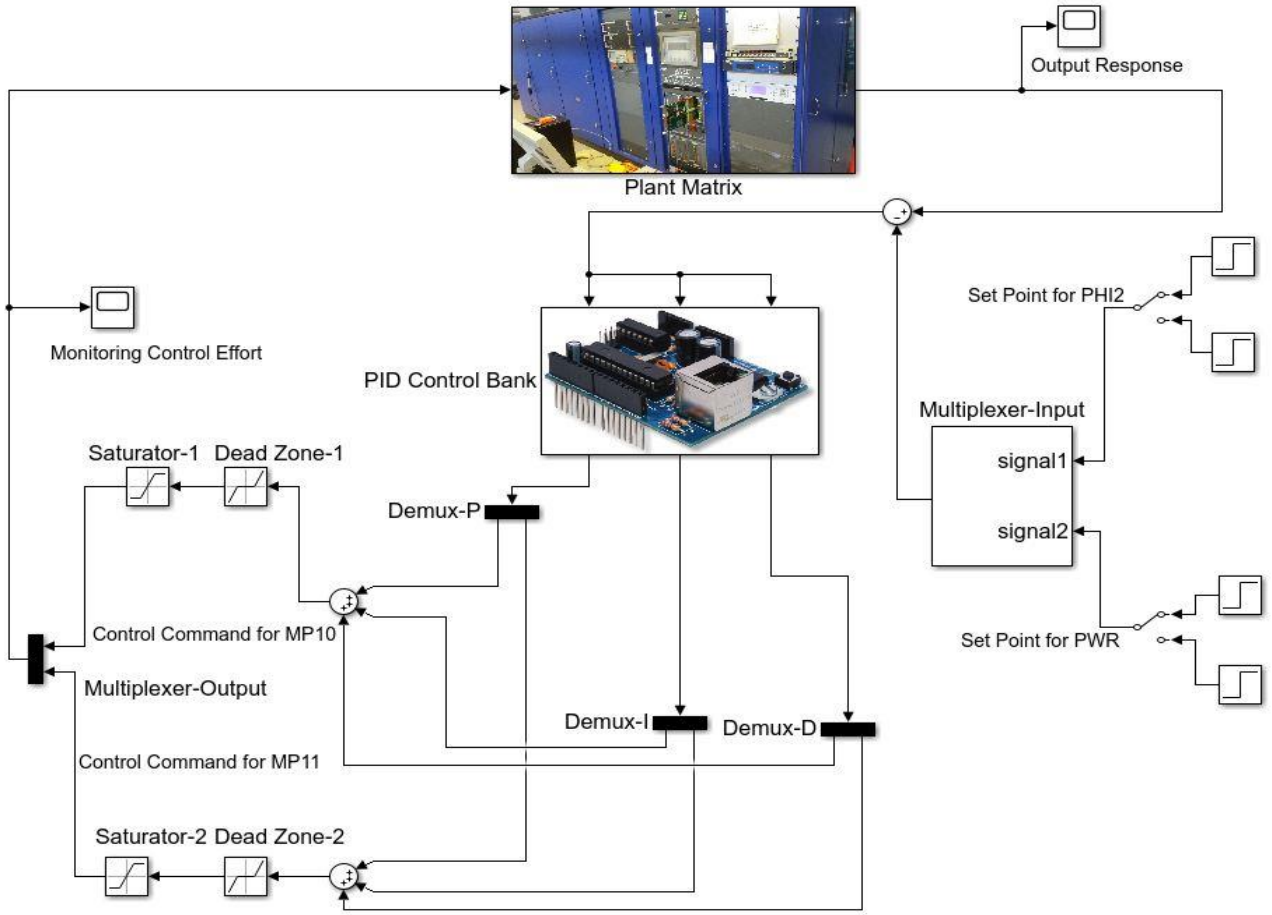

Figure 24: MATLAB – Simulink Diagram of Closed Loop Plant

CHAPTER 5
IMPLEMENTATION

This chapter discusses a convenient method to implement a hardware setup for testing proposed controller designed in previous chapter. Complete setup comprises a data acquisition and processing part supported by a linear analog circuit part. Section 5.1 clearly describes the way of replacing the existing fine tuning algorithm by developed hardware. Section 5.2 explains a method how proposed controller can be embedded in ATMEL MEGA-328P, high speed microcontroller [25] which is coming with an Arduino developing plat form. Section 5.3 presents a way of using existing hardware itself to finalize the design attractively.

5.1 Replacing Existing Hardware

The existing controller is placed between measured variables, PHI2, PWR and control voltages of two servo amplifiers (Figure 10). According to the manufacturer's design, fine tuning algorithm of final RF stage is activated at the end of the overall tuning procedure. Meanwhile tuning process, fine tuning of RF driver stage is working as well. Because we are dealing with only fine tuning of final RF stage, its coarse tuning and tuning of RF driver stage shouldn't be interrupted. Motor control commands of both, fine tuning and coarse tuning are issued through a same output port of existing motor control board. Therefore it is necessary to disconnect servo amplifiers from existing motor control board at the very beginning of fine tuning. Then input ports of two servo amplifiers are connected to output ports of proposed controller. This configuration is maintained until transmitter is retuned to another frequency as it needs to run the coarse tuning. This interchange of connections is accomplished with helps of transmitter's main control section and a single switching relay device. This methodology can be depicted as in Figure 25.

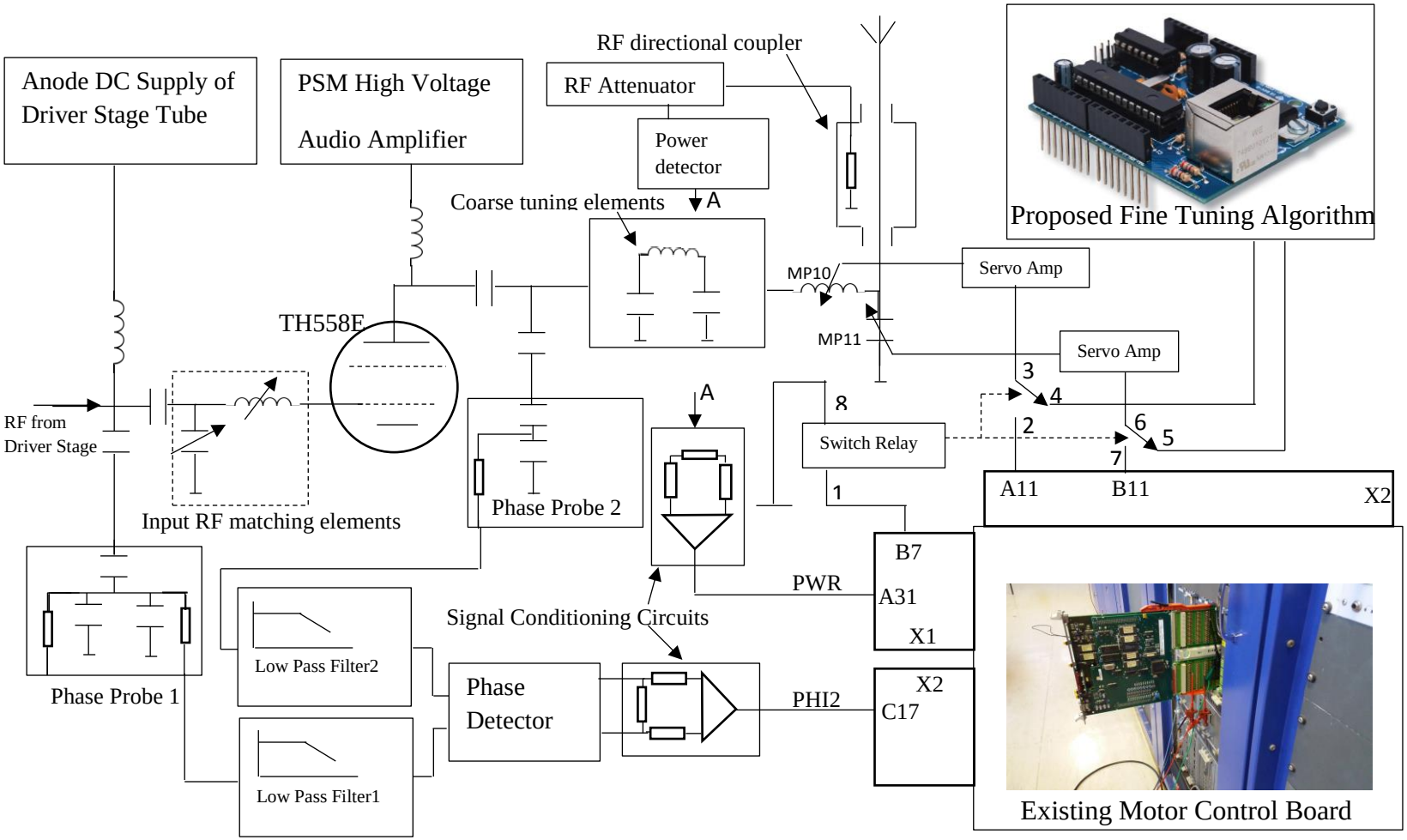

Figure 25: The Way of Introducing Proposed Controller to Plant

Existing motor control board has two plugin terminals designated as X1 and X2. Each terminal has 96 input/output pins via which different kind of electrical signals are coming in to the board and going out from the board. How these two terminals are presence with the board is shown in Figure 26.

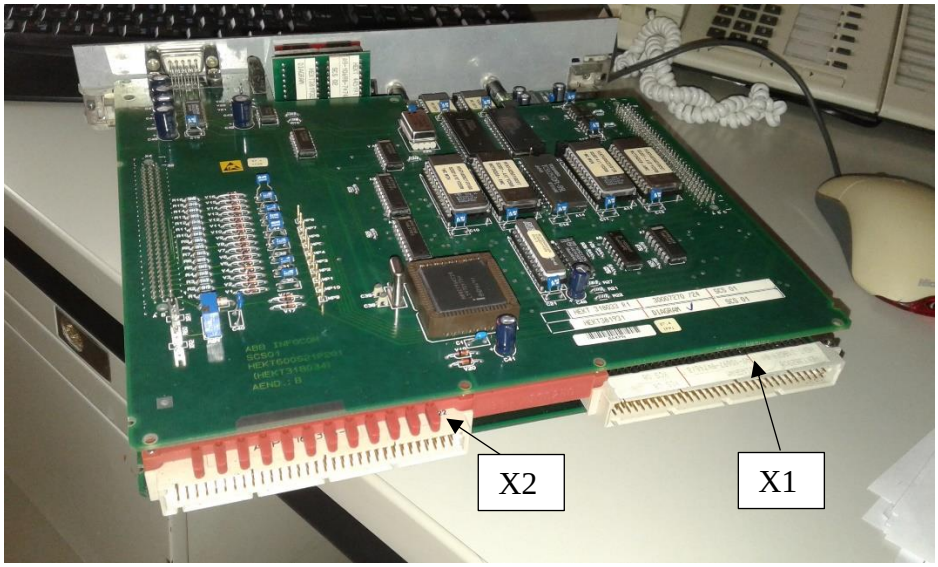

Figure 26: Two Input/output Terminals of Motor Control Board

96 pins belong to a one terminal are again divided in to three sub classes named A, B and C. Measured variable PWR is coming in to the board through X1/A31 pin while PHI2 is coming through X2/C17 pin. This is clearly shown in Figure 25 .These two signals are tapped by connecting an extending plugin board as shown in Figure 14 and Figure 25. Then those measured variables are fed as inputs to the proposed controller. Two control commands for servo amplifiers of MP10 and Mp11 are going out through X2/A11 and X2/B11 respectively. Because these two output pins are used themselves in coarse tuning too, it is not possible to connect servo amplifiers with proposed controller directly. That is why, a switching relay is employed to interchange the control commands for servo amplifiers from existing motor control board to proposed controller when fine tuning is going to be started. A 24V DC voltage is issued via X1/B7 from existing motor control board to the main control section of transmitter as an acknowledgement to confirm whether coarse tuning is achieved successfully.

This 24V signal itself is used in our design to interchange two controllers. A relay designated as G2R-2, a product of Omron [26] is employed as the interchanger. Its operating voltage is 24V DC and power consumption of activating coil is around 0.5W which is less than the maximum power handling capability of the sub circuitry connected to X1/B7. Therefore relay can be powered directly using this acknowledgement signal. This relay is shown in Figure 27.

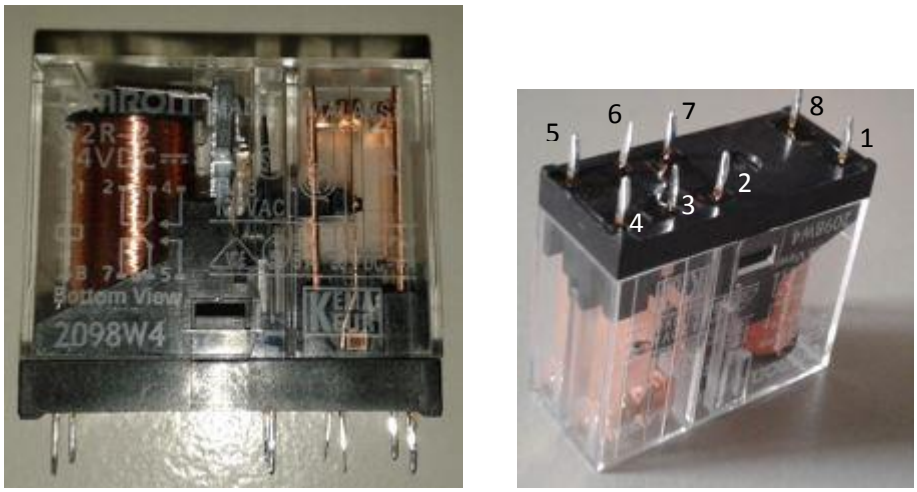

Figure 27: The Switching Relay Used as Controller's Changeover

The numbers marked in Figure 27 represent the pin numbers designated by manufacturer of relay. 24V DC coil supply is given across pin 1 and pin 8. Pin numbers 2, 3 and 6, 7 are normally closed (NC) contacts while pin numbers 3, 4 and 5, 6 are normally opened (NO) contacts. Therefore, relevant pins are connected within the proposed circuit as shown in Figure 25. After two parameters, PHI2 and PWR are optimized or at end of the fine tuning, acknowledgement signal issued through X1/B7 is set to 0V by existing motor control board. Then switching relay is deactivated and hence outputs of existing motor control board, X2/A11 and X2/B11 are again connected with two relevant servo amplifiers. Therefore it ensures the coarse tuning motor control commands are handled by existing motor control board while fine tuning commands are manipulated by the proposed controller.

5.2 Programing ATMEL MEGA 328P for Decentralized PID Controllers

The most convenient way of implementing the closed loop decentralized PID controller which guarantees the stability of augmented plant and expected time domain performances is to synthesize it using a discrete microcontroller. The origin of our design is based on a continuous time LTI system. Therefore, the design should be reconsidered in discrete time domain as microcontroller doesn't process continues signals. The high speed microcontroller, ATMEL MEGA-328P which has as same characteristics as microcontroller, INTEL 80C196KC20 [28] used in existing motor control board owns, is selected to synthesize proposed controller. MATLAB simulation results of two continuous time PID controllers of which gains are found by ILMI algorithm given in figure 23, confirm our all expectations. Therefore it is reasonable to convert only the controller in to discrete domain by using finite difference and backward difference approximations [27]. The outputs of two continuous time PID controllers can be formulated in's' domain by having the gain values from (108), (109) and (110) as given by (111) and (112) [5].

$$P_1(s) = 1.2491E_1(s) + \frac{0.0162}{s}E_1(s) + 2.2805.s.E_1(s) \quad (111)$$

$$P_2(s) = 1.5108E_2(s) + \frac{0.0616}{s}E_2(s) + 3.9334.s.E_2(s) \quad (112)$$

The relationship between s and z can be expressed as in (113)

$$z^{-1} = e^{-s*\Delta t} \qquad (113)$$

By expanding the right side of (113) using Taylor's series, we have

$$z^{-1} = e^{-s*\Delta t} = 1 - (s.\Delta t) + \frac{s^2.\Delta t^2}{2!} + \cdots \qquad (114)$$

By considering the fact that sampling time Δt is so small such that the values of Δt^2 and its higher order terms are negligible compared with first two terms of right side of (113), equation is reasonable to approximate as in (114)

$$z^{-1} = e^{-s*\Delta t} = 1 - (s.\Delta t) \qquad (115)$$

(114) Can be rearranged to have an expression for s

$$s \cong \frac{1 - z^{-1}}{\Delta t} \qquad (114)$$

Equations (111) and (112) are discretized when (114) is substituted in them. Relevant equations are given in (115) and (116)

$$P_1(z) = 1.2491E_1(z) + \frac{0.0162\Delta t}{(1 - z^{-1})}E_1(z) + \frac{2.2805(1 - z^{-1})E_1(z)}{\Delta t} \quad (115)$$

$$P_2(z) = 1.5108E_2(z) + \frac{0.0616\Delta t}{(1 - z^{-1})}E_2(z) + \frac{3.9334(1 - z^{-1})E_2(z)}{\Delta t} \quad (116)$$

Equations (115) and (116) can directly be used in MATLAB Simulink by introducing a Zeroth Order Hold (ZOH) in between controller and plant which is still modeled in 's' domain. Figure 28 shows the Simulink model where $T_s = \Delta t$, sampling time.

Selection of sampling time period is critical on stability and performances of closed loop system. Therefore, stability check is firstly carried out for sampling time which is used by existing motor control board. Let's revisit the continuous time state space realization of augmented plant.

$\dot{z} = \bar{A}z + \bar{B}1w + \bar{B}2u$ (99)

$\bar{y}_r = \bar{C}_r z + Du$ (101)

$u = \bar{F}\bar{y}_s$ (103)

One of state space representation (A, B, and C, D) of plant transfer function matrix described by equations (20), (21), (22) and (23) is presented by the equations from (117) to (120). This realization is taken in canonical form as it doesn't make numerical difficulties in the algorithm used to find continuous time PID gains.

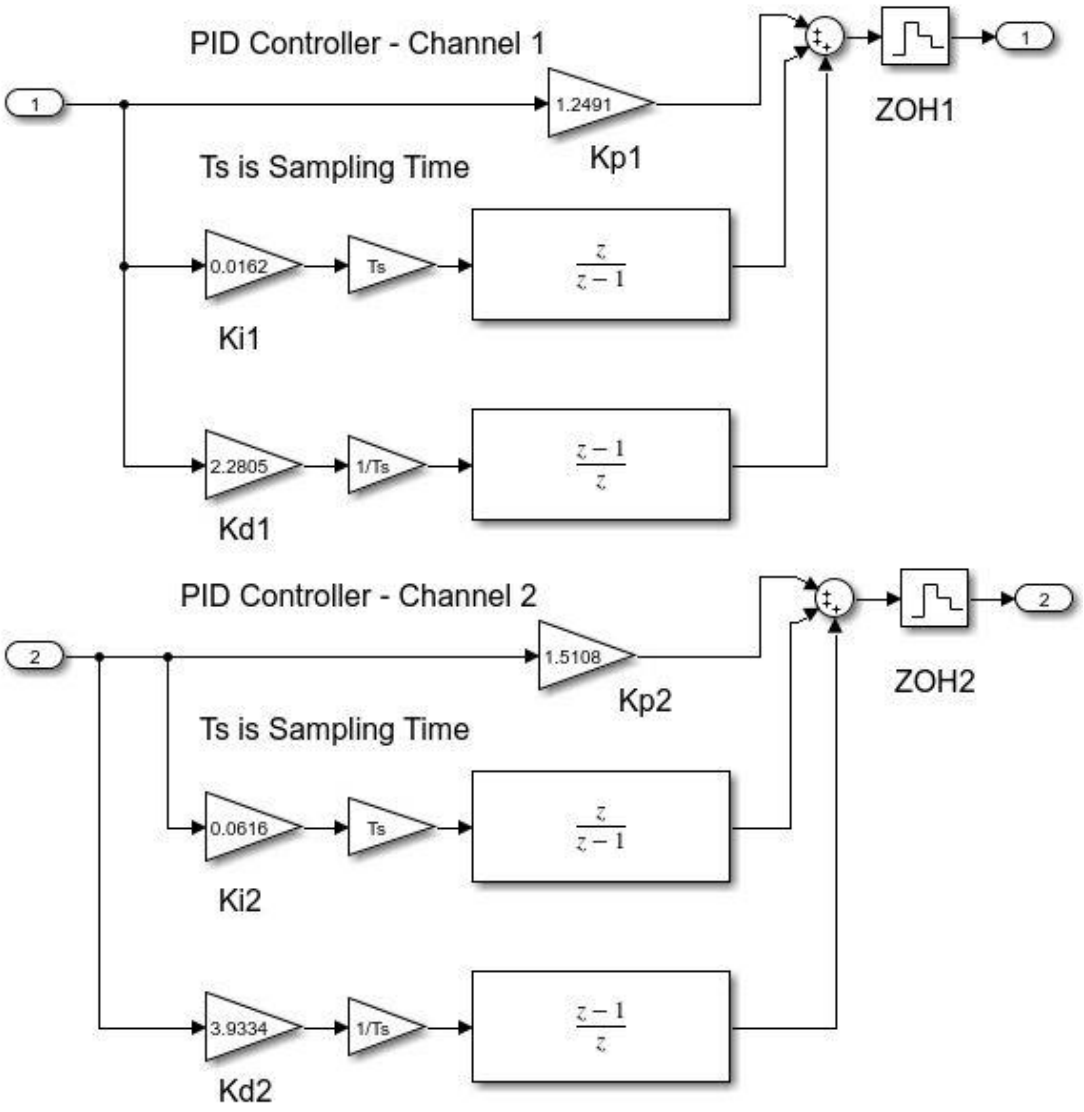

Figure 28: Simulink Model of Discretized Two PID Controllers

$$A=\begin{bmatrix} -71.38 & -3.13 & 0 & 0 & 0 & 0 & 0 & 0 & 0 & 0 & 0 & 0 \\ 4 & 0 & 0 & 0 & 0 & 0 & 0 & 0 & 0 & 0 & 0 & 0 \\ 0 & 0.25 & 0 & 0 & 0 & 0 & 0 & 0 & 0 & 0 & 0 & 0 \\ 0 & 0 & 0 & -0.71 & -0.15 & 0 & 0 & 0 & 0 & 0 & 0 & 0 \\ 0 & 0 & 0 & 1 & 0 & 0 & 0 & 0 & 0 & 0 & 0 & 0 \\ 0 & 0 & 0 & 0 & 1 & 0 & 0 & 0 & 0 & 0 & 0 & 0 \\ 0 & 0 & 0 & 0 & 0 & 0 & -0.09 & -0.026 & 0 & 0 & 0 & 0 \\ 0 & 0 & 0 & 0 & 0 & 0 & 0.125 & 0 & 0 & 0 & 0 & 0 \\ 0 & 0 & 0 & 0 & 0 & 0 & 0 & 0.25 & 0 & 0 & 0 & 0 \\ 0 & 0 & 0 & 0 & 0 & 0 & 0 & 0 & 0 & -0.21 & -0.12 & 0 \\ 0 & 0 & 0 & 0 & 0 & 0 & 0 & 0 & 0 & 0.5 & 0 & 0 \\ 0 & 0 & 0 & 0 & 0 & 0 & 0 & 0 & 0 & 0 & 1 & 0 \end{bmatrix} \quad (117)$$

$$B=\begin{bmatrix} 2 & 0 \\ 0 & 0 \\ 0 & 0 \\ 0.25 & 0 \\ 0 & 0 \\ 0 & 0 \\ 0 & 0.0625 \\ 0 & 0 \\ 0 & 0 \\ 0 & 0.125 \\ 0 & 0 \\ 0 & 0 \end{bmatrix} \quad (118)$$

$$C=\begin{bmatrix} 0 & 0 & -2.33 & 0 & 0 & 0 & 0 & 0 & 0.033 & 0 & 0 & 0 \\ 0 & 0 & 0 & 0 & 0 & -0.12 & 0 & 0 & 0 & 0 & 0 & -0.072 \end{bmatrix} \quad (119)$$

$$D=\begin{bmatrix} 0 & 0 \\ 0 & 0 \end{bmatrix} \quad (120)$$

As it is derived in (49) and (64), augmented matrices $\bar{A}$, $\bar{B}_2$, $\bar{B}_1$, $\bar{C}$ and $\bar{D}$ can be derived from original plant matrices given in equations from (117) to (120). These augmented matrices are presented in equations from (121) to (125).

$$\bar{A} =$$

$$\begin{bmatrix} -71.38 & -3.13 & 0 & 0 & 0 & 0 & 0 & 0 & 0 & 0 & 0 & 0 & 0 & 0 \\ 4 & 0 & 0 & 0 & 0 & 0 & 0 & 0 & 0 & 0 & 0 & 0 & 0 & 0 \\ 0 & 0.25 & 0 & 0 & 0 & 0 & 0 & 0 & 0 & 0 & 0 & 0 & 0 & 0 \\ 0 & 0 & 0 & -0.71 & -0.15 & 0 & 0 & 0 & 0 & 0 & 0 & 0 & 0 & 0 \\ 0 & 0 & 0 & 1 & 0 & 0 & 0 & 0 & 0 & 0 & 0 & 0 & 0 & 0 \\ 0 & 0 & 0 & 0 & 1 & 0 & 0 & 0 & 0 & 0 & 0 & 0 & 0 & 0 \\ 0 & 0 & 0 & 0 & 0 & 0 & -0.092 & -0.026 & 0 & 0 & 0 & 0 & 0 & 0 \\ 0 & 0 & 0 & 0 & 0 & 0 & 0.125 & 0 & 0 & 0 & 0 & 0 & 0 & 0 \\ 0 & 0 & 0 & 0 & 0 & 0 & 0 & 0.25 & 0 & 0 & 0 & 0 & 0 & 0 \\ 0 & 0 & 0 & 0 & 0 & 0 & 0 & 0 & 0 & -0.218 & -0.12 & 0 & 0 & 0 \\ 0 & 0 & 0 & 0 & 0 & 0 & 0 & 0 & 0 & 0.5 & 0 & 0 & 0 & 0 \\ 0 & 0 & 0 & 0 & 0 & 0 & 0 & 0 & 0 & 0 & 1 & 0 & 0 & 0 \\ 0 & 0 & -2.33 & 0 & 0 & 0 & 0 & 0 & 0.033 & 0 & 0 & 0 & 0 & 0 \\ 0 & 0 & 0 & 0 & 0 & -0.12 & 0 & 0 & 0 & 0 & 0 & -0.072 & 0 & 0 \end{bmatrix}$$

(121)

$$\bar{B}_2 = \begin{bmatrix} 2 & 0 \\ 0 & 0 \\ 0 & 0 \\ 0.25 & 0 \\ 0 & 0 \\ 0 & 0 \\ 0 & 0.0625 \\ 0 & 0 \\ 0 & 0 \\ 0 & 0.125 \\ 0 & 0 \\ 0 & 0 \\ 0 & 0 \\ 0 & 0 \end{bmatrix} \quad (122) \qquad \bar{B}_1 = \begin{bmatrix} 2 \\ 0 \\ 0 \\ 0.25 \\ 0 \\ 0 \\ 0.0625 \\ 0 \\ 0 \\ 0.125 \\ 0 \\ 0 \\ 0 \\ 0 \end{bmatrix} \quad (123)$$

$$\bar{C}_r = \begin{bmatrix} 0 & 0 & -2.33 & 0 & 0 & 0 & 0 & 0 & 0.033 & 0 & 0 & 0 & 0 & 0 \\ 0 & 0 & 0 & 0 & 0 & -0.12 & 0 & 0 & 0 & 0 & 0 & -0.07 & 0 & 0 \\ 0 & 0 & 0 & 0 & 0 & 0 & 0 & 0 & 0 & 0 & 0 & 0 & 1 & 0 \\ 0 & 0 & 0 & 0 & 0 & 0 & 0 & 0 & 0 & 0 & 0 & 0 & 0 & 1 \\ 0 & -0.58 & 0 & 0 & 0 & 0 & 0 & 0.0084 & 0 & 0 & 0 & 0 & 0 & 0 \\ 0 & 0 & 0 & 0 & -0.12 & 0 & 0 & 0 & 0 & 0 & -0.072 & 0 & 0 & 0 \end{bmatrix} \quad (124)$$

$$\bar{D} = \begin{bmatrix} 0 & 0 \\ 0 & 0 \\ 0 & 0 \\ 0 & 0 \\ 0 & 0 \\ 0 & 0 \end{bmatrix} \qquad (125)$$

Disturbance and noise matrix $\bar{B}_1$ is selected such that a disturbance is added at the input of each actuator (servo amplifier) as shown in Figure 29. G11, G12, G21 and G22 in Figure 29 represent the transfer functions given in equations (20), (21), (22) and (23) respectively. External disturbances are represented by d1 and d2.

By converting this continuous state space representation in to discrete form and evaluating its transition matrix, it is possible to say that closed loop system is stable in discrete domain if all eigenvalues of transition matrix are within the unit circle of which origin is zero in the z – plane [27]. Discretized transition matrix, $\bar{\emptyset}(t)$ can be derived for any sampling time period T_s from continuous time transition matrix, $(\bar{A} + \bar{B}_2\bar{F}\bar{C})$ as shown by (126) [21].

$$\bar{\emptyset}(t) = \mathrm{L}^{-1}[(sI - (\bar{A} + \bar{B}_2\bar{F}\bar{C}))^{-1}] \qquad (126)$$

Here $\mathrm{L}^{-1}()$ is inverse Laplace transformation. Then discretized transition matrix for sampling time $T_s = 0.01s$ can be expressed as given by (127).

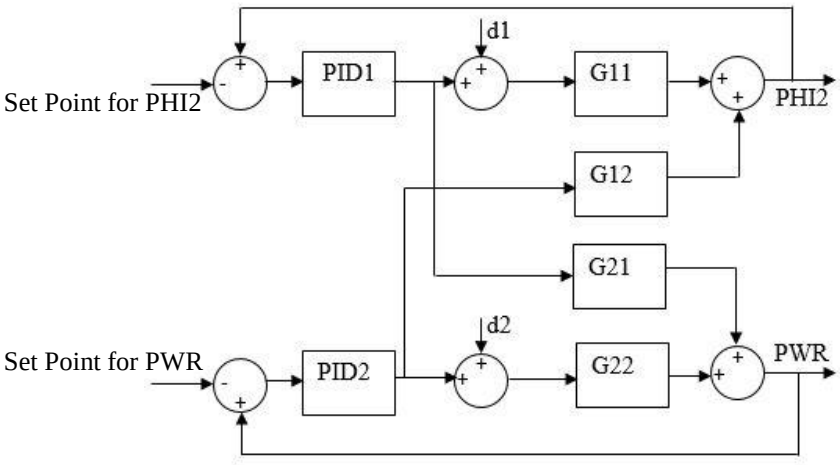

Figure 29: System Representation with External Disturbances

$$\bar{\emptyset}(t) = \begin{bmatrix} 0.4890 & -0.0415 & -0.0417 & 0 & 0 & 0 & 0 & 0.0003 & 0.0006 & 0 & 0 & 0 & 0.0002 & 0 \\ 0.0286 & 0.9991 & -0.0009 & 0 & 0 & 0 & 0 & 0 & 0 & 0 & 0 & 0 & 0 & 0 \\ 0 & 0.0025 & 1 & 0 & 0 & 0 & 0 & 0 & 0 & 0 & 0 & 0 & 0 & 0 \\ 0 & -0.0033 & -0.0073 & 0.9929 & -0.0016 & 0 & 0 & 0 & 0 & 0 & 0 & 0 & 0 & 0 \\ 0 & 0 & 0 & 0.01 & 1 & 0 & 0 & 0 & 0 & 0 & 0 & 0 & 0 & 0 \\ 0 & 0 & 0 & 0 & 0.01 & 1 & 0 & 0 & 0 & 0 & 0 & 0 & 0 & 0 \\ 0 & 0 & 0 & 0 & -0.0003 & -0.0001 & 0.99 & -0.0003 & 0 & 0 & -0.0002 & -0.0001 & 0 & 0 \\ 0 & 0 & 0 & 0 & 0 & 0 & 0.0012 & 1 & 0 & 0 & 0 & 0 & 0 & 0 \\ 0 & 0 & 0 & 0 & 0 & 0 & 0 & 0.0025 & 1 & 0 & 0 & 0 & 0 & 0 \\ 0 & 0 & 0 & 0 & -0.0006 & -0.0002 & 0 & 0 & 0 & 0.9978 & -0.0016 & -0.0001 & 0 & 0 \\ 0 & 0 & 0 & 0 & 0 & 0 & 0 & 0 & 0 & 0.0050 & 1 & 0 & 0 & 0 \\ 0 & 0 & 0 & 0 & 0 & 0 & 0 & 0 & 0 & 0 & 0.01 & 1 & 0 & 0 \\ 0 & 0 & 0 & 0 & -0.0234 & 0 & 0 & 0 & 0.0003 & 0 & 0 & 0 & 1 & 0 \\ 0 & 0 & 0 & 0 & 0 & 0 & 0 & -0.0013 & 0 & 0 & 0 & -0.0007 & 0 & 1 \end{bmatrix} \quad (127)$$

The eigenvalues of this discretized transition matrix are given in equation (128)

$$
\begin{aligned}
\lambda_1 &= 0.4914 + 0.0000i \\
\lambda_2 &= 0.9964 + 0.0017i \\
\lambda_3 &= 0.9964 - 0.0017i \\
\lambda_4 &= 0.9984 + 0.0023i \\
\lambda_5 &= 0.9984 - 0.0023i \\
\lambda_6 &= 0.9994 + 0.0024i \\
\lambda_7 &= 0.9994 - 0.0024i \\
\lambda_8 &= 0.9996 + 0.0005i \\
\lambda_9 &= 0.9996 - 0.0005i \\
\lambda_{10} &= 0.9999 + 0.0000i \\
\lambda_{11} &= 0.9994 + 0.0003i \\
\lambda_{12} &= 0.9994 - 0.0003i \\
\lambda_{13} &= 0.9990 + 0.0000i \\
\lambda_{14} &= 0.9990 + 0.0000i
\end{aligned}
\qquad (128)
$$

Equation (128) clearly shows that all eigenvalues are within the unit circle on z-plane. Therefore sampling time, $T_s = 0.01s$ is feasible to implement the digital test circuit with ATMEL MEGA-328P microcontroller.

Voltage ranges used in fine tuning control of transmitter and ATMEL microcontroller must be mapped each other. Measured variables, PHI2 and PWR vary within the range of 0V…+10V. Input control voltage for two servo amplifiers must vary within the range of -10V...+10V. Therefore these voltage ranges must be converted to ranges which can be handled by microcontroller. Microcontroller can accept and generate voltages within the range of 0V…+3.3V. Therefore two measurements are fed via resistor dividers so as maximum 10V maps to 3.3V. Output control voltages issued by microcontroller are mapped by an external linear amplifier which is made of operational amplifiers. Control voltage mapping is accomplished as shown in Table 2. The complete circuit diagram which consists microcontroller, linear amplifier, resistor dividers and servo amplifiers of two motors is depicted in Figure 31. TL074CN, low noise operational amplifier is used as linear amplifiers. Developed test hardware module is shown in Figure 30. Relevant programing code written in language C is given in Appendix ‘C’.

Table 2: Mapping of Control Voltages between Microcontroller and Plant

Control Voltage Issued by Microcontroller/V	Output Voltage from Linear Amplifier/V (I/P to the Servo Amplifier)
0	+10
1.65 (=3.3/2)	0
3.3	-10

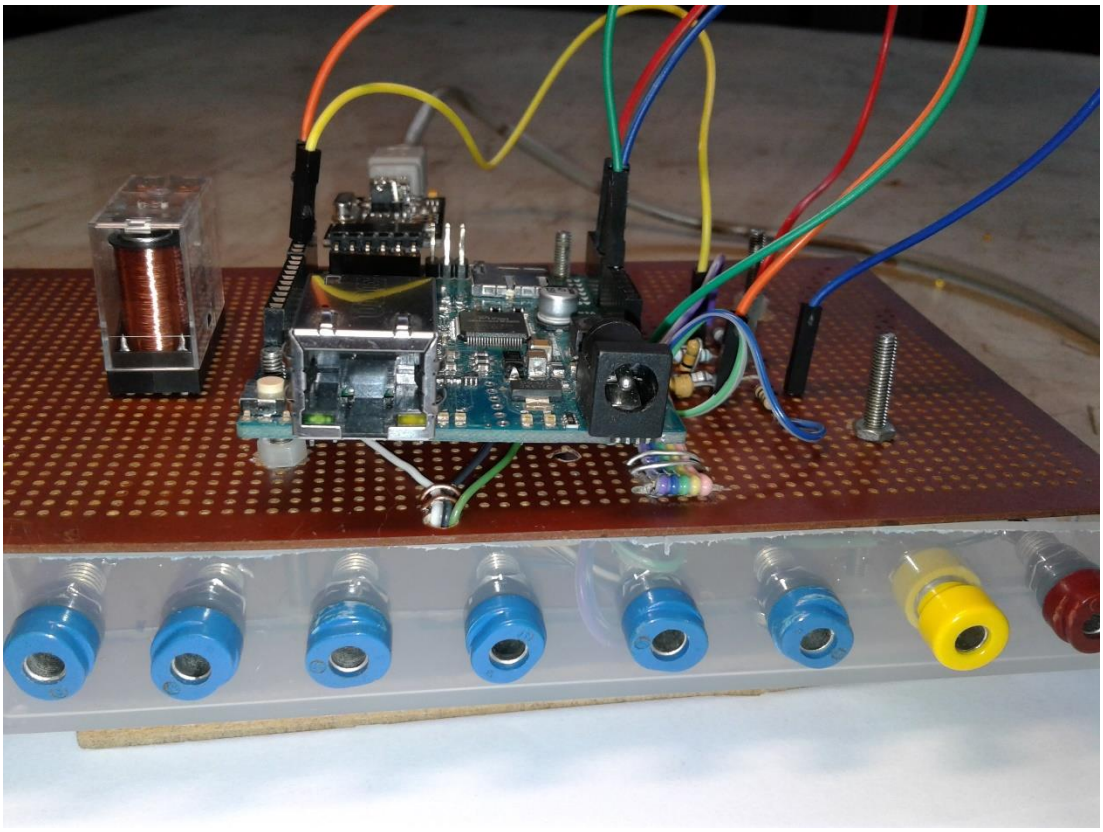

Figure 30: Test Hardware Module

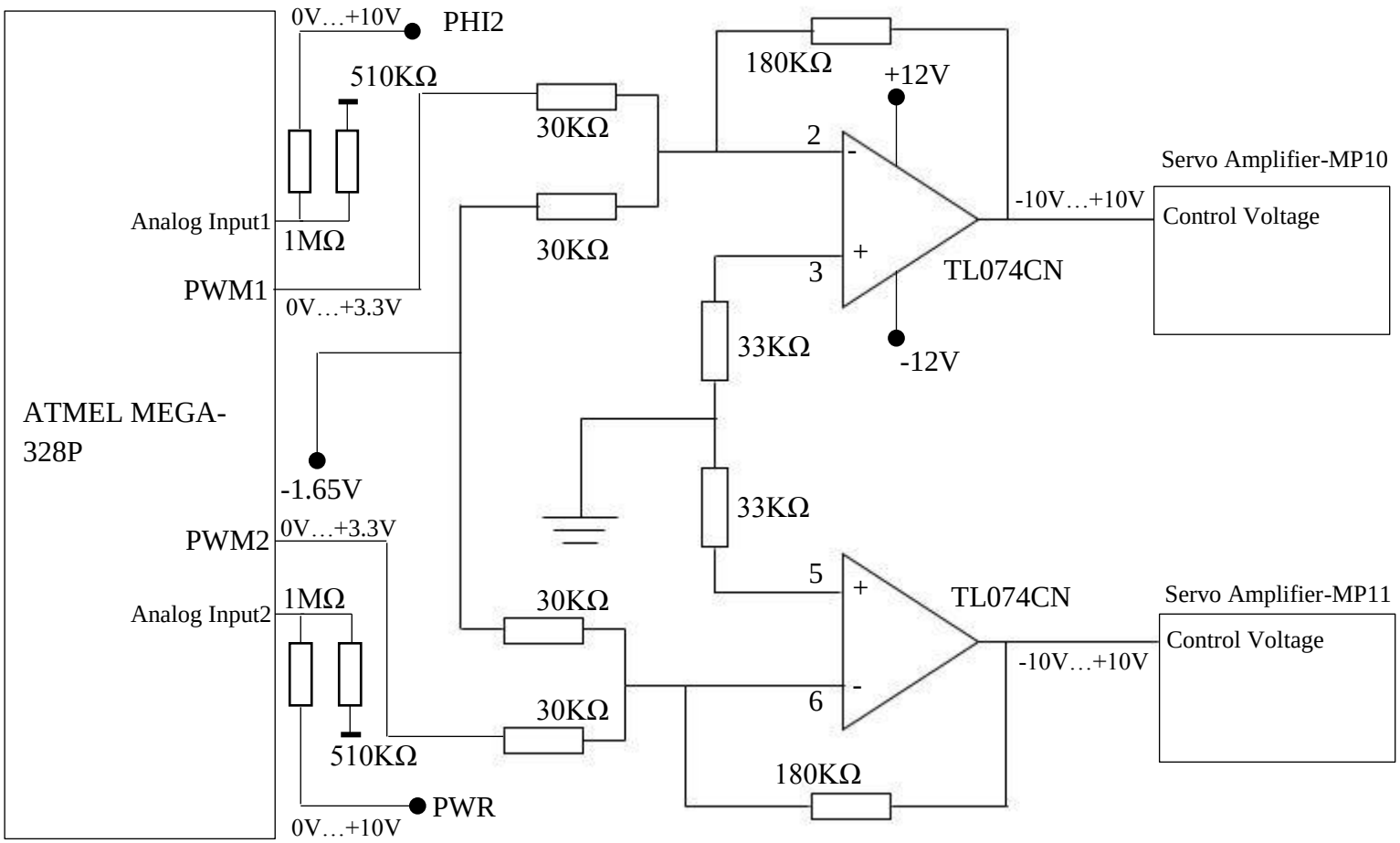

Figure 31: Complete System of Plant and Digital Controller Implemented with ATMEL MEGA-328P

5.3 Embedding the Proposed Algorithm in Existing Hardware

Fine tuning algorithm of final RF stage and many other algorithms are embedded in express microcontroller, INTEL 80C196KC20 [28]. This microcontroller is the main processing device of existing motor control board. It is operated by a 12MHz clock signal. It has a built in analog to digital converter which has a resolution of 10 bits. This converter is used in measuring of two controlled variables PHI2 and PWR. This microcontroller has an address range of 64KB, which is partly connected to an external RAM and a ROM. Existing algorithm is programmed by language C. Therefore it is not difficult to download the proposed algorithm with some minor modifications in to INTEL 80C196KC20 as our program is also written in C. Anyway, existing program comprises many other code segments as well. Those are related to other algorithms in addition to the algorithm of final RF stage fine tuning. They are related to coarse tuning, fine tuning of driver stage, safety loops, so on. Therefore it is necessary to have complete program for modifying the code segment devoted to fine tuning of final RF stage. But manufacture of transmitter doesn't share program with their customers as it is an intellectual property belongs to manufacturer. At the end of a series of requests, they agreed to replace only code segment related to their fine tuning algorithm by our proposed algorithm. After that, only compiled binary file of modified complete program was sent us for downloading it in to INTEL 80C196KC20. It is obvious to see that results are same as the results taken from test circuit which employs ATMEL MEGA-328P microcontroller. Those results are discussed in the Chapter 6, results and conclusion.

CHAPTER 6
RESULTS, DISCUSSION AND CONCLUSION

6.1 Results

This final chapter has three sections. In section 6.1, all test results taken with Simulink of discrete controller and with developed test hardware setup are depicted. Section 6.2 is devoted to discuss the results. Results delivered from proposed controller are compared with experimental results taken from existing controller. Discussion reveals the validity of proposed control scheme. Finally, section 6.3 summarizes success of research project as conclusion.

6.1.1 Simulation Results

The proposed SOF-H_∞-PID controller of which control gain matrices are found by the algorithm given in Figure 23, is simulated in MATLAB-SIMULINK. Step response is traced as it takes the response of full frequency spectrum of closed loop system in to account. The control efforts are also depicted to show their low and feasible actuator inputs which can practically be realized. Firstly, Simulation results for P, PI and PD controllers are depicted from Figure 32 to Figure 34. Poor time domain performances of such control scenarios over the PID ensures the necessity of PID controlling for automatic fine tuning. Secondly, step response of digital PID controller, with respect to corresponding reference values (5V for PHI2 and 6.3V for PWR) is shown in Figure 35. Corresponding control effort is depicted in Figure 36. Then, decoupling nature of main control loops is simulated by breaking a one loop each time. Figure 37 and Figure 38 show the capability of controller to withstand in such a situation as one control loop is accidently broken. That scenario reveals the decoupling capability of two individual control loops. When one loop is out of order, controller maintains the expected performance from other loop to ensure an uninterruptible service.

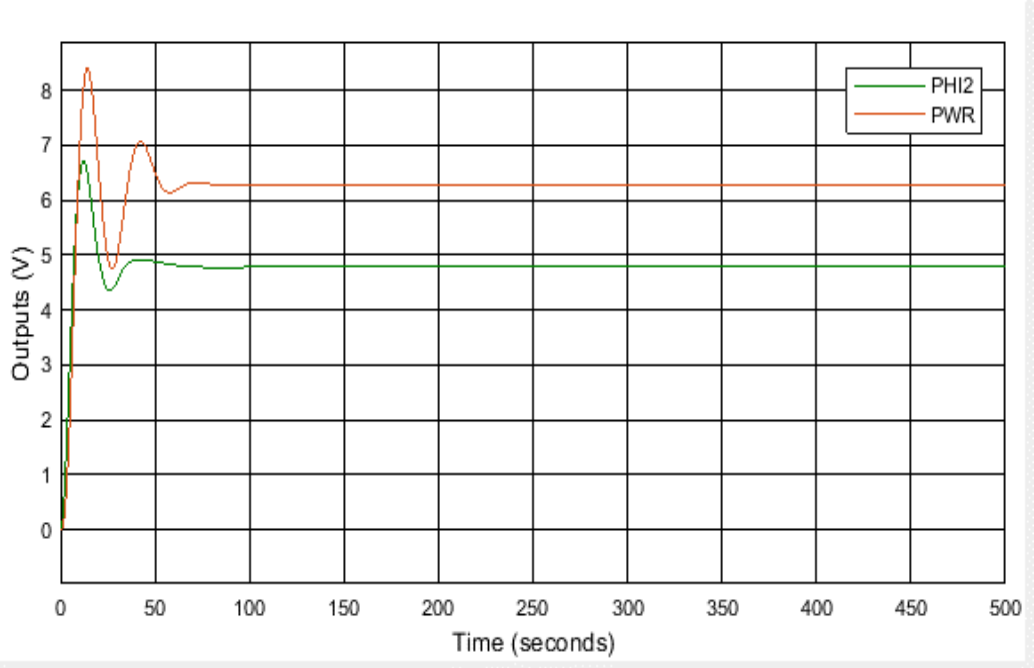

Figure 32: Step Response of Closed Loop System for Proportional (P) Digital Controller

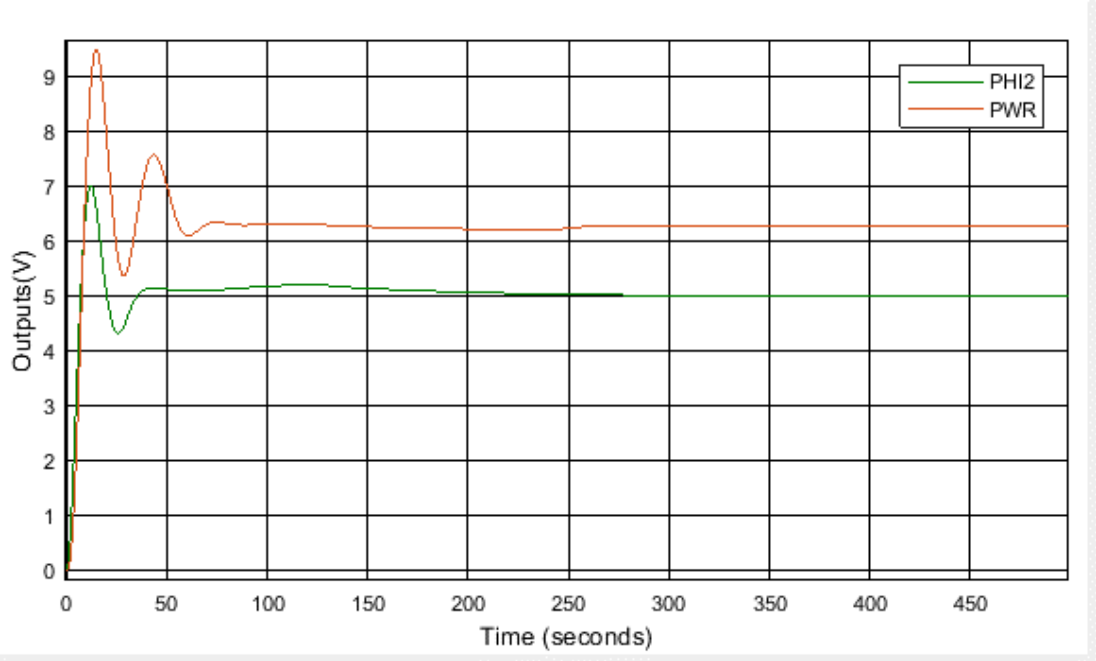

Figure 33: Step Response of Closed Loop System for Proportional-Integral (PI) Digital Controller

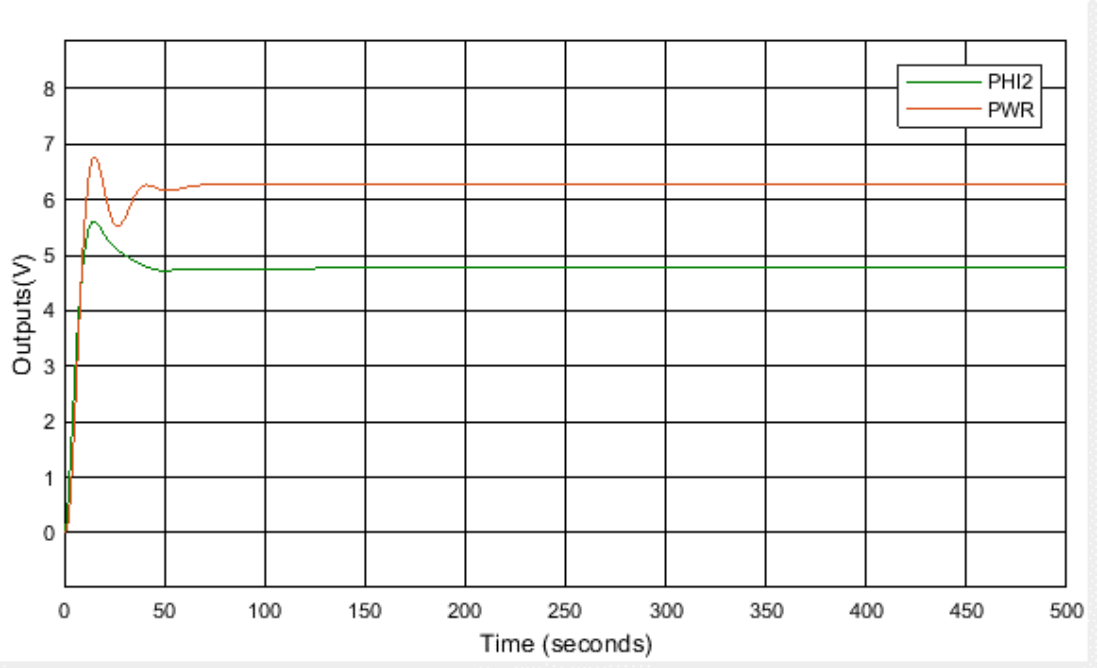

Figure 34: Step Response of Closed Loop System for Proportional-Derivative (PD) Digital Controller

Figure 32 clearly reveals the fact that only a proportional controller of which gains are found by using same ILMI algorithm is not capable to deliver satisfied time domain performances as there exists a high peak over shoot and a steady state error for both output variables. It is obvious to see that both output RF power and efficiency have their over shoots at same time. This indicates a huge power wasting as heat inside the emission tube. Figure 33 shows that PI controlling can ensure a zero steady state error while there exist huge over shoots for both output variables. Figure 34 depicts the time domain performances for a PD controller. That type of controller can minimize the over shoots successfully. But at the end of fine tuning, it is rest with steady state errors for both output variables. The steady state error for PHI2 indicates a steady power wastage throughout the operating time of emission tube. It is not good for both efficiency and life time of the tube. Therefore it is necessary to employ a PID controller which should be capable to ensure an expected performances as revealed by Figure 35.

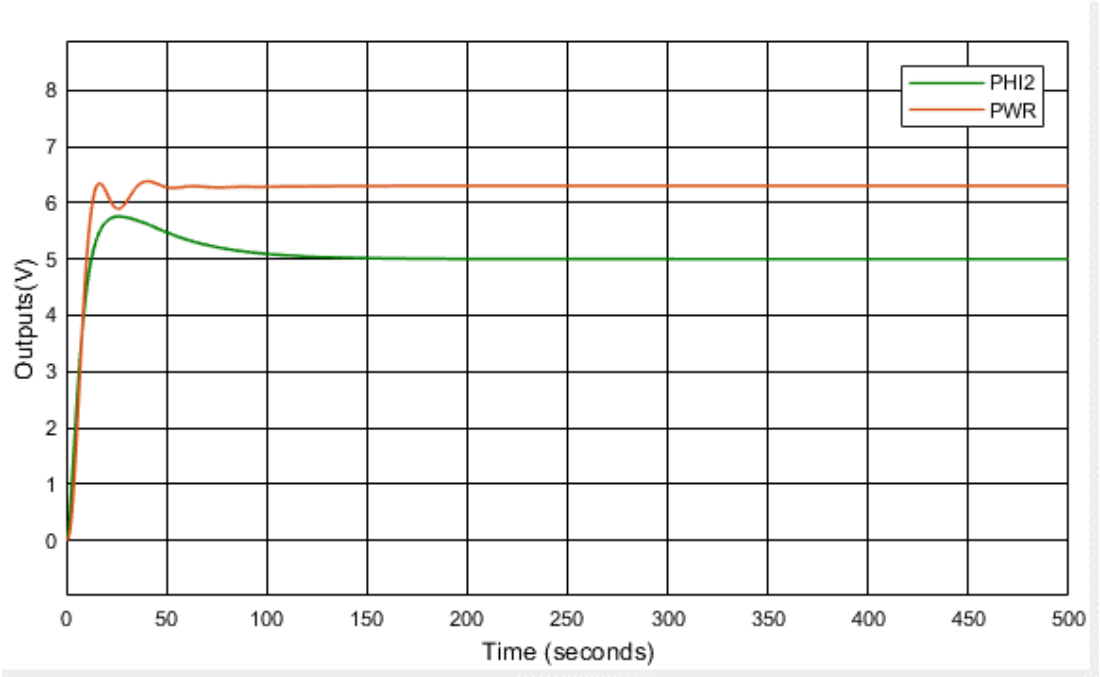

Figure 35: Step Response of Closed Loop System with Proposed PID Digital Controller

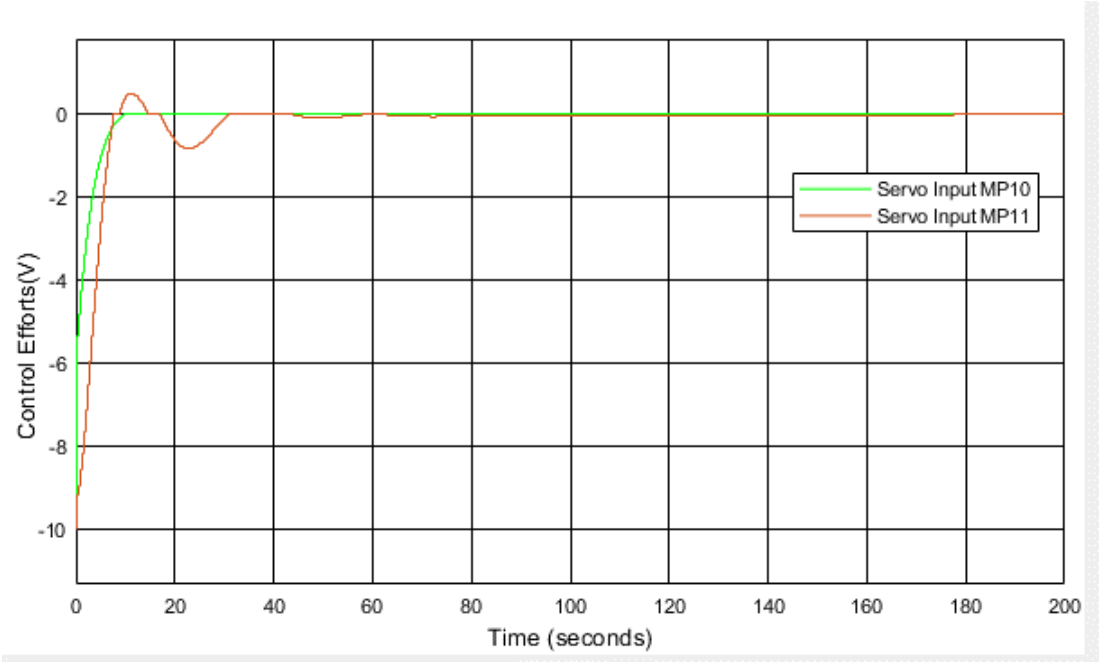

Figure 36: Control Efforts for Step Response of Closed Loop System with Proposed PID Digital Controller

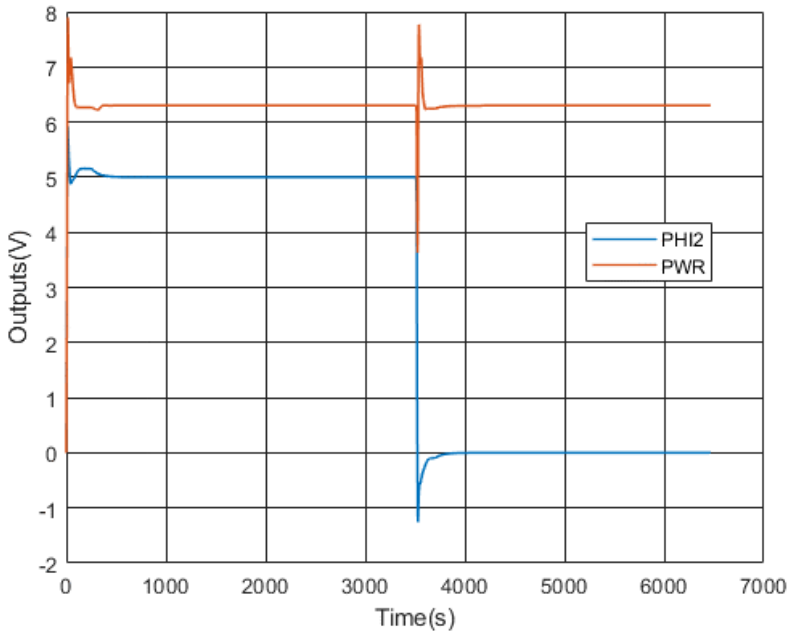

Figure 37: Response of Closed Loop System with Proposed PID Digital Controller while PHI2 Loop is opened at 3500s

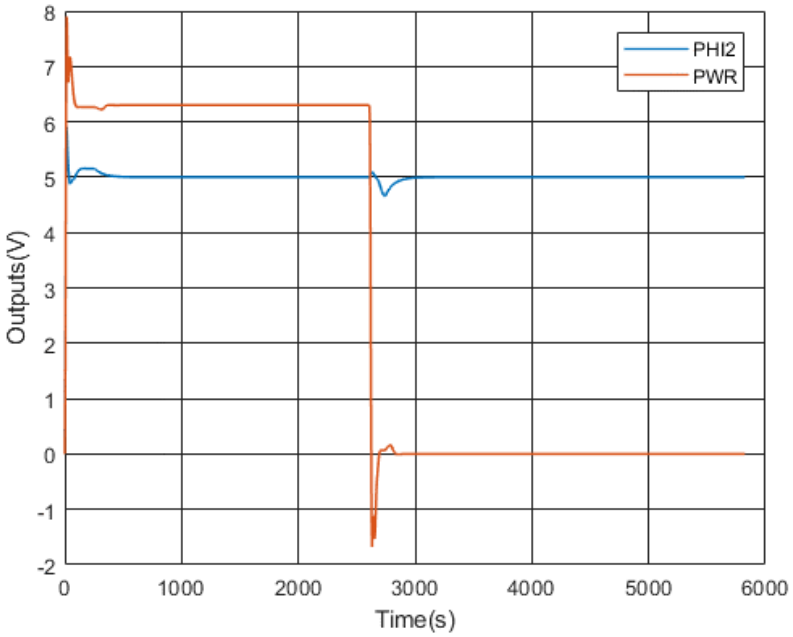

Figure 38: Response of Closed Loop System with Proposed PID Digital Controller while PWR Loop is opened at 2600s

The controller's behavior while low frequency disturbance is present at inputs of both servo amplifiers is depicted in Figure 39. Figure 40 shows the SIMULINK diagram used to simulate this scenario. A step disturbance is present at time 720s and it disappears in time 2170s. Saturators at the output of controller are placed due to the fact that both servo amplifiers are saturated beyond the range of control input -10 V- +10V. Dead zones which have a range of -0.3V - +0.3V represent the control input voltage range within which output variables don't response at all.

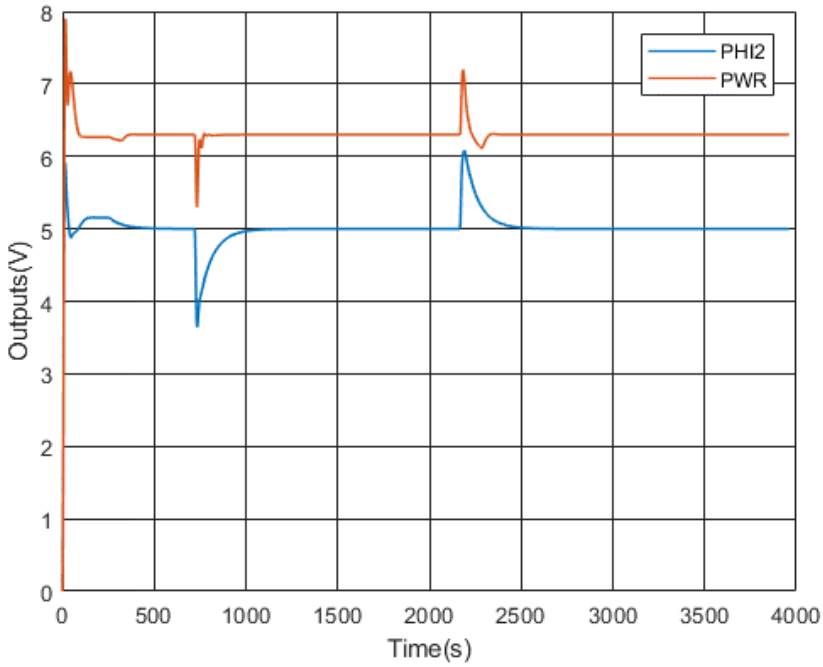

Figure 39: Output Response while Presence of a unit disturbance at input of Actuators within the time from 720s to 2170s

Because plant is operating in an environment of high frequency RF is abundant due to other transmitters in the premises, a high frequency, low amplitude noise is also added to the point from where output variables are measured. The nature of this noise is depicted in Figure 41. The step response of the closed loop plant while high frequency noise is present, is depicted in Figure 42.

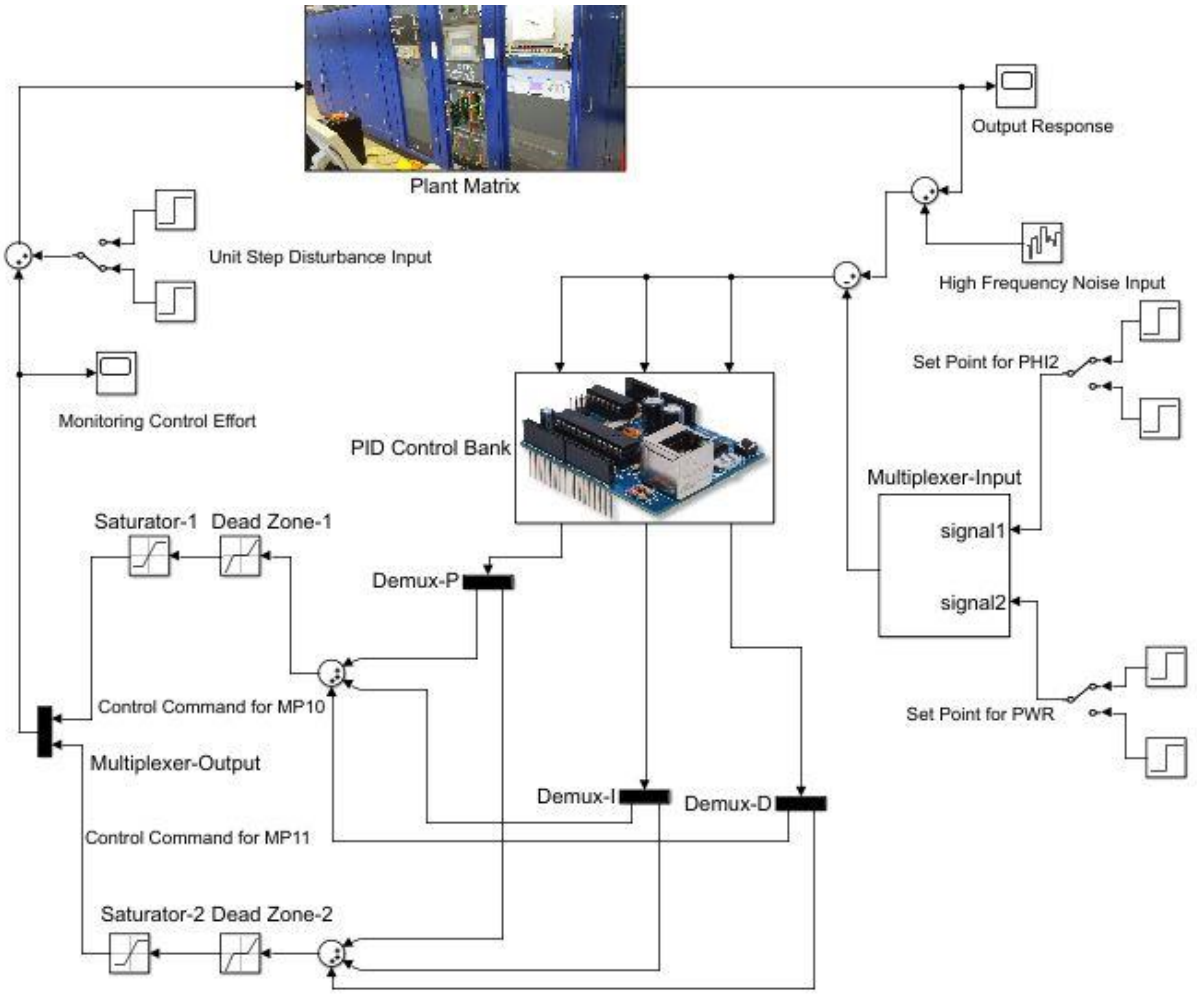

Figure 40: MATLAB-SIMULINK Diagram with Presence of Actuator Disturbances and High Frequency Noises at Outputs

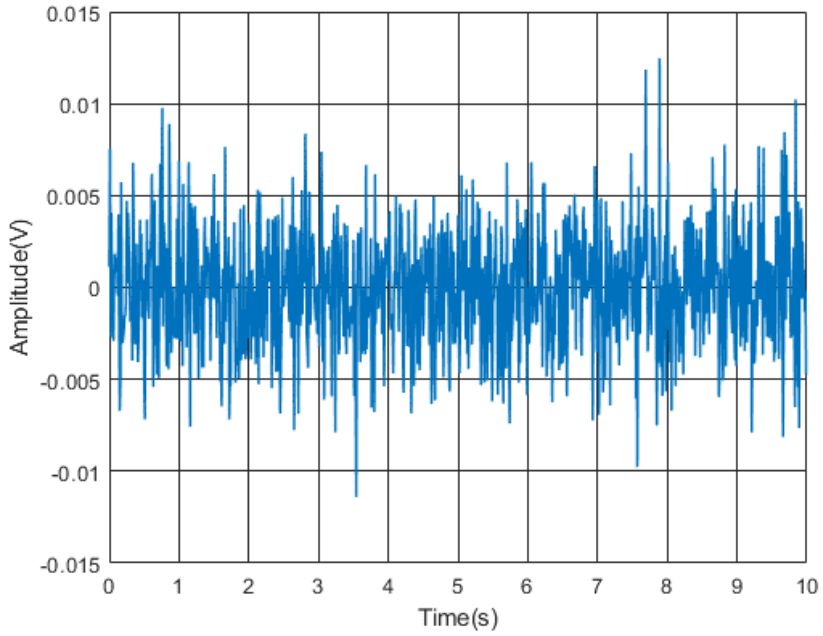

Figure 41: The Nature of High Frequency Noise Added to the Plant's Output

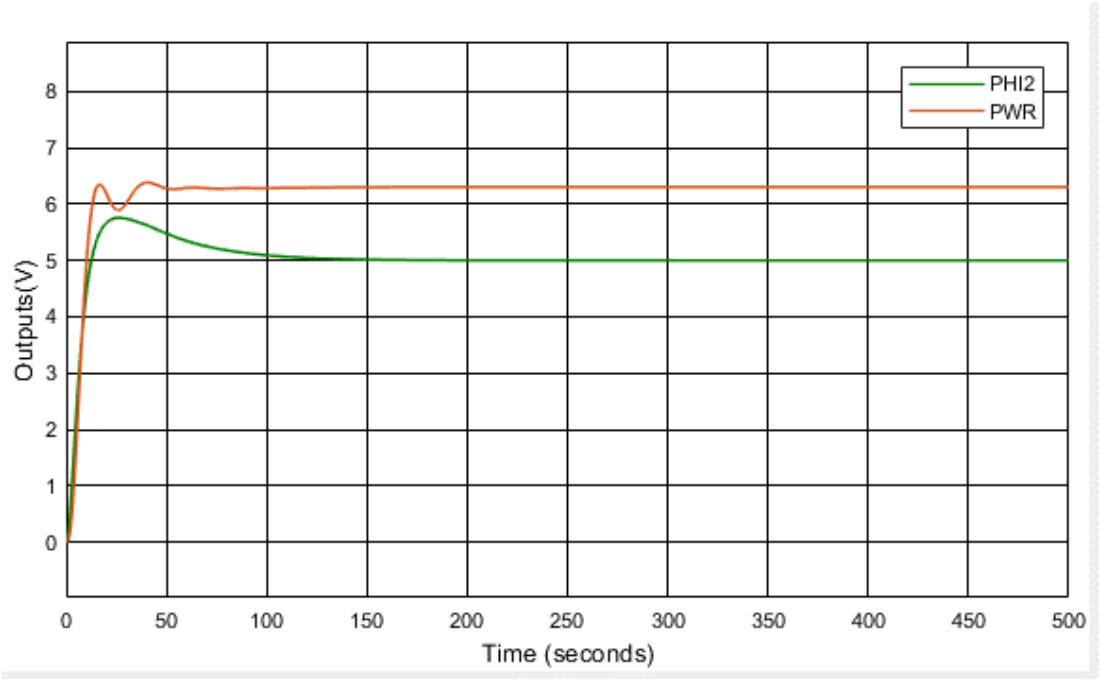

Figure 42: Output Response while Presence of High Frequency Noise in Measured Variables

6.1.2 Test Results Taken Using Developed Prototype Hardware

Test Results are taken for two operating frequencies which drive the RF amplifier. Existing controller normally experiences malfunctions for these test frequencies. We compare the behavior of output variables, PHI2 and PWR which are taken with proposed and existing controllers. All the tests are carried out with half RF power, 125kW. Therefore reference set point for controlled variable PWR is 3.125V. Reference value for controlled variable PHI2 doesn't change as it represents the efficiency of amplifier.

6.1.2.1 Output Response for Test Frequency 9720 KHz

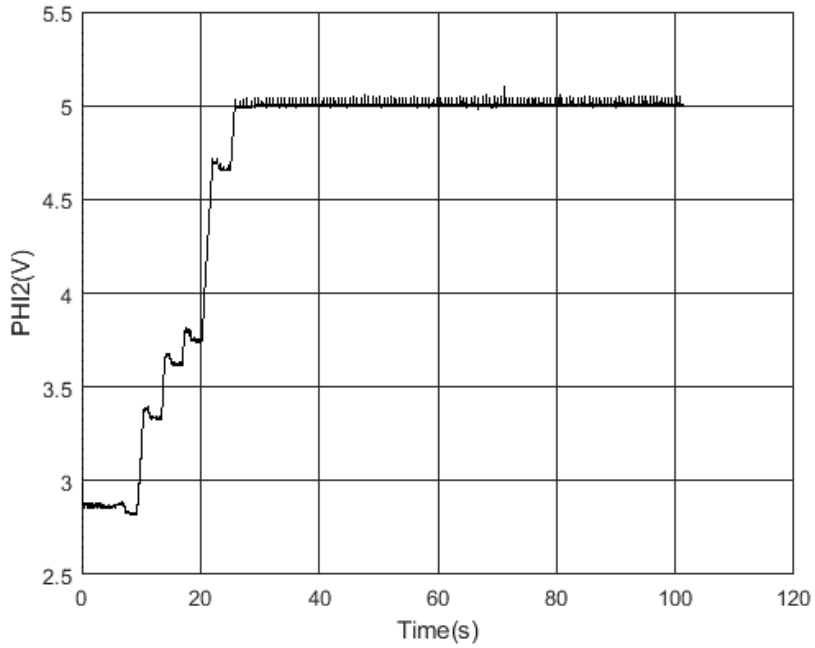

Figure 43: The Variation of PHI2 with Proposed Controller for 9720 kHz Test Frequency

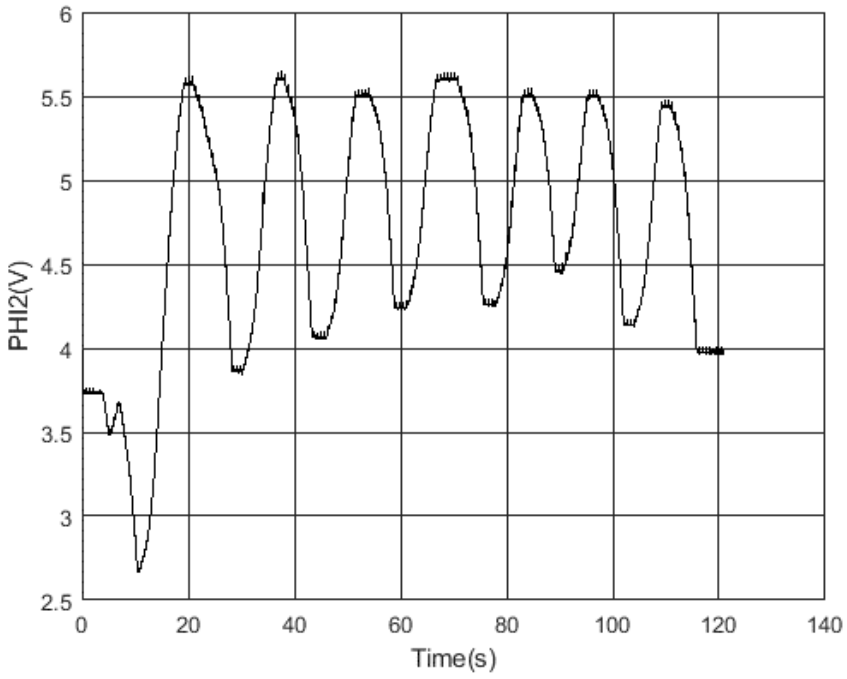

Figure 44: The Variation of PHI2 with Existing Controller for 9720 kHz Test Frequency

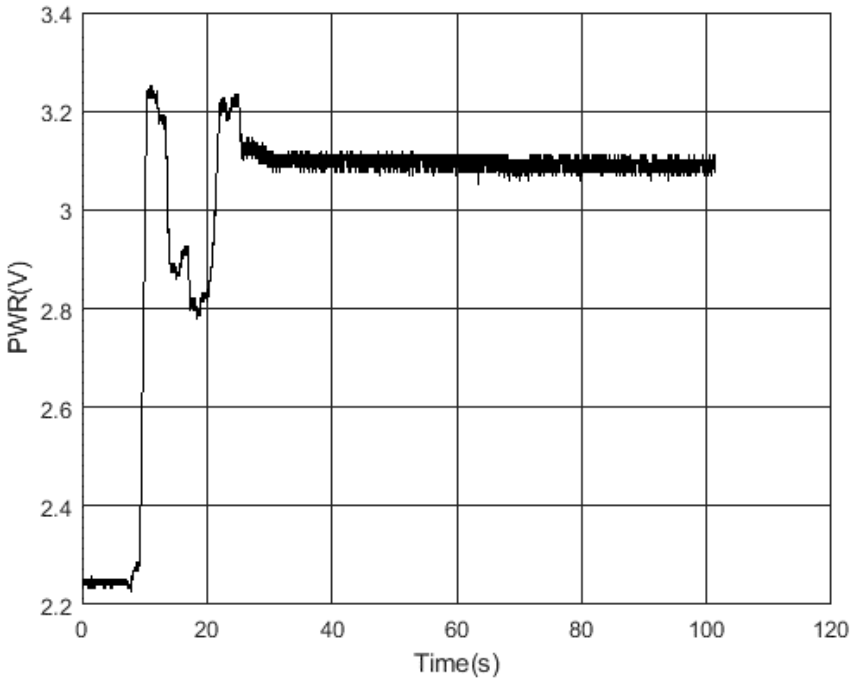

Figure 45: The Variation of PWR with Proposed Controller for 9720 kHz Test Frequency

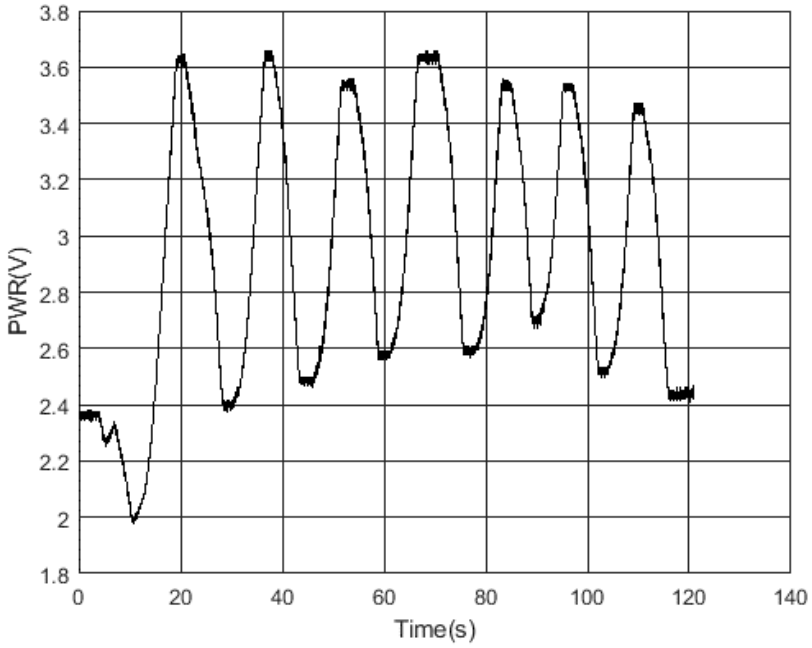

Figure 46: The Variation of PWR with Existing Controller for 9720 kHz Test Frequency

6.1.2.2 Output Response for Test Frequency 15155 KHz

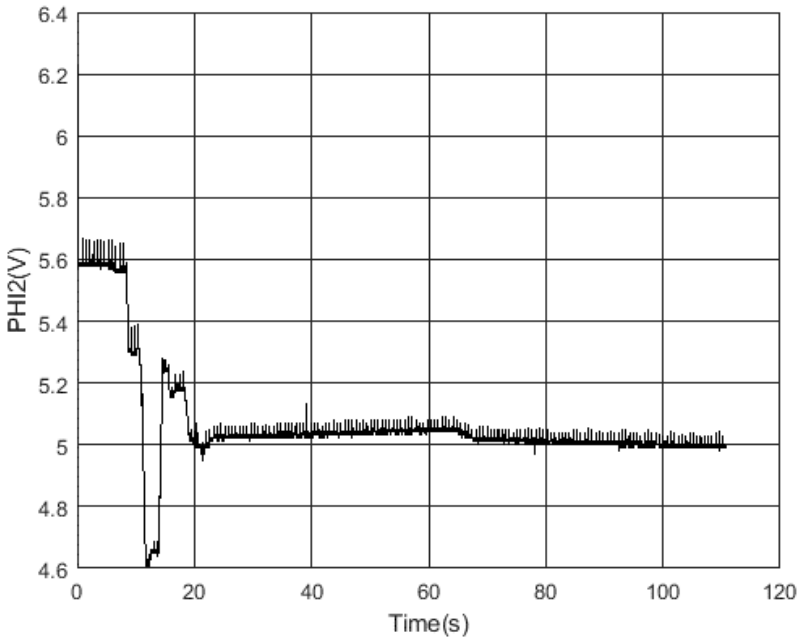

Figure 47: The Variation of PHI2 with Proposed Controller for 15155 kHz Test Frequency

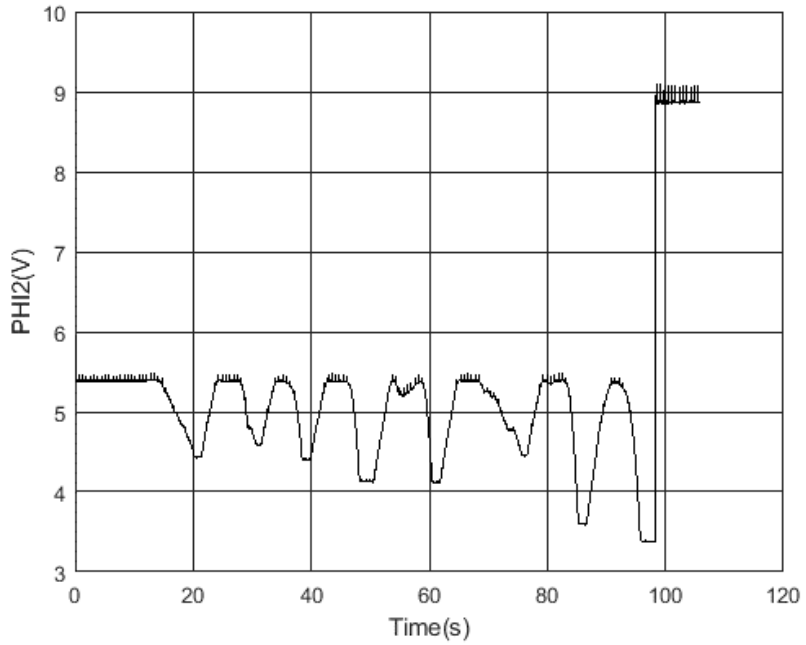

Figure 48: The Variation of PHI2 with Existing Controller for 15155 kHz Test Frequency

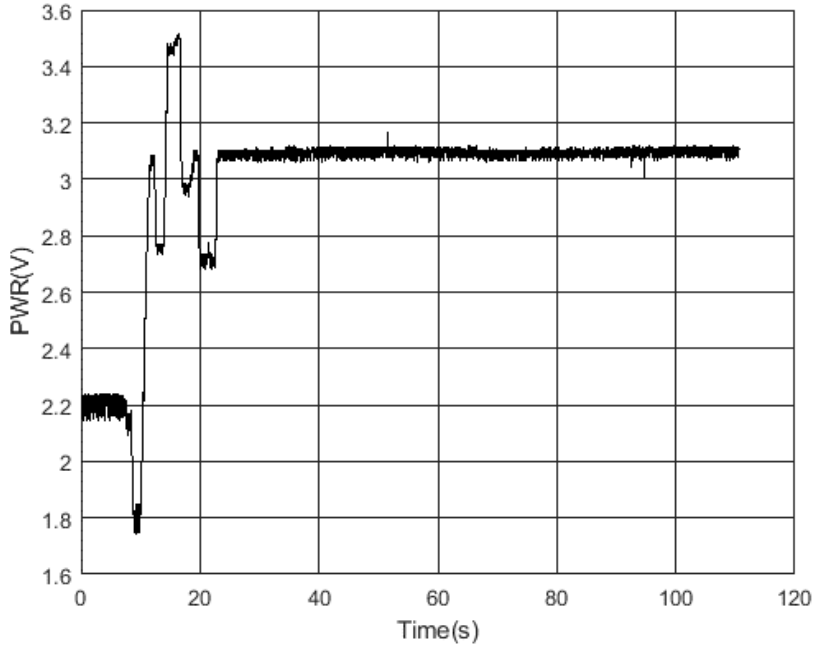

Figure 49: The Variation of PWR with Proposed Controller for 15155 kHz Test Frequency

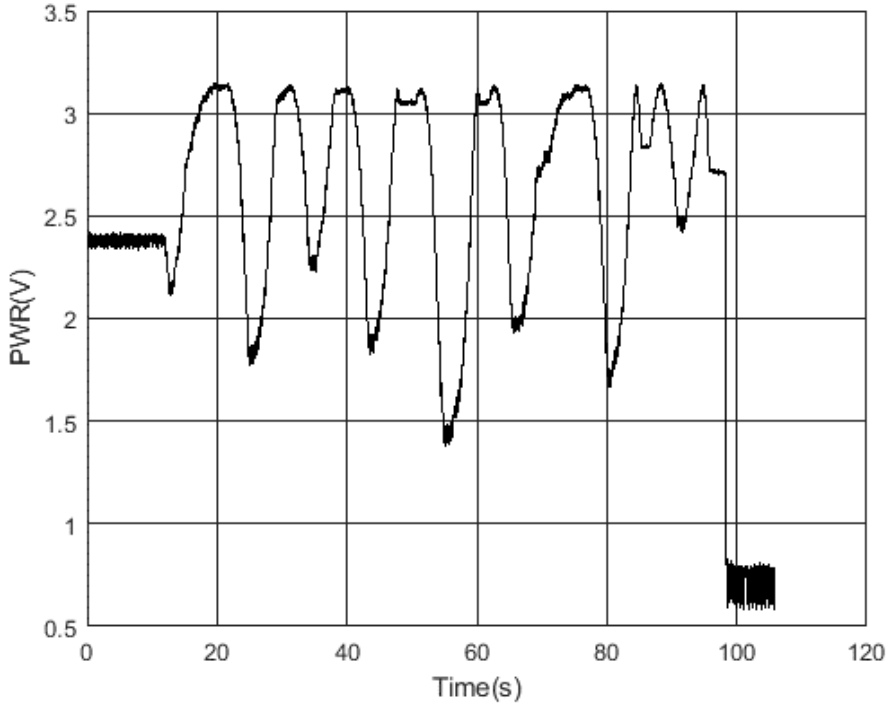

Figure 50: The Variation of PWR with Existing Controller for 15155 kHz Test Frequency

6.2 Discussion

The instability behaviour of existing controller when it tries to optimize controlled variables, PHI2 and PWR are clearly depicted in Figures 44, 46, 48 and 50. As shown by Figure 43, the RF power efficiency which relates to the controlled variable PHI2 has a response which can be approximated to a critically damped behaviour. Therefore it doesn't experience any over shoot or under shoot. But, several overshoots and under shoots can be observed for controlled variable PWR which represents the output RF power, as shown by Figure 45. This behaviour doesn't make any bad impact on the interior structure of emission tube since controlled variable, PHI2 has its optimum controlling behaviour. Otherwise an excessive amount of heat could be dissipated within the tube while fine tuning is working. Anyway, at the end of fine tuning, output RF power reaches expected value by ensuring zero steady state error.

Due to the fact that the controller for fine tuning of final RF stage is activated at a moment when values of controlled variables reach around the set point values, settling time gets shorter than the time that takes in simulation which starts the regulation of controlled variables from zero. This scenario can be observed by comparing the Figures 35 and 43. As shown by Figure 35, the settling time is around 120s in simulation, while Figures 43 and 45 show that it is only 25s for synthesised test hardware.

Settling time for test frequency, 15155 kHz is around 70s. Transmitter's main control system doesn't let audio to modulate with carrier until PHI2 stabilizes around set value with a maximum tolerance of 2%. In other words, PHI2 must stabilize within the range of +4.9V…+5.1V. Therefore it takes 70s to finalize the fine tuning so as at the end, audio could be modulated with the carrier frequency, 15155 kHz. This is an acceptable time duration because there is a 3 minutes time gap between successive broadcasting programs which have different frequencies.

Since controlled variable, PHI2 for both test frequencies settles without a steady state error, power wastage as heat during the run time of transmitter is minimized to a small value. That reveals the fact that efficiency of emission tube is at its best. This observation is directly related to the total operation cost of the transmitter. Therefore proposed control scheme ensures not only extended life time of emission tube but also reduced expenditures.

6.3 Conclusion

In this research work, a new feedback control scheme is proposed for fine tuning of final stage of the RF amplifier employed in SK 53 C3-3-P 250kW short wave transmitter, due to the fact that existing control scheme gets malfunction for several operating frequencies. Even though suspected causes for this poor behaviour are unknown, a robust control scheme is designed to stabilize the closed loop system. The most convenient way we follow to attain this matter is the black box approach. The direct relationships or so called mathematical transfer functions between inputs and outputs are experimentally analysed rather than formulating the physics of each independent unit of plant. The method called nonlinear least squares could approximate the transfer functions with an accuracy more than 90%. Because simulation results reveal the success of proposed control scheme in every aspect, PID gain matrices found by proposed ILMI algorithm are used to synthesise the test hardware as well. The main goal of this research, proposing a robust controller which can ensure the stability, and thereby high power efficiency of emission tube is proven by results given in Figures 43, 45, 47 and Figure 49. The sub goal, expected time domain performances are also achieved in addition to the main goal.

Synthesised hardware is tested for other frequencies which are coming under standard SW frequency bands. All frequencies are tuned properly with expected performances. Existing motor control board of which fine tuning algorithm is replaced by proposed controller is tested. It delivers same results as test hardware does. Therefore it is concluded that proposed controller is capable to satisfy our main and sub goals as we expect at the design phase. It has proven that H-infinity optimality criterion can mitigate unexpected plant's responses created by model errors and external disturbances. However, the proposed controller may have a maximum tolerance of model error and a limitation of external disturbances beyond which controller may not perform as we expect. Therefore a chance still exists to fail the proposed control scheme in a situation where electrical or mechanical properties of components coming with RF circuit and control circuit are perturbed in a huge amount. But the time to occur such a deviation of properties takes many years.

BIBLIOGRAPHY

[1] F. M. Bayat, "An Iterative LMI Approach for H ∞ Synthesis of Multivariable PI/PD Controllers for Stable and Unstable Processes," *Chemical Engineering Research and Design* , vol. 132, no. 2018, pp. 606-615, 2018.

[2] S. Boyd, M. Hast and K. J. Astrom, "MIMO PID tuning via iterated LMI restriction," *Int. J. Robust Nonlinear Control*, vol. 26, no. 2016, pp. 1718-1731, 2016.

[3] Y. Y. Cao, J. Lam and Y. X. Sun, "Static Output Feedback Stabilization: An ILMI Approach," *Automatica*, vol. 34, no. 12, pp. 1641-1645, 1998.

[4] K. Zhou, J. C. Doyle and K. Glover, Robust and Optimal Control, New Jersey: Prentice Hall, 1996.

[5] D. E. Seborg, T. F. Edgar and D. A. Mellichamp, Process Dynamics and Control, 2nd ed., New Jersey: Wiley, 2003.

[6] P. Gahinet and P. Apkarian, "A linear matrix inequality approach to H-infinity control," *Int. J. Robust Nonlinear Control*, vol. 4, no. 5, pp. 421-448, 1994.

[7] S. Skogestad and I. Postlethewaite, Multivariable Feedback Control, 2nd ed., New York: Wiley, 1996.

[8] G. Gu, "On the existence of linear optimal control with output feedback," *SIAM J. Contr. Optim*, vol. 28, no. 3, pp. 711-719, 1990.

[9] T. Iwasaki and R. E. Skelton, "Parametrization of all stabilizing controllers via quadratic Lyapunov functions," *J.Optim. Theory Appl*, vol. 85, pp. 291-307, 1995.

[10] T. Iwasaki, R. E. Skelton and J. C. Geromel, "Linear quadratic suboptimal control with static output feedback," *Systems Control Lett*, vol. 18, pp. 421-430, 1994.

[11] M. C. Oliveira and J. C. Geromel, "Numerical comparison of output feedback design methods," in *Proc. of America Control Conf*, Albuquerque, U.S.A, 1997.

[12] D. Teschl, "Dynamical Systems," in *Ordinary Differential Equations and Dynamical Systems*, Rhode Island, American Mathematical Society, 2012, pp. 198-203.

[13] M. C. Razali, N. A. Wahab, P. Balaguer, M. F. Rahmat and S. I. Samsudin, "Multivariable PID controllers for dynamic process," in *2013 9th Asian Control Conference (ASCC)*, Istanbul, Turkey, 2013.

[14] J. Hu, C. Bohn and H. R. Wu, "Systematic H-infinity weighting function selection and its application to the real-time control of a vertical take-off aircraft," *Control Engineering Practice*, vol. 8, pp. 241-252, 2000.

[15] K. J. Astrom, K. H. Johansson and Q. G. Wang, "Design of Decoupled PID Controllers for MIMO Systems," in *American Control Conference*, Arlington, 2001.

[16] R. Kalpana, H. Kandath, J. Senthilkumar, G. Balasubramanian and S. G. Abhay ,"PrePrints," 25.12.2017. [Online]. Available: https://www.preprints.org/manuscript/201712.0184/v1. [Accessed 27 12 2018].

[17] Thales Electron Devices,"Industrial High-Power Tetrode, " TH558E datasheet, Dec. 2012 .

[18] "SLBC," [Online]. Available: http://www.slbc.lk/.

[19] Dunkermotoron Corporation,"Permanent Magnet DC Motor," GR 53×58 datasheet, Oct. 2012.

[20] "THALES Group ," [Online]. Available: https://www.thalesgroup.com/en/global/activities/market-specific-solutions/microwave-imaging-sub-systems/radio-frequency-microwav-0.

[21] "Ampegon Corporation ," [Online]. Available: https://ampegon.com/products/sw-tube-transmitter/.

[22] Thales Electron Devices,"Industrial High- μ Triode," CTK 12-1 datasheet, Dec. 2012 .

[23] "L34A: The Bounded Real Lemma," Control System Synthesis, 1 March 2017. [Online]. Available: https://www.youtube.com/watch?v=EsykpnnpPhM. [Accessed 12 10 2018].

[24] "Mosek LMI Solver ," [Online]. Available: https://www.mosek.com/products/mosek/. [Accessed 12 10 2018].

[25] MicroChip Corporation,"8-bit Microcontroller with 4/8/16/32K Bytes In-System Programmable Flash," ATmega328P datasheet, Feb. 2009.

[26] Omron Electronics Components,"PCB Power Relay," G2R-2 datasheet, Jan. 2019 .

[27] B. C. Kuo, Digital Control Systems, 2nd ed., New York: Oxford University Press Inc, 2007.

[28] M. C. Razali, N. A. Wahab, P. Balaguer, M. F. Rahmat and S. I. Samsudin, "Multivariable PID controllers for dynamic process," in *2013 9th Asian Control Conference (ASCC)*, Istanbul, Turkey, 2013.

[29] "APMonitor Regression Solver ," [Online]. Available: https://www.apmonitor.com/wiki/index.php/Main/MATLAB. [Accessed 12 10 2018].

APPENDIXES

Appendix A – H-infinity ILMI Algorithm in MATLAB

Appendix B – H-infinity ILMI Algorithm in MATLAB

Appendix C – Microcontroller Programing Code of Decentralized PID Controller

Appendix A

Non Linear Least Square Error Algorithm in MATLAB and APM Model

```
%MATLAB Code for Calling Non Linear Least Square Algorithm Built in
%APM

clear all;
close all;
clc;

addpath('apm')

s='http://byu.apmonitor.com';
a='data_regression';

apm(s,a,'clear all');

apm_load(s,a,'model.apm');
csv_load(s,a,'data.csv');

apm_info(s,a,'FV','epsilon')
apm_info(s,a,'FV','ohmegan')

apm_option(s,a,'zeta.status',1);
apm_option(s,a,'ohmegan.status',1);
apm_option(s,a,'nlc.imode',2);

output=apm(s,a,'solve');
disp(output)

y=apm_sol(s,a);
z=y.x;

disp('solution')
disp(['zeta = ' num2str(z.zeta(1))])
disp(['ohmegan = ' num2str(z.ohmegan(1))])

figure(1)
plot(z.t,z.valm,'o')
hold on
plot(z.t,z.modval,'x');
```

%APM Model for a Second Order System with an Integrator

```
Model
  Parameters
   zeta
   ohmegan
   t
   valm
  End Parameters


  Variables
    modval
  End Variables

  Equations
      modval=t - (2*zeta)/ohmegan + (2*zeta*exp(-
      ohmegan*t*zeta)*(cosh(ohmegan*t*(zeta^2 - 1)^(1/2)) -
      (sinh(ohmegan*t*(zeta^2 - 1)^(1/2))*(ohmegan*zeta + (-
      4*ohmegan*zeta^2 + ohmegan)/(2*zeta)))/(ohmegan*(zeta^2 -
      1)^(1/2))))/ohmegan
  End Equations

    minimize (((valm-modval)/valm)^2)

End Model
```

Appendix B

H-infinity ILMI Algorithm in MATLAB

This MATLAB program calculates three gain matrices of decentralized PID controller

```
clear all;
close all;
clc;

num11=-0.37237;
den11=[0.0797 5.689 1 0];
G11=tf(num11,den11);
num12=0.019761;
den12=[301.091 27.693 1 0];
G12=tf(num12,den12);
num21=-0.2018;
den21=[6.315 4.5234 1 0];
G21=tf(num21,den21);
num22=-0.07345;
den22=[16.112 3.523 1 0];
G22=tf(num22,den22);
GMIMO=[G11 G12;G21 G22];

SYS=ss(GMIMO);%Find ss in diagonal canonical form

A=SYS.A;
B=SYS.B;
C=SYS.C;
D=SYS.D;

delta=0;
gamma=10;

[~,l]=size(B);%no of inputs
[m,~]=size(C);%no of outputs

%making a random symmetric and positive definite matrix
n=length(A);%no of states
Q0 = rand((n+m),(n+m));
Q0 = 0.5*(Q0+Q0');
Q0 = Q0 + (n+m)*eye(n+m);

%Defining LMI matrix variables
P=sdpvar(n+m);
```

```
alpha=sdpvar(1);

F111=sdpvar(1);
F122=sdpvar(1);

F211=sdpvar(1);
F222=sdpvar(1);

F311=sdpvar(1);
F322=sdpvar(1);

F1=[F111 0;0 F122];
F2=[F211 0;0 F222];
F3=[F311 0;0 F322];

F=[F1 F2 F3];

%Defining augmented system matrices
Abar=[A zeros(n,m);C zeros(m,m)];
Bbar=[B;zeros(m,l)];
B1bar=[2 0 0 0.25 0 0 0.0625 0 0 0.125 0 0 0 0]';
C1=[C zeros(m,m)];
C2=[zeros(m,n) eye(m,m)];
C3=[(C*A) zeros(m,m)];
Cbar=[C1' C2' C3']';
[~,c]=size(Bbar);%no of inputs
[r,~]=size(Cbar);
Dbar=zeros(r,c);

for i=1:1:inf
    if(i==1)
        %solving Riccati equation
        [X,L,GG] = care(Abar,Bbar,Q0);

        %defining LMI constraint matrix
       M11=(Abar'*P)+(P*Abar)-(X*(Bbar*Bbar')*P)-
     (P*(Bbar*Bbar')*X)+(X*(Bbar*Bbar')*X)-(alpha*P);
        M12=P*B1bar;
        M13=((Cbar)+(Dbar*F*Cbar))';
        M14=((Bbar'*P)+(F*Cbar))';
        M21=(B1bar'*P);
        M22=-(gamma^2)*eye(1,1);
        M23=zeros(1,3*m);
        M24=zeros(1,l);
        M31=((Cbar)+(Dbar*F*Cbar));
        M32=zeros(3*m,1);
        M33=-eye(3*m,3*m);
        M34=zeros(3*m,l);
```

```
        M41=((Bbar'*P)+(F*Cbar));
        M42=zeros(l,1);
        M43=zeros(l,3*m);
        M44=-eye(l,l);
        M11=(M11+M11')/2;
        M=[M11 M12 M13 M14;M21 M22 M23 M24;M31 M32 M33
    M34;M41 M42 M43 M44];

        %defining LMI constraints

        constr = [(M<=0),(0<=P)];

        %select LMI solver plugged in to MATLAB
        options=sdpsettings('solver','mosek','debug',1);
        %solve LMI by minimizing alpha
        diagnostics = bisection(constr,alpha,options);
        alphasol=double(alpha);% The value of minimized
alpha
        Fsol=double(F);
        if(alphasol<=-0.05)% -0.05 is the value to which
alpha is minimized
            fprintf('The value of alpha is %d',alphasol);
            F1bar=Fsol(:,1:2);
            F2bar=Fsol(:,3:4);
            F3bar=Fsol(:,5:6);

          %PID gain matrices
            F3=F3bar/(eye(size(C*B*F3bar))+(C*B*F3bar))
            F2=(eye(size(F3*C*B))-(F3*C*B))*F2bar
            F1=(eye(size(F3*C*B))-(F3*C*B))*F1bar
            break;
        else
        %defining LMI constraint matrix
       M11=(Abar'*P)+(P*Abar)-(X*(Bbar*Bbar')*P)-
    (P*(Bbar*Bbar')*X)+(X*(Bbar*Bbar')*X)-(alphasol*P);
        M12=P*B1bar;
        M13=((Cbar)+(Dbar*F*Cbar))';
        M14=((Bbar'*P)+(F*Cbar))';
        M21=(B1bar'*P);
        M22=-(gamma^2)*eye(1,1);
        M23=zeros(1,3*m);
        M24=zeros(1,l);
        M31=((Cbar)+(Dbar*F*Cbar));
        M32=zeros(3*m,1);
        M33=-eye(3*m,3*m);
        M34=zeros(3*m,l);
        M41=((Bbar'*P)+(F*Cbar));
        M42=zeros(l,1);
```

```
        M43=zeros(l,3*m);
        M44=-eye(l,l);
        M11=(M11+M11')/2;
        M=[M11 M12 M13 M14;M21 M22 M23 M24;M31 M32 M33
M34;M41 M42 M43 M44];
        %defining LMI constraints
        constr = [(M<=0),(0<=P)];
        options=sdpsettings('solver','mosek');
        optimize(constr,trace(P),options);
        Psol=double(P);%optimized Pi-1
        PX=double(P);%optimized P is assigned to PX in
1st iteration
        N=norm(X*Bbar-Psol*Bbar);% Compare X & P
        N1=N
        alphasol

        if(N<delta)% Check feasibility of solution
            disp('The System May not be stabilizable for
this delta value');
            break;

        end
        end

    else
        %This segment is run from 2nd iteration
        %defining LMI constraint matrix
        Ptemp=double(PX);
       M11=(Abar'*P)+(P*Abar)-(PX*(Bbar*Bbar')*P)-
     (P*(Bbar*Bbar')*PX)+(PX*(Bbar*Bbar')*PX)-(alpha*P);
        M12=P*B1bar;
        M13=((Cbar)+(Dbar*F*Cbar))';
        M14=((Bbar'*P)+(F*Cbar))';
        M21=(B1bar'*P);
        M22=-(gamma^2)*eye(1,1);
        M23=zeros(1,3*m);
        M24=zeros(1,l);
        M31=((Cbar)+(Dbar*F*Cbar));
        M32=zeros(3*m,1);
        M33=-eye(3*m,3*m);
        M34=zeros(3*m,l);
        M41=((Bbar'*P)+(F*Cbar));
        M42=zeros(l,1);
        M43=zeros(l,3*m);
        M44=-eye(l,l);
        M11=(M11+M11')/2;
        M=[M11 M12 M13 M14;M21 M22 M23 M24;M31 M32 M33
M34;M41 M42 M43 M44];
```

```
        %defining needed constraints
        constr = [(M<=0),(0<=P)];
        %select solver
        options=sdpsettings('solver','mosek');
        %solve LMI by minimiying alpha
        diagnostics = bisection(constr,alpha,options);
        alphasol=double(alpha);
        Fsol=double(F);
        alphasol

        if(alphasol<=-0.05)

            fprintf('The value of alpha is %d',alphasol);

            F1bar=Fsol(:,1:2);
            F2bar=Fsol(:,3:4);
            F3bar=Fsol(:,5:6);

F3=F3bar*inv(eye(size(C*B*F3bar))+(C*B*F3bar))
            F2=(eye(size(F3*C*B))-(F3*C*B))*F2bar
            F1=(eye(size(F3*C*B))-(F3*C*B))*F1bar
            break;


        else
       M11=(Abar'*P)+(P*Abar)-(PX*(Bbar*Bbar')*P)-
     (P*(Bbar*Bbar')*PX)+(PX*(Bbar*Bbar')*PX)-
     (alphasol*P);
        M12=P*B1bar;
        M13=((Cbar)+(Dbar*F*Cbar))';
        M14=((Bbar'*P)+(F*Cbar))';
        M21=(B1bar'*P);
        M22=-(gamma^2)*eye(1,1);
        M23=zeros(1,3*m);
        M24=zeros(1,l);
        M31=((Cbar)+(Dbar*F*Cbar));
        M32=zeros(3*m,1);
        M33=-eye(3*m,3*m);
        M34=zeros(3*m,l);
        M41=((Bbar'*P)+(F*Cbar));
        M42=zeros(l,1);
        M43=zeros(l,3*m);
        M44=-eye(l,l);
        M11=(M11+M11')/2;
        M=[M11 M12 M13 M14;M21 M22 M23 M24;M31 M32 M33
M34;M41 M42 M43 M44];
```

```
        constr = [(M<=0),(0<=P)];
        options=sdpsettings('solver','mosek');
        optimize(constr,trace(P),options);
        PX=double(P);
        N=norm(Ptemp*Bbar-PX*Bbar);
        N2=N
        alphasol

        if(N<delta)
            disp('The System May not be stabilizable for
this delta value');
            break;

        end

        end
    end
end
```

Appendix C

Microcontroller Programing Code of Decentralized PID Controller

```
double InputRaw1;
double InputRaw2;
double ErrorLast1=0;
double ErrorLast2=0;
double ErrorPresent1;
double ErrorPresent2;
double Setpoint1;
double Setpoint2;
double Integral1;
double Integral2;
double Derivative1;
double Derivative2;
double PWM_MP10;
double PWM_MP11;
double readings1;
double readings2;


double Kp1=1.2491, Ki1=0.0162, Kd1=2.2805 ;
double Kp2=1.5108, Ki2=0.0616, Kd2=3.9334;

double pidOut1;
double pidOut2;

void setup() {
  // put your setup code here, to run once:

  analogReference(DEFAULT);
  Serial.begin(9600);

  Setpoint1=0.5;
  Setpoint2=0.4;

  InputRaw1=analogRead(0);
  InputRaw2=analogRead(1);

  readings1=(10.6*InputRaw1)/(1024);
  readings2=(9.0*InputRaw2)/(1024);

  ErrorLast1=readings1-Setpoint1;
  ErrorLast2=readings2-Setpoint2;
```

```
  Integral1=0;
  Integral2=0;
}

void loop() {
  // put your main code here, to run repeatedly:

  InputRaw1=analogRead(0);
  InputRaw2=analogRead(1);

  readings1=(10.6*InputRaw1)/(1024);
  readings2=(9.0*InputRaw2)/(1024);

  ErrorPresent1=readings1-Setpoint1;
  ErrorPresent2=readings2-Setpoint2;

  Derivative1=ErrorPresent1-ErrorLast1;
  Derivative2=ErrorPresent2-ErrorLast2;
  Integral1=Integral1+ErrorPresent1;
  Integral2=Integral2+ErrorPresent2;
  ErrorLast1=ErrorPresent1;
  ErrorLast2=ErrorPresent2;


pidOut1=(Kp1*ErrorPresent1)+(Ki1*Integral1)+(Kd1*Derivati
ve1);

pidOut2=(Kp2*ErrorPresent2)+(Ki2*Integral2)+(Kd2*Derivati
ve2);

  PWM_MP10=((1.65)-(pidOut1/6.0606))*(255/3.3);//PWM3
  PWM_MP11=((1.65)-(pidOut2/6.0606))*(255/3.3);//PWM5

  analogWrite(3,PWM_MP10);
  analogWrite(5,PWM_MP11);

  Serial.println(ErrorPresent1);

  delay(10);//Sampling time Ts=0.01s
}
```